MODELLING THE RELATIONSHIP BETWEEN PHYSIOLOGICAL MEASURES OF MOTION SICKNESS

OLUWASEYI ELIZABETH SHODIPE

A THESIS SUBMITTED TO
THE FACULTY OF GRADUATE STUDIES
IN PARTIAL FULFILLMENT OF THE REQUIREMENTS
FOR THE DEGREE OF MASTER OF APPLIED SCIENCE

GRADUATE PROGRAM IN ELECTRICAL ENGINEERING AND COMPUTER SCIENCE
YORK UNIVERSITY
TORONTO, ONTARIO

May 2023

ABSTRACT

Car sickness is anticipated to occur more frequently in self-driving vehicles because of their design. This thesis involved an investigation using machine learning techniques with physiological measures to detect and predict the severity of car sickness in real-time every two minutes. A total of 40 adults were exposed to two conditions, each involving a 20-minute ride on a motion-base simulator. Car sickness incidence and severity were subjectively measured using the Fast Motion Sickness (FMS) and Simulator Sickness Questionnaire (SSQ). Car sickness symptom was successfully elicited in 31 participants (77.5%) while avoiding simulator sickness. Results showed that head movement had the strongest relationship with car sickness, and there was a moderate correlation between heart rate and skin conductance. The machine learning models revealed a medium correlation between the physiological measures and the FMS scores. An acceptable classification score distinguishing between motion-sick and non-motion-sick participants was found using the random forest model.

ACKNOWLEDGEMENTS

My most profound appreciation goes to God for the gift of life and the opportunity to successfully complete this thesis. My sincere appreciation also goes to my husband (Olawale Shodipe) and my two(2) kids, Ire and Ayo, for their immense patience and support throughout this programme.

I also thank my supervisor, Professor Robert Allison, for his assistance and guidance in helping me carry out this research.

Finally, I thank my mum, sisters and close friends for their emotional support and encouragement through this journey.

TABLE OF CONTENTS

LIST OF TABLES

LIST OF FIGURES

ABBREVIATIONS

ANOVA	Analysis of Variance
ECG	Electrocardiogram
EDA	Electrodermal Activity
EOG	Electrooculogram
FMS	Fast Motion Sickness
HF	High-Frequency Power
HRV	Heart Rate Variability
IMU	Inertial Measurement Unit
LF	Low-Frequency Power
MS	Motion Sickness
MSSQ	Motion Sickness Susceptibility Questionnaire
NDRT	Non-Driving Related Task
PDI	Pensacola Diagnostic Index
SCR	Skin Conductance Response
SSQ	Simulator Sickness Questionnaire
VIMS	Visual-Induced Motion Sickness
VR	Virtual Reality

CHAPTER ONE – INTRODUCTION

1.1 INTRODUCTION

Motion sickness (also known as kinetosis) is a common negative reaction to travel in a wide variety of vehicles, including ships, trains, spacecraft, airplanes, and cars. Some studies suggest that it dates back to shortly after man adopted other transportation modes apart from walking (Dobie, 2019). It is characterized by a wide range of symptoms, including pallor, burping, stomach awareness, headaches, fatigue, cold sweating, alterations in gastric rhythm, nausea, and vomiting (Bronstein et al., 2020, Reason, 1978). These symptoms are often disabling, causing drowsiness, lack of concentration, and disorientation in those who experience them (Li et al., 2022). Over 60% of people say they have experienced car sickness at least once in their lifetime, with over 50% reporting it happened during the past five years (Schmidt et al., 2020). Symptoms are more likely to occur when engaging in tasks like reading or writing (Krueger et al., 2017; Schmidt et al., 2020) or when unable to view outside of the car (Turner & Griffin, 1999).

Car sickness is anticipated to occur more frequently in self-driving vehicles because of their design, which includes electronics and seating arrangements optimized for work and entertainment (Diels & Bos, 2016; Iskander et al., 2019). Therefore, mitigating motion sickness is a crucial research area that is essential to the effective use of electronics in autonomous vehicles and, ultimately, their broad adoption. Motion sickness commonly occurs in scenarios when sensory information signalling self-motion has unexpected or conflicting correlations (Money, 1970). For instance, when reading on a smartphone as a passenger in a moving car, the head moves with the device as the outside world passes by. Although the head is relatively stable with respect to the device and the car's interior, the head is moving in space as indicated by cues like the inner ear's vestibular system during acceleration.

The most prevalent theories of motion sickness are sensory conflict theories. For instance, according to the sensory rearrangement theory, motion sickness develops when there is a significant difference between the expected pattern of sensory inputs anticipated when we move (based on prior experience) and the actual sensory inputs received (Oman, 1990; Reason, 1978). This theory and its adaptations are popular because they explain why some conflicts cause motion sickness, why drivers are less susceptible to motion sickness than passengers, and how we adjust and become desensitized over time. Additionally, it agrees with the observation that having a view of the outside world, especially the view of the road in front of the vehicle, helps prevent car sickness while driving (Griffin & Newman, 2004).

In line with this theory, several researchers have proposed visual display-based mitigation strategies to minimize or eliminate visual conflicts with other senses or enhance sensory input expectations (Karjanto et al., 2018; McGill et al., 2017; Cho & Kim, 2022), but results have been mixed (Feenstra et al., 2011; Griffin & Newman, 2004). The diversity, location, and quality of the displays probably contribute to some of this variability. Stimuli in the visual field can influence car sickness, and these effects can be advantageous or detrimental. Similarly, a type of motion sickness known as visually-induced motion sickness (VIMS) can be elicited solely from vision (Keshavarz, 2015). The nature, placement, size, and perceived relationship of stationary and moving components of the scene relative to the head are important factors in effectively predicting and mitigating motion sickness (Andersen & Braunstein, 1985; Foulkes et al., 2013; Harris et al., 2012; Pavard et al., 1976; Stern et al., 1990; Warren & Rushton, 2008; Webb & Griffin, 2003). Moreover, it is essential to comprehend this flow parsing and segregation (Koenderink, 1986) to predict how additional visual stimuli affect sensory conflict and motion sickness (Vogel et al., 1982).

1.2 RESEARCH MOTIVATION

Investigating motion sickness issues in the context of real or simulated driving requires real-time measurement of car sickness. However, the real-time, continuous assessment of motion sickness symptoms without the user's direct involvement or interference poses a challenge for research and practical mitigation. Consequently, there has been a lot of research interest in assessing and monitoring motion sickness from physiological and behavioural measures. Numerous potential signals have been studied, including eye movements (Flanagan et al., 2004; Krueger et al., 2017; Webb & Griffin, 2002), facial or body temperature (Pham Xuan et al., 2021), skin conductance (Dahlman et al., 2009; Himi et al., 2004), heart rate (Cowings & Toscano, 1993; Himi et al., 2004; Holmes & Griffin, 2001; Mullen et al., 1998), head and body movements (Arcioni et al., 2019; Cloutier, 2006; Palmisano et al., 2020; Riccio & Stoffregen; 1991; Stoffregen et al., 2017), and electroencephalogram (Himi et al., 2004, Lin et al., 2007).

Additionally, there are documented commonalities and differences between the etiology, symptoms, and susceptibility of the different types of motion sickness (Golding, 2006). These variances are significant enough that predicting a person's vulnerability to car sickness based on other types of motion sickness is impossible. Similarly, the objective measures applicable to one variant may not necessarily apply to another. This research is a step toward establishing the suitability of batteries of objective measurements as indicators and predictors of car sickness, including developing and validating such batteries using a model. A model can prove useful in determining the likelihood of car sickness severity in individual users, allowing intervention before the onset of motion sickness. Therefore, establishing the best physiological indicators of simulator sickness could shed more light on the likelihood and exact triggering time of the

syndrome, allowing a more accurate description of the temporal characteristics of car sickness and more informed interventions.

1.3 RESEARCH BACKGROUND

The Greek physician Hippocrates is credited with first describing motion sickness when he stated that "sailing on the sea indicates that motion disturbs the body". Irwin used the term "motion sickness" in 1881 to characterize a condition brought on by frequent oscillatory movements of the body. It refers to a feeling of illness or discomfort that occurs while travelling by land, sea, or air as well as while using a car, train, elevator, amusement ride, swing, or, less frequently, an animal like a camel (Leung & Hon, 2019; Golding, 2016; Leung & Coenegrachts, 2011). Similar symptoms are commonly reported on entering and leaving space.

However, real motion is not a prerequisite for this malady, as motion perception can also cause motion sickness (Gahlinger, 1999). So, even though the affected individuals are not actually moving, they can suffer motion sickness symptoms while watching a big moving field or participating in virtual reality rides in amusement parks (Koch et al., 2018). For these situations, some authors prefer to use the terms "pseudo motion sickness" or "pseudokinetosis" (Schmäl, 2013). Motion sickness can also be referred to as space sickness, automobile sickness, seasickness, travel sickness, and simulator/cinema/cybersickness, depending on the environment in which it occurs (Koch et al., 2018).

A motion-base simulator provides an ideal scenario for studying motion sickness because it allows for a wider range of research that may be risky in a normal car, like the transfer of control in autonomous vehicles. Typical autonomous vehicles are designed to facilitate automated driving on certain roads, with a brief handover back to the passenger when travelling through an area that does not support automated driving. However, as passengers engage in other activities during automated driving, their outside view may be restricted, increasing the likelihood or severity of car sickness (Griffin and Newman, 2004). Another area of research that can benefit from studying car sickness in a simulator is the development of countermeasures against motion sickness. These measures can include providing additional sensory information to reduce sensory conflict and improve anticipation of motion (Rolnick and Bles, 1989) and have already been proven effective in simulators for flight and ship travel (Tal et al., 2014; Feenstra et al., 2011).

1.4 RESEARCH AIM AND OBJECTIVES

The specific goals of this thesis included using signal processing, quantitative analysis, and machine learning (ML) approaches to (1) detect and identify changes in physiological and behavioural measures

linked to the onset of car sickness and (2) categorize participants as sick or not sick based on physiological and behavioural measures. Although there were anticipated alterations in participants' physiological responses as they experienced car sickness, there were no precise predictions regarding the physiological measures that would be the most accurate indicators of car sickness, given the variety of results published by earlier research in this domain. Consequently, ML techniques were anticipated to increase the likelihood of identifying patterns of physiological measures linked to car sickness.

1.5 STRUCTURE OF THESIS

This thesis report comprises five chapters; Chapter 1 is this introduction. Chapter 2 reviews related literature on motion sickness to understand the epidemiology, types, measurement techniques and state-of-the-art. Chapter 3 discusses the research methodology, including the experiment's stimulus, participants, apparatus, data collection and data preprocessing techniques. Chapter 4 provides a comprehensive overview of the data collection and results of the data analysis, including a correlation of the motion sickness measures and a presentation of the developed machine learning models. Chapter 5 covers an extensive discussion of the research findings, limitations of the study, suggestions for future work and the conclusion.

CHAPTER TWO-LITERATURE REVIEW

2.1 INTRODUCTION

The preceding chapter detailed the research background while outlining the research objectives this thesis aims to address. This chapter builds on this and provides a comprehensive review of relevant and related research work in the area of motion sickness.

This chapter is subdivided into five main sections. Section 2.2 outlines the epidemiology of motion sickness to provide valuable insights into the prevalence, incidence, and risk factors associated with this condition, while section 2.3 provides a general overview of the most popular motion sickness theories. Section 2.4 highlights the various types of motion sickness, while the various ways motion sickness can be measured are presented in section 2.5, including justifications for the measures chosen in this thesis. The last section summarizes the literature review chapter.

2.2 MOTION SICKNESS EPIDEMIOLOGY

Many people have experienced motion nausea at least once (Herron, 2010), with seasickness reportedly being the most prevalent and well-known type (Koch et al., 2018). The word "nausea", a primary symptom of motion sickness, comes from the Greek word naus, meaning "nautical," or a ship. Within two to three days following the start of an ocean cruise, up to twenty-five (25) percent of passengers on a large ship will develop motion sickness (Leung and Hon, 2019; Leung and Coenegrachts, 2011). With bad weather and smaller vessels, the incidence is higher. In the most extreme of cases, as many as sixty (60) percent of passengers, including experienced crew members, may be affected (Koch et al., 2018).

The incidence of motion sickness necessitating medical consultations was 4.2 per 1000 people per day, according to an extensive study of 2366 passengers who had collectively taken part in 26 cruise voyages for 34,501 person-days (Schutz et al., 2014). Up to four percent of drivers of rally vehicles and passengers who are reading a book or sitting in the back seats during the trip are likely to experience motion sickness (Leung & Hon, 2019; Leung & Coenegrachts, 2011; Koch et al., 2018; Golding & Gresty, 2015). In pressurized commercial aircraft, just one percent of passengers experience motion sickness and even fewer (0.13%) get sick on trains (Leung & Hon, 2019; Leung & Coenegrachts; Koch et al., 2018; Golding & Gresty, 2015). Student pilots report experiencing motion sickness ranging from 10-31%. The overall incidence gradually declines as these student pilots gain experience (Samuel and Tal, 2015). Up to eighty

(80) percent of astronauts experience space sickness during the first three days of a space mission (Heer and Paloski, 2006).

It is believed that motion sickness can occur in anyone if the movements being applied to the body are substantial enough. However, there is a high level of individual susceptibility to motion sickness caused by gene-environment interaction (Priesol, 2017; Takov and Tadi, 2019; Zhang et al., 2016). This susceptibility is connected with particular traits. According to studies by Leung & Hon, 2019; Leung & Coenegrachts; Koch et al., 2018; Schmäl, 2013; Lawther & Griffin, 1988; Paillard et al., 2013; and Golding (2016), women are more likely than men of the same age to experience greater frequency and intensity of symptoms, particularly during menstruation. Similarly, pregnant women are more prone to motion sickness due to hormonal changes during pregnancy (Takov & Tadi, 2019; Zhang et al., 2016). Children under two rarely experience motion sickness, presumably because of their limited visual experience (Gahlinger, 1999; Schmäl, 2013).

Young infants are also frequently in a reclined position, which makes them less prone to motion sickness (Gahlinger, 1999). The most vulnerable are children aged six to twelve, peaking between ages nine and ten (Golding, 2016; Gahlinger, 1999; Koch et al., 2018; Takov & Tadi, 2019). The susceptibility decreases through adolescence and afterward, presumably due to habituation (Gahlinger, 1999; Murdin et al., 2011; Takov & Tadi, 2019; Reavley et al., 2006). Motion sickness is less common in adults and rarely happens after age 50 (Leung & Hon, 2019; Leung & Coenegrachts, 2011; Schmäl, 2013; Paillard et al., 2013). Compared to their age-matched male counterparts, females experience a transient increase in vulnerability around menopause (Paillard et al., 2013).

Although people of all races can experience motion sickness, considerable racial disparities exist (Golding, 2006). Chinese people have been found to be more prone to motion sickness than white people (Zhang et al., 2016; Klosterhalfen et al., 2005; Stern et al., 1996). Motion sickness may run in families (Reavley et al., 2006), and the likelihood that a child would experience motion sickness is twice as high if either parent experienced it as a child (Leung & Hon, 2019; Leung & Coenegrachts, 2011). Car sickness may have a hereditary component because monozygotic twins experience it 2.5 times more frequently than dizygotic twins (Leung & Hon, 2019; Leung & Coenegrachts, 2011), with estimates of heritability ranging from 57–70%. Hromatka et al. (2015) conducted a genome-wide study on motion sickness involving eight thousand four hundred and ninety-four (80,494) people surveyed about car sickness. The authors found 35 single-nucleotide polymorphisms associated with motion sickness. The motion sickness genes are located on chromosome four. (Peddareddygari et al., 2019).

2.3 MOTION SICKNESS THEORIES

2.3.1 SENSORY CONFLICT THEORY

There are physiological factors responsible for motion sickness. The sensory conflict theory is currently the most widely accepted theory that has withstood over forty years of dispute. The theory initially proposed in 1975 in reference to flight simulators (Reason and Brand, 1975) argues that the compelling visual sensation of motion, without the associated vestibular or proprioceptive inputs, causes the physiological side effects characterizing motion sickness (Stanney and Kennedy, 2009; Groen and Bos 2008; Nichols and Patel, 2002; Reason and Brand, 1975). The vestibular system provides information about linear and angular acceleration, including the body's position with respect to gravity (Cohen et al., 2005). The visual system also offers information about body motion and orientation as it relates to the visual world, and the kinesthetic or proprioceptive system offers information about limb and body position (Barratt and Pool, 2008). Normally, these sensory signals are consistent and provide complementary or redundant information about self-motion and orientation.

Reason and Brand's (1975) theory states that a replica of a self-generated movement is combined with the resulting sensory inputs to create a predicted pattern of sensory cues or an engram (Reason, 1978). The sensory inputs are then compared to the engrams stored in a comparator module. A mismatch signal is produced when there is a disparity between the input and the engram, which in turn causes motion sickness. The number of sensory modalities in conflict, the extent of the discrepancy and prior exposure to the conflicting stimuli decide the strength of the mismatch signal. Similarly, the latency and intensity of motion sickness symptoms correlate with the mismatch signal's strength. When people are immersed in situations where they perceive self-motion through vection (the illusion of self-motion produced by viewing an optic flow pattern), visual cues that suggest movement conflict with vestibular inputs, indicating the user is stationary. Consequently, a mismatch signal is issued when no matching engram is detected, resulting in motion sickness (Reason, 1978; Reason and Brand, 1975).

While modern versions of Reason and Brand's (1975) theory are widely accepted, it fails to explain motion sickness onset and progression. Firstly, this concept lacks a convincing physiological foundation that would clarify the significance of mismatch signals in facilitating sickness (Oman, 1988). Secondly, this theory cannot explain individual variations in motion sickness (Davis et al., 2014; Warwick-Evans et al., 1995). For instance, it is unclear why women are more likely than men to have motion sickness (Chen et al., 2015; Flanagan et al., 2005; Kim et al., 2008; Stanney et al., 1999, 2003). Finally, the argument falls short in addressing why some sensory cues are more likely to result in sickness than others. It is unknown why

certain stimuli are more nauseogenic than others because, according to the theory, any sensory conflict that causes a mismatch signal should make a person feel nauseous. For instance, in a VR environment, scenes with oscillations are more likely to result in cybersickness than scenes without oscillations (Lo and So, 2001; So and Lo, 1999).

To address some of the unanswered questions by the sensory conflict theory, Oman (1988) hypothesized that desired body states trigger muscle activity and postural adjustments. These modifications provide signals that various sensory modalities can detect. Thus, a difference vector is produced by comparing an internal model of all sensory modalities with actual sensory inputs. More sensory conflicts result in a larger vector, which may reflect severe sickness. Bles et al. (1998) and Bos et al. (2008) presented a more restricted description of sensory conflict that built on the ideas of Oman (1988) by proposing that the only salient conflict was in the perception of the subjective vertical. The importance of subjective vertical, created from integrated sensory data from vision, proprioception, and the vestibular organs, is attributed to its role as a frame of reference to successfully interact with the external environment (Barra et al., 2010).

2.3.2 POISON THEORY

Although it is not apparent how or why sensory conflicts result in sensations like nausea, the Poison Hypothesis is one widely cited theory (Treisman, 1977) suggesting that sensory mismatches are a component of an early warning system when an animal consumes poisons. Hence, nausea is an evolved, adaptive reaction to a sensory conflict that helps an animal eliminate toxic substances (Treisman, 1977). Although many experts think this concept is not a convincing or testable explanation for motion sickness, it is a viable explanation for the nausea symptoms of the condition. However, it does not account for other symptoms, such as oculomotor or disorientation symptoms (Davis et al., 2015; LaViola, 2000; Oman, 2012).

2.3.3 ECOLOGICAL THEORY

Over the years, other theories have been proposed to explain motion sickness. The Ecological Theory (sometimes referred to as the Postural Instability theory) is one such theory, and it explains that motion sickness is caused by prolonged instability in postural control (Riccio and Stoffregen, 1991; Bonnet et al., 2008). People are likely to experience motion sickness when they encounter novel situations for which they have not yet learnt techniques to stabilize their posture (Stoffregen et al., 2000; Villard et al., 2008). For instance, Stoffregen and Smart (1998) discovered increases in postural sway preceding visual-induced motion sickness symptoms when participants were exposed to low-amplitude optical flow in an immersive

environment. In addition, Smart et al. (2002) discovered that pitch velocity and vertical variability of body sway could predict which subjects will become sick following exposure to optic flow stimulation.

The causal relationship between motion sickness and postural instability is still unclear. For instance, Dennison and D'Zmura (2017) reported that postural sway patterns of participants were similar before and during VR exposure, and motion sickness increased alike when participants were seated (and thus unlikely to have an unstable posture) and when standing (and thus subject to greater postural demands and the potential for instability). Similar findings were made by Warwick-Evans et al. (1995), who found that participants experienced motion sickness watching a movie both while standing up and while being constrained in a chair. Also, Akiduki et al. (2003) showed that postural instability (specifically, body sway) was only substantially different post-exposure to virtual reality, thus, suggesting that instability is more a result of cybersickness than a cause.

2.4 TYPES OF MOTION SICKNESS

2.4.1 CAR SICKNESS

Cars, the most popular form of land transportation, elicit a specific form of motion sickness known as car sickness (Murdin et al., 2011). Car sickness is more common in passengers than in drivers, who are much less likely to have symptoms of nausea, dizziness, retching, or vomiting (Diels & Bos, 2015). According to studies (e.g., Kuiper et al., 2020; Diels & Bos, 2015; Stoffregen et al., 2014), this may be because driving involves controlling the vehicle, and thus the driver can predict the trajectory of the car better than a passenger, particularly one in the back. Also, limiting the passengers' field of view and increasing their participation in activities unrelated to driving may lead to a sensory conflict between the passengers' visual, vestibular, and somatosensory systems (Diels & Bos, 2015; Griffin & Newman, 2004; Salter et al., 2019).

Sensory conflict is frequently cited as the fundamental mechanism causing motion sickness (Dobie, 2019). A fixed-base driving simulator illustrates an ideal scenario where such conflicts might occur because, as the driving simulation progresses, the user only experiences the visual sensation of self-motion, without all other related sensations of an actual driving experience except the hands on the steering wheel. According to the sensory conflict theory, motion sickness can also happen when various cues contradict the expectations based on prior personal experiences. Regardless of the scenario, vestibular cues play an essential role in this theory, as people without functional vestibular systems do not experience motion sickness (Money, 1972; Cheung et al., 1991).

2.4.2 SEASICKNESS

Seasickness is a classic form of motion sickness and one that is mentioned in the earliest extant literature (Lawther & Griffin, 1986). Typically, subjective symptoms appear between one and twelve hours into a sea cruise. After being exposed to ship motion continuously for 12 to 96 hours, adaptation usually takes place. Even among those who do not get seasick, the body sways at sea differs from sway on land (Mayo, Wade, & Stoffregen, 2011; Stoffregen et al., 2011). According to the postural instability theory of motion sickness, there will be disparities in postural activity between those who subsequently experience seasickness and those who do not. The postural sway of sick people also changes over time with ongoing exposure to a ship's motion. It takes many days for the body to adjust to ship motion. However, according to the theory, subjective symptoms should disappear when a person develops stable postural control in response to ship motion.

Postural activity in fully adapted individuals will not be the same as prior to the start of subjective symptoms or before exposure to a ship's motion, and a return to stable control does not necessarily mean a return to previously steady movement patterns as the sway of the same people on land and at sea in properly adapted seafarers differ (Mayo et al., 2011; Bos et al., 2008). Mal de debarquement is a re-adaptation process that can cause motion sickness-like sensations to persist for several hours (even days or months) after returning to the land (Cha, 2009). Consequently, when a person goes ashore after thoroughly adapting to life at sea, they must re-adapt to the lack of ship motion.

2.4.3 AIRSICKNESS

Airsickness is a type of motion sickness. The phenomenon was documented as far back as World War II when airborne military personnel were "neutralized" and unable to complete their mission despite arriving at their destination (Estrada et al., 2007). The size, structure of the aircraft, flight speed, profile, and weather all affect the severity of airsickness symptoms when flying. The relationship between flying direction, the subjective vertical, and the true vertical gravity vector also significantly impacts how airsickness develops. The low-frequency lateral and vertical motion axes are noted as the most likely to cause symptoms of motion sickness (Turner et al., 2000).

Visual cues may contribute to sensory mismatch in aviation (Turner et al., 2000). This situation is further complicated when travelling through clouds and air pockets without visual information. Unlike the pilots at the controls, passengers who cannot anticipate aircraft movement may experience additional discomfort. This experience is similar to how car sickness affects drivers and passengers differently (Rolnick and

Lubow, 1991). Due to their frequent, regular flying and control of the aircraft, pilots have a higher potential for habituation. Another factor unique to the aerospace environment is hypoxia. Hypoxia is minimal in compressed aircraft cabins, but a study shows that even moderate hypoxia can worsen motion sickness symptoms induced by optokinetic stimuli (Zhang et al., 1998).

Airsickness is a condition that many passengers have experienced. It is a common source of severe discomfort, primarily due to nausea and fatigue, for which pharmacological support is often required. Between 1946 and 1947, the most extensive study in the field was carried out on more than a million airline passengers (Ledera & Kidera, 1954). According to the study, three of every four travellers experienced some form of airsickness. Females were more likely to experience the symptoms than males, and it was more prevalent in smaller rather larger aircraft. Subsequent research showed that the prevalence of motion sickness on commercial passenger flights was declining, most likely due to advancements in aviation technology. According to a British study conducted in 2000 on 923 domestic airline passengers, 48% complained of airsickness-related symptoms. Interestingly, those seated near the wing or at the back of the plane experienced more severe symptoms (Turner et al., 2000).

2.4.4 VISUAL-INDUCED MOTION SICKNESS AND CYBERSICKNESS

Visual induced motion sickness (VIMS) differs slightly from traditional motion sickness syndromes like car, sea, and air sickness, which are caused by the vehicle's actual movement (Golding, 2016; Reason and Brand,1975). However, it does share some similarities with other motion sickness types. VIMS is related to or a factor in a number of other syndromes, including cybersickness (McCauley and Sharkey, 1992; Davis et al., 2014), simulator sickness (Kennedy et al., 1992; Hettinger and Haas, 2003), gaming sickness (Chen et al., 2016; Oldenburg, 2018), and virtual reality sickness (e.g., Guna et al., 2019; Saredakis et al., 2020). VIMS is a kind of MS predominantly brought on by stimulation of the visual system without actual physical movement, and it encompasses some of the above types of motion sickness (Keshavarz et al., 2014).

Cybersickness is an uncomfortable sensation comprising of nausea, fatigue, eyestrain, and disorientation resulting from exposure to immersive virtual reality environments, with display lags historically being a major contributor. According to Hill and Howarth (2000), Keshavarz et al. (2015), Reason and Brand (1975) and Rebenitsch & Owen (2016), cybersickness is caused by visually-induced illusory motion in an immersive VR environment, in which an optic flow provides motion information in the absence of corresponding vestibular signals. Cybersickness can be differentiated from other forms of motion sickness

using the Disorientation, Nausea and Oculomotor (D>N>O) symptom profile (Rebenitsch & Owen, 2016; Stanney et al., 1997). According to this profile, cybersickness is characterized by severe and frequent disorientation symptoms, followed by nausea symptoms, and least by oculomotor symptoms. Whereas simulator sickness has an O>N>D profile, seasickness is characterized by an N>O>D profile, and space sickness by an N>D>O profile (Rebenitsch and Owen, 2016; Stanney et al., 1997).

Many theories have been proposed to explain VIMS, such as those based on the role of postural control or eye movements (Riccio and Stoffregen, 1991; Ebenholtz et al., 1994), but the true etiopathogenic and the biological mechanisms underpinning VIMS are still unknown. According to the framework of sensory conflict theory, arguably the most widely acknowledged theory for the development of VIMS today (Reason and Brand, 1975), VIMS is brought on by the following: contradictory information from the visual, vestibular, and somatosensory senses or a mismatch between the arrangement of these three senses and what would be expected from prior experience. For instance, the vestibular and somatosensory senses communicate stasis, yet the visual stimulation in an immersive but stationary driving simulator may specify the self-motion of the driver. In certain situations (such as when there are not adequate adaptive mechanisms), this visual-vestibular conflict might cause VIMS.

Many VR applications use vection, an optic flow pattern that creates the illusion of self-motion. For instance, a VR driving simulator offers precise optic flow patterns of the road, buildings, and other environmental features, producing distinct vection sensations. The visual signals inform the user that they are travelling with a specific acceleration in a particular direction. However, because the user is not actively moving, the vestibular organs provide signals indicating there is no linear or angular acceleration. This sensory conflict results in VIMS because visual signals for self-motion are not supported by inertial forces communicated through the vestibular system (Keshavarz et al., 2015).

Positional trackers are a common feature of modern VR head-mounted displays (HMD), allowing users to walk around physically in the real world while exploring the virtual environment (Harsora et al., 2017). Visual cues are supported by vestibular information when moving about in VR, greatly reducing the conflict between the sensory modalities and, consequently, causing VIMS. However, vection is considerably stronger when users move their heads, possibly contributing to VIMS (Ash et al., 2011). Palmisano et al. (2022) proposed that large amplitude, time-varying patterns of differences in virtual and physical head pose caused by head movements and motion-to-photon-based display lag during HMD-based VR are the primary triggers for cybersickness.

2.5 MOTION SICKNESS MEASUREMENT

2.5.1 SUBJECTIVE MEASURES OF MOTION SICKNESS

Motion sickness evaluations have often been measured subjectively using clinical observation, interview methods and predefined questionnaires. Traditionally, subjective self-reports have been used to investigate the occurrence of motion sickness. The Simulator Sickness Questionnaire (see Figure 2.1) by Kennedy et al. (1993) is one of the most frequently used tools, and it is a 16-item questionnaire that assesses various symptom categories of MS, with responses given on a 4-point scale (i.e., none, slight, moderate and severe). This questionnaire divides symptoms of motion sickness into three main groups: nausea (N), which includes stomach awareness, increased salivation, and nausea itself. Disorientation (D) includes symptoms like dizziness, vertigo, and difficulty focusing, while Oculomotor (O) includes eyestrain, headache, and blurred vision. Based on previous studies, the highest Fast Motion Sickness rating reported during stimulus presentation has been found to strongly correlate with the SSQ (Keshavarz and Hecht, 2014; Peck et al., 2020).

The Motion Sickness Susceptibility Questionnaire (MSSQ) evaluates the number of times participants had previously experienced motion sickness when riding in automobiles, buses, coaches, trains, aeroplanes, small boats, ships (such as channel ferries), playground swings, playground roundabouts, big dippers, or other amusement park rides. Participants are given the options of not applicable/never travelled, never felt sick, seldom felt sick, occasionally felt sick, and frequently felt sick. The questionnaire is subdivided into two major sections: a section about MS experienced as a child and a second section about adulthood experiences in the past ten years. A raw score for the entire MSSQ scale can be derived and converted into percentile values based on the population norms listed in Golding (2006), and higher scores indicate a stronger susceptibility to motion sickness. This questionnaire was adopted for this thesis because of its usefulness in predicting the individual differences in motion sickness caused by various stimuli.

The Fast Motion Sickness(FMS) questionnaire (Keshavarz & Hecht, 2011) is a verbal questionnaire designed to specifically measure the nausea aspect of motion sickness (including stomach awareness and general discomfort). Its rating scale ranges from 0 (no sickness) to 20 (frank sickness). The FMS questionnaire allows for repeated, frequent assessment of motion sickness. It was selected as one of the preferred questionnaires for this thesis because it is easy to administer and records the time course of MS when applied frequently, for instance, every two minutes. Additionally, because it consists of only one question, it simplifies its repeated use during the experiment and overcomes the drawbacks associated with

many motion sickness questionnaires that are either too long or too complex to be utilized during an experiment.

No_____ Date_____

SIMULATOR SICKNESS QUESTIONNAIRE

Kennedy, Lane, Berbaum, & Lilienthal (1993)***

Instructions : Circle how much each symptom below is affecting you right now.

1. General discomfort	None	Slight	Moderate	Severe
2. Fatigue	None	Slight	Moderate	Severe
3. Headache	None	Slight	Moderate	Severe
4. Eye strain	None	Slight	Moderate	Severe
5. Difficulty focusing	None	Slight	Moderate	Severe
6. Salivation increasing	None	Slight	Moderate	Severe
7. Sweating	None	Slight	Moderate	Severe
8. Nausea	None	Slight	Moderate	Severe
9. Difficulty concentrating	None	Slight	Moderate	Severe
10. « Fullness of the Head »	None	Slight	Moderate	Severe
11. Blurred vision	None	Slight	Moderate	Severe
12. Dizziness with eyes open	None	Slight	Moderate	Severe
13. Dizziness with eyes closed	None	Slight	Moderate	Severe
14. *Vertigo	None	Slight	Moderate	Severe
15. **Stomach awareness	None	Slight	Moderate	Severe
16. Burping	None	Slight	Moderate	Severe

* Vertigo is experienced as loss of orientation with respect to vertical upright.

** Stomach awareness is usually used to indicate a feeling of discomfort which is just short of nausea.

Last version : March 2013

***Original version : Kennedy, R.S., Lane, N.E., Berbaum, K.S., & Lilienthal, M.G. (1993). Simulator Sickness Questionnaire: An enhanced method for quantifying simulator sickness. *International Journal of Aviation Psychology, 3*(3), 203-220.

Figure 2.1. Simulator Sickness Questionnaire (Figure borrowed from Kennedy et al., 1993)

Another type of questionnaire, the Misery Scale (MISC) rating scale (Bos et al. 2005), usually ranges from zero (0) to ten (10) (see Figure 2.2), and reliable estimates may be given as frequently as every 30 seconds. The scores on the scale represent varying degrees of motion sickness symptoms. A score of 1 indicates that the participant is experiencing uneasiness, while scores 2-5 represent varying symptom levels such as dizziness, warmth, headache, stomach awareness, or sweating. Scores 6-9 are assigned for varying degrees of nausea. A major drawback in its use is that querying participants with the MISC may impact other experimental task performance and sickness development due to increased retrospection.

Symptoms		MISC
No problems		0
Some discomfort, but no specific symptoms		1
Dizziness, cold/warm, headache,	Vague	2
stomach/throat awareness, sweating,	Little	3
blurred vision, yawning, burping,	Rather	4
tiredness, salivation, . . . but no nausea	Severe	5
	Little	6
Nausea	Rather	7
	Severe	8
	Retching	9
Vomiting		10

Figure 2.2. The Misery Scale (MISC) rating scale (Figure borrowed from Bos et al. 2005)

Pensacola Diagnostic Index (PDI) is one of the most popular questionnaires for evaluating motion sickness. Although researchers have widely used it for a long time, its major drawback is that it only produces a single score based on the combined intensity of the symptoms of nausea, headache, dizziness, warmth, and perspiration. These univariate PDI scores suggest that motion sickness is a construct that ranges along a single continuum, from a mild encounter to a severe one (Gianaros et al., 2001). Alternatively, it is possible to quantify motion sickness more accurately as a multidimensional construct with various symptom components using questionnaires like the SSQ.

All these questionnaires rely on individual interpretation and experience (Cain 2007); therefore, the repeatability and validity of subjective assessments are frequently questionable due to individual variances

in interpretation (Annett 2002; Cain 2007). Additionally, the results of these measurements do not adequately consider physiological mechanisms to allow for an accurate interpretation of the phenomenon of motion sickness. To avoid the subjective nature of self-report and to better link to mechanisms, many researchers have argued that there is a need for objective evaluation measures.

2.5.2 PHYSIOLOGICAL AND BEHAVIOURAL MEASURES OF MOTION SICKNESS

In contrast to subjective rating measures, psychological measurements promise an objective way to evaluate motion sickness by considering physiological and psychological processes. The selected physiological measures for this thesis are electrocardiogram (ECG) and cardiovascular measures such as heart rate and heart rate variability (HRV), Electrodermal activity (EDA), respiration, and participant body movement. These physiological measures were selected because they are frequently linked to psychological stressors like motion sickness (Chouk'er et al., 2010). Secondly, they best reflect some of the cardinal signs and symptoms of motion sickness (e.g., EDA for sweating; respiration; and body movement for general discomfort and fatigue), and thirdly, they are some of the more useful markers for classic motion sickness based on previous studies and more recent literature suggesting their relevance to car sickness (Irmak et al., 2021; Pham Xuan et al., 2021; Stoffregen et al., 2017).

SKIN CONDUCTANCE

Skin conductance on the palm and sole is associated with autonomic responses, anxiety and arousal. It involves measuring electrodermal skin conductance levels throughout the session and phasic changes (skin conductance responses) in response to significant driving events (accelerations and decelerations). Several studies have been conducted to measure electrodermal activity in motion sickness (e.g., Wan, Hu & Wang, 2003; Dahlman et al., 2009; Himi et al., 2004) because one of its primary symptoms is cold sweating (Lackner,2014). Hence, electrodermal activity has been researched extensively as a potential motion sickness correlate. Many studies (Hu et al., 1991; Warwick-Evans et al., 1987) demonstrated an increase in skin conductance level as motion sickness severity increased; however, other investigations were unable to detect a difference in skin conductance levels between participants who were motion-sick and those who were not (Dahlman et al., 2009; Smyth et al., 2021).

HEART RATE

The electrocardiogram (ECG) has been used to measure heart rate (e.g., Cowings and Toscano 1993; Holmes and Griffin 2001; Mullen et al. 1998) and heart rate variability (Holmes and Griffin 2001; Himi et al. 2004; Lin et al. 2011; Ohyama et al. 2007; Dahlman et al. 2009) in motion sickness studies. Several

studies have shown that car sickness is associated with increased heart rate, particularly during the early stages of exposure to motion sickness (Kennedy et al., 1992). One proposed mechanism for the increase in heart rate during car sickness is through activation of the autonomic nervous system, specifically the sympathetic nervous system. The sympathetic nervous system is responsible for the "fight or flight" response, which increases heart rate, among other physiological changes (Ohyama et al., 2007). According to Bos et al. (2008), motion sickness can cause an increase in heart rate, particularly in response to certain types of motion, such as pitch and roll, thus suggesting that the sympathetic nervous system may be involved in response to motion sickness. Similarly, Cowings et al. (1986) suggest that the activation of the sympathetic nervous system in response to sensory conflict can lead to increased heart rate and other symptoms of motion sickness.

The spectral analysis of heart rate variability examines the components of low-frequency (LF) and high-frequency (HF) power as well as the ratio of LF:HF power (or "autonomic balance"). For instance, Holmes & Griffin (2001) investigated the changes in both heart rate and heart rate variability before and after the onset of nausea. Participants in the study sat in an optokinetic drum (a visual stimulus), rotating at five revolutions per minute (rpm) for a maximum of 32 minutes. Heart rate variability, heart rate and motion sickness ratings were recorded both at rest before the exposure and during optokinetic stimulation. The analysis of variance (ANOVA) showed that HF power and LF:HF power varied significantly with the subjective ratings of sickness, while the Newman-Keuls tests showed that this result was typically attributable to decreasing HF power and increasing LF:HF power with increasing ratings of sickness. Pairwise comparisons showed that (1) HF power was lower at ratings four and six (“mild-moderate nausea” and “moderate nausea, want to stop”) than at ratings 0 (“no symptoms”), (2) LF:HF power ratio was higher at ratings 5 and 6 than at 0, and (3) there were no significant differences in LF power across rating levels (Holmes & Griffin, 2001).

RESPIRATION

Respiration physiology (RSP) has been used in past studies to measure motion sickness (e.g., Keshavarz et al., 2022; Kiryu et al., 2008; Kim et al., 2005). Existing studies suggest that the degree of respiratory synchronization with motion frequency could be a factor in the development of motion sickness (Denise et al., 2009). Sherwood (2006) found that the mechanical frequencies that cause motion sickness are interestingly within the range of natural breathing frequency (0.2-0.3 Hz), which raises the possibility of a connection between respiration and motion sickness. It has also been proposed that changes in breathing patterns may be a physiological response to the stress and discomfort associated with motion sickness and that these changes may exacerbate the symptoms of motion sickness. According to a study by Yen Pik Sang

et al. (2005), motion sickness can alter breathing patterns, particularly during the onset of symptoms. Similarly, a study by Rahimzadeh et al. (2023) found that breathing exercises can improve symptoms of motion sickness, suggesting that there may be a connection between respiration and motion sickness.

BRAIN ACTIVITY

According to Chen et al. (2010) and Schmäl (2013), the multimodal integration of sensory inputs of the brain appears to be a major factor in the development of motion sickness. The occipital cortex processes visual input, while the parietal integrate vision with proprioceptive and vestibular inputs. The integration and coordination of these different areas normally provide a precise and reliable perception of an individual's mobility relative to their environment (Schmäl, 2013). Electroencephalography (EEG) is the preferred technique for assessing cerebral activity in motion sickness (Chen et al., 2010; Naqvi et al., 2015) because of its portability, non-invasiveness and high temporal precision.

Several studies support the hypothesis that the severity of motion sickness symptoms is positively correlated with changes in cortical activity, as measured by EEG, in brain regions associated with vestibular processing and autonomic regulation. For instance, Lin et al. (2013) found that motion sickness induced changes in EEG spectral power in multiple frequency bands, increased delta and theta power in occipital and frontal regions, and decreased alpha and beta power in temporal and parietal regions. Moreover, these changes were more pronounced in individuals who reported higher motion sickness symptoms than those who did not. Another study by Chen et al. (2010) investigated the relationship between motion sickness severity and EEG coherence, a measure of functional connectivity between brain regions. The authors found that changes in EEG coherence between occipital and temporal regions and between frontal and temporal regions were positively correlated with motion sickness severity.

ELECTROOCULOGRAPHY (EOG)

In recent years, human-computer interaction (HCI) applications have employed EOG signals because they are simple to record and non-invasive using surface electrodes positioned around the eye. The EOG signal arises from the electrical potential difference between the eye's anterior and posterior poles, which changes orientation when the eye rotates (Banerjee et al., 2014). The magnitude of the EOG picked up at electrodes on the face changes approximately sinusoidally with the angle between the sensor plane and the gaze direction (Chakraborty et al., 2020). Thus, based on the small angle approximation of the sinusoid, there is a nearly linear association between eye movement and EOG amplitude for a modest range of eye movements (Banerjee et al., 2015). The EOG signal's amplitude typically ranges from 0.05 mV to 3.5 mV

per degree of eyeball rotation, with most of the relevant frequency domain energy ranging from 0.1 to 15 Hz (Banerjee et al., 2015; Erkaymaz et al., 2015).

One hypothesis explaining the relationship between increases in car motion sickness and eye movement is that the frequency and intensity of eye movements can exacerbate the sensory conflict that leads to motion sickness. According to Reason and Brand (1975), eye movements, such as those made while reading or looking at a screen, can increase the likelihood of experiencing motion sickness in a moving vehicle. This is because the eyes constantly shift focus and provide new visual information, which can cause a greater discrepancy between the visual and vestibular inputs to the brain. Similarly, Golding et al. (2003) suggest that increases in eye movement frequency, particularly in the horizontal plane, can lead to greater motion sickness susceptibility. Therefore, it can be hypothesized that as eye movement frequency and intensity increase, so too does the likelihood and severity of car motion sickness.

HEAD AND BODY MOVEMENT

Measures of sway magnitude during quiet stances, such as the velocity or positional variability of the head, torso, or centre of pressure, have been found to differ between individuals who are motion sick and those who are not (e.g., Bonnet et al., 2006, 2008; Stoffregen & Smart, 1998; Stoffregen et al., 2008; Villard et al., 2008). In addition to these effects, some studies have discovered disparities between the motion sick and healthy in the dynamics of postural activity as demonstrated by detrended fluctuation analysis (e.g., Dong et al., 2011; Stoffregen et al., 2010; Villard et al., 2008).

MULTIVARIATE MEASURES

Numerous studies have measured multiple independent objective and subjective metrics of motion sickness (see Table 2.1). For instance, Irmak, Pool and Happee (2021) investigated the objective and subjective responses to motion sickness in individuals and groups. They simulated the temporal evolution of motion sickness using a very dynamic sickening drive and discovered that motion sickness did not significantly impact head roll. Also, motion sickness and time both caused a small electrocardiogram (ECG) variation. Furthermore, Electrodermal Activity (EDA) varied with motion sickness, especially where the tonic and phasic EDA increased by 42.5 percent and 90 percent over baseline at high Misery scale (MISC) levels, respectively. Complicating its use as a motion sickness marker, EDA also increased with time independently of motion sickness, accompanied by significant dispersion.

Table 2.1. Sample Related Studies on Motion Sickness Measurement

Author	**Stimuli**	**Measurement**	**Participants**
Keshavarz et al. (2022)	Projector: First-person viewpoint video	Electrodermal Activity, Electrocardiogram, Electrogastrogram, Body temperature, Facial skin Temperature, Respiration, Body Movement, SSQ,	56
Henry et al. (2022)	Car: Driving	Electroencephalography	9
Irmak et al. (2021)	Car: Driving	MISC scale, Head roll, Galvanic Skin Response (GSR), and electrocardiography (ECG)	24
Chuang et al. (2016)	Projector(Simulator): Driving	Motor, parietal, occipital alpha, gamma, MSSQ	19
Malinska et al. (2015)	HMD: Virtual Work Station	Heart Rate, Autonomic Balance (LF, HF)	19
Nalivaiko et al. (2015)	HMD: Rollercoaster	Temperature, Heart Rate, MSSQ	26
Zuzewicz et al. (2011)	Head-Mounted Display (HMD) Simulator: Forklift	Heart Rate, Autonomic Balance (LF, HF)	24
Kiryu et al. (2008)	First-person viewpoint video	Autonomic balance (LF, HF), Respiration (RR, HF, RSA), Blood pressure (LF), SSQ	27
Kim et al. (2005)	Projector : 3D Virtual Environment	Heart Rate, Temperature, Skin Conductance, Respiration (RR, HF, RSA), gastric tachyarrhythmia, F3, T3—delta, F3—slow Beta, T3—beta, Eye Blink	61

Additionally, several studies have attempted to establish a psychophysiological connection between an individual's subjective experience of MS and physiological parameters, with conflicting and inconclusive results (Bertin et al., 2005; Crampton, 1990; Dahlman et al.,2009; Money, 1970; Ohyama et al., 2007; Otto et al., 2006). For example, some studies have shown a weak to moderate correlation between MS and gastric activity (Cheung and Vaitkus, 1998; Muth et al., 1996), heart rate (Cowings et al., 1986), electrodermal activity (Golding, 1992; Warwick-Evans et al., 1987) and respiration rate (Kim et al., 2005).

However, we know of no clear and unambiguous pattern of physiological measurements unique to car sickness.

In a recent study, Keshavarz et al. (2022) investigated the possibility of detecting and predicting the severity of visually-induced motion sickness (VIMS) in real-time, using a random forest analysis in conjunction with physiological measures like ECG, EDA, electrogastrogram (EGG), respiration, body and skin temperature, and body movement. The study involved showing a 15-minute VIMS-inducing video to forty-three (43) participants. The Simulator Sickness Questionnaire (SSQ) and the Fast Motion Sickness (FMS) Scale were used to measure the subjective severity of VIMS. According to the findings, variations in facial skin temperature and body movement had the strongest correlation with VIMS. Also, ML models showed a medium correlation between the physiological measures (ECG, EDA, EGG, respiration) and the FMS scores on a one-minute basis. They concluded that although physiological measures may be beneficial for measuring VIMS, they are not a reliable stand-alone approach to detecting or predicting the severity of VIMS in real-time.

Li et al. (2022) explored the multi-dimensional and objective assessment of motion sickness severity using several ML techniques: support vector machine (SVM), random forest (RF), K-nearest neighbour (KNN), and multilayer perceptron (MLP). The study involved inducing motion sickness in 51 participants using a Coriolis acceleration stimulus. The results showed that the severity of motion sickness is associated with increasing levels of gastric electrical activity, facial skin tone, skin temperature, and nystagmus. Also, based on these factors, the support vector machine classifier exhibited the best performance among the ML assessment models, with an accuracy of 88.24 percent, a sensitivity of 91.43 percent, and a specificity of 81.25 percent. Pham Xuan et al. (2021) described a methodology to identify changes in facial skin temperatures in a real-driving study. It involved adjusting commonly available techniques to meet the requirements of in-car recording and objectively estimating variations in facial temperature caused by car motion sickness. They concluded that detecting variations in facial skin temperature using thermal infrared imaging while driving is challenging.

Stoffregen et al. (2017) investigated the relationship between users' experience driving real automobiles and motion sickness when driving virtual automobiles. The study revealed that drivers with approximately 30 years of driving experience became motion sick more rapidly than non-drivers or drivers with less than 15 years of experience driving virtual automobiles. However, the driving experience did not affect the frequency or intensity of motion sickness during virtual driving. Different movement patterns were observed depending on the driver's driving experience. Participants who later experienced motion sickness moved differently from those who did not. Specifically, positional variability of the head and torso in the

AP and ML axes was greater among non-drivers than drivers, meaning that approximately 30 years of driving experience reduced the spatial magnitude of body movement during virtual driving. Most importantly, patterns of postural activity that occurred during the virtual drive and before the onset of motion sickness were influenced by the physical driving experience. Their findings support the postural instability theory of motion sickness and provide insight into the connections between real and virtual vehicle driving controls.

Dennison et al. (2016) exposed 20 participants to a virtual environment and assessed their level of MS using the Simulator Sickness Questionnaire and a subjective rating scale. They collected a range of physiological measures such as electrocardiograms, electrogastrograms, electrooculograms, pulse oximeter readings, respiration, and electrodermal activity (EDA). They found the strongest correlation with the EGG measures at r = -0.335, and linear regressions revealed that physiological measures could only account for about 10% of the total variance in the SSQ nausea data. Also, correlations between the SSQ nausea subscale and all physiological measures were weak to moderate and not statistically significant.

More recently, deep learning and machine learning (ML) approaches have been suggested as a viable way to understand better the connection between physiological changes and the subjective experience of visually-induced motion sickness (Tauscher et al., 2020). For instance, Li et al. (2019) demonstrated that based on measurements of Electroencephalography (EEG), postural sway, and head and waist motion tracking, it was possible to classify users in a VR application as sick or non-sick with a high accuracy rate. Similarly, Recenti et al. (2021) classified their participants post hoc as sick or not sick by combining EEG with postural sway. However, neither study examined whether ML approaches accurately estimate VIMS severity during stimulus presentation or the ability to identify the onset of symptoms quickly and reliably.

2.6 LITERATURE REVIEW SUMMARY

No recent study that the researcher is aware of has investigated how machine-learning techniques can be used to detect patterns derived from multiple physiological measures that are diagnostic and predictive of an episode of car sickness. Although existing studies have identified a plethora of independent objective metrics of motion sickness, it is unknown what the precise relationships are between these measures. Additionally, while studies relating motion sickness with physiological measures exist, most recent work has focused on VIMS. However, these have not been validated for car sickness, especially device usage in a car. Therefore, this thesis aims to bridge this research gap by investigating the correlation between several independent objective measures of motion sickness in the context of reading in a car and developing a

model that connects these objective measures to predict motion sickness from a combination of these signals.

The outcome will be a better understanding of motion sickness symptoms' likelihood and potential impact during device use in various automotive scenarios based on so-called "objective measures". The measurement of postural instability, specifically the head/body movement, is motivated by the important theoretical role of this construct in the seasickness and airsickness literature. Evaluating the head/body movement was an important subgoal of this project as it is unclear how well this transfers to car sickness and how to measure it in a seated individual best. The specific goals of this research include using quantitative analysis and machine learning (ML) approaches to, firstly, detect and identify changes in physiological and behavioural measures linked to the onset of car sickness and, secondly, serve as foundational research towards categorization of participants as sick or not sick based on physiological and behavioural measures using real-time estimates.

CHAPTER THREE – METHODOLOGY

3.1 STIMULUS

3.1.1 APPARATUS (HARDWARE AND SOFTWARE)

The experiment involved simulated driving using a limited motion-base, left-hand drive, traffic driving simulator with three (3) mechanical degrees of freedom (heave, roll, pitch), as shown in Table 3.1. The SCANeR® studio simulator software (SCANeR, 2022) was installed on a desktop server with Microsoft Windows Professional operating system (version 10.0.19042, build 19042), 64GB memory and model HP Z1 G8 tower. The simulator software controlled the motion-base driving simulator and was used to create the road geometry, landscape and traffic scenario. It affords a graphical environment that includes modules for vehicle dynamics, sensor models, data recording, configuring, preparing, running simulations and analyzing results. For these experiments, the visual displays were turned off.

This software could also replicate vehicle dynamics and induce motion sickness sensations like on a real road. Kuiper et al. (2019) argue that motion-base simulators can elicit car sickness for research purposes using a lateral sinusoidal motion at 0.2 Hz if visual-induced simulator sickness is avoided. As the focus here is reading from a mobile device during car rides, it was possible to accomplish this. Consequently, a rotation on the pitch axis at a frequency of 0.2 Hz was adopted for the base of the driving simulator during the main test as it was confirmed to elicit adequate motion sickness levels during pilot testing. The pitch axis was in the simulator base below the participant's feet, and therefore the stimulus included forward/backward and up/down translation as the head pitched. The pitch axis was in the simulator base below the participant's feet, and therefore the stimulus included forward/backward and up/down translation as the head pitched. There was minimal lighting to aid movement around the room, and the simulated car cabin was dimly visible. The simulator cabin/room temperature was also controlled and monitored at 24 degrees Celsius.

Table 3.1: Limits for the degree of freedom of the motion-base simulator

	Vertical Axis (Metres)	Roll (Radian)	Pitch (Radian)
Minimum	-0.0381	-0.066279	-0.063048
Maximum	0.0381	0.066279	0.063048

The Biosignalplux™ signal acquisition system with multiple sensors and the Muse™ S (Gen 2) model Headset were adopted for the real-time data collection of the physiological and behavioural measures. These devices can also save the data collected in Comma Separated Value (CSV) files at the end of the experiment

sessions for subsequent statistical analysis. The data analyses involved using MATLAB, EEGLAB software tools, and Python programming language. The reading task was presented using a 10-inch Huawei Mobile device with an Android Operating system.

3.1.2 PROCEDURE

Before starting the experiment, participants sat with sensors attached for about ten minutes to acclimatize and stabilize the electrode interfaces after providing informed consent and demographic information, and the experiment was explained. After that, the initial response from the Simulator Sickness Questionnaire (SSQ) shown in Figure 2.1 was recorded before the participants were directed to sit in the motion-base simulator. This pre-exposure SSQ helped to ensure that participants were not already motion sick before the experiment and were aware of the subjective symptoms of motion sickness, thus providing a baseline against which to compare post-exposure results.

Following checks of biosignal integrity, the experiment commenced with an eye-tracking calibration procedure to support subsequent analysis of the EOG data. The calibration was necessary because eye movements are measured in degrees while the EOG electrode signals are in volts. Therefore, a calibration curve is necessary to determine the relationship between the amplitude of the recorded voltage and the actual eye movements generated by participants. The calibration session involved participants sitting 55 cm away from a target box with six equidistant markers; each spaced 4.1 cm apart in a cross pattern. Then, participants were asked to fixate on each of the six markers for 30 seconds by moving their eyes to the left-center-right and up-center-down positions of the markers. The eye movements were recorded using an EOG sensor at a frequency of 300 Hz

The motion-base simulator was started, and participants experienced a dynamically controlled sinusoidal oscillation while accomplishing a Non-Driving Related Task (NDRT) on a mobile device's screen or while performing no task. The NDRT task involved reading comprehension passages (Borojeni et al., 2018) on a mobile device with recall questions to ensure the participants were attending to the task. This task was chosen due to its cognitive similarity to reading, writing text messages, or conversing, which are expected tasks in an automated driving context. Participants were required to read comprehension passages and answer some follow-up questions related to the comprehension passages to ensure they were attending to the reading task. The no-task condition simulated a normal passenger experience with no task to perform; participants were required to look straight ahead without focusing on any particular object, thus affording

the participants the flexibility to look at any object within their frontal view while maintaining a standard posture with their feet on the floor.

The automatically simulated car drive lasted 20 minutes for each Task condition, with a ten-minute break between the conditions to allow any motion sickness symptoms from the first condition to wear off before the onset of the second condition. However, participants were permitted to stop if they experienced motion sickness symptoms that necessitated stopping. During the ride, objective measures such as electroencephalogram (EEG), electrocardiogram (ECG), electrooculogram (EOG) and Electrodermal activity (EDA), respiration and behavioural measures such as head/body movement, were recorded and analyzed.

Participants were asked to verbally rate their current motion sickness status every two minutes during the session using a Fast Motion Sickness (FMS) questionnaire with prompts administered as an audio recording via the sound module of the motion-base simulator server. The FMS questionnaire was necessary to assess the incidence and degree of car motion sickness. It is a verbal rating scale ranging from 0 (no sickness) to 20 (frank sickness) and focuses on subjects' general discomfort, nausea, and stomach problems (Keshavarz & Hecht, 2011). Participants were instructed to base their ratings on relevant symptoms like nausea, general discomfort and stomach problems but ignore likely distorting effects such as nervousness, boredom or fatigue.

Participants' incidence and severity of motion sickness using the SSQ were evaluated multiple times. In addition to the pre-exposure SSQ administered at the beginning of the experiments, participants were also required to give detailed feedback on their motion sickness status using the SSQ at the end of each simulated drive. According to Kennedy et al. (1993), simulator sickness differs significantly from motion sickness (MS) because it is less severe and affects a smaller portion of the exposed population. Therefore, researchers often eliminate from the SS analyses the MS symptoms reported less infrequently or showing no changes in frequency or severity reported before and after simulator exposure leaving sixteen (16) symptoms grouped into three subscales: oculomotor (O), disorientation (D) and nausea (N). The subscale analysis of the SSQ is necessary to confirm that participants experienced car sickness symptomology rather than simulator sickness (SS) as symptoms in the nausea (N) subscale, such as general discomfort, stomach awareness and increased salivation, should be dominant.

3.1.3 DESIGN

The experiment was fully within subjects with the following NDRT task as the independent variable with two levels:

- No task
- Reading Task

The NDRT variable was necessary to ensure adequate data collection and to elicit a suitable range of car sickness. The independent variable was assigned alternately with twenty (20) participants per order to counterbalance and control for sequence or order effects.

The dependent variables in this experiment were (1) the repeated FMS and SSQ responses, (2) the physiological and behavioural time-series measures: electroencephalogram (EEG), electrocardiogram (ECG), respiration (RIP), electrooculogram (EOG), electrodermal activity (EDA), and head movement, and (3) the measured platform motion profile.

3.2 PARTICIPANTS

A non-probabilistic sampling method, specifically convenience sampling, was used in sourcing the research population because of its ease and availability of research volunteers. The study entailed a simulated driving scenario, and a pilot test was conducted before the main experiment. The pilot test was necessary to assist the researcher in exploring and analyzing various physiological measures in order to adopt the most suitable subset for the project based on the outcome of the pilot studies. Ten Huawei employees were recruited for the pilot experiments.

The main study involved 40 participants, comprising 20 male and 20 female participants recruited from the broader York Community. The researcher had no previous relationship with the participants in the main experiments. Participants in the main study were required to confirm normal or corrected to normal vision using contact lenses or eyeglasses because of the reading task. The study was designed in accordance with common ethical research principles and approved by York University's Research Ethics Board. All participants provided written consent before the commencement of the study. Participants were also informed about their rights to withdraw from the study at any time without negative consequences. A $25 compensation was given to the participants to reimburse them for their time commitment and travel to the study. As part of the demographic information collected, the participants' susceptibility to car sickness was assessed based on their self-evaluated subjective ratings using the Motion Sickness Susceptibility Questionnaire-Short (Golding, 1998).

3.3 PHYSIOLOGICAL MEASURES

The physiological data of the participants were recorded using a number of sensors. The Biosignalsplux™ sensor was used to measure the Respiration, EOG and EDA, while the Muse™ Headset was used to record

the EEG and head movement. The Biosignalsplux® is a multi-sensor device designed for biosignal acquisitions at a selectable sampling frequency ranging from 300Hz to 1000Hz. It can collect and digitize biosignals, transmit them via Bluetooth® and is integrated with OpenSignals®, an easy-to-use, versatile software useful for real-time biosignals data recording and visualization.

ELECTROCARDIOGRAM (ECG)

The ECG activity was recorded using three gelled self-adhesive Ag/AgCl electrodes placed on the participant's body using BiosignalPlux's recommended configuration. The Biosignalsplux ECG is a triode configuration primarily designed to acquire single-lead ECG data using the Einthoven configuration (see Figure 3.1), which allows the positioning of the electrode cables using three different ECG leads. Lead I was positioned to measure from the right arm (RA) to the left arm (LA), Lead II measured from the RA to the left foot (LF), and Lead III measured from the LA to the LF. The electrodes were placed under the right clavicle, left clavicle, and below the left rib cage. The ECG signal was then used to calculate heart rate (HR) in beats per minute (BPM) and HRV parameters, including the RR interval (RR-I), root mean square of successive differences (RMSSD), and percentage of adjacent RR-I's that differ by more than 50 ms (pNN50). RR-I represents the time between consecutive heartbeats in the ECG waveform. RMSSD reflects the beat-to-beat variance in HR, while pNN50 is a common metric used to measure short-term variability within the RR-I series during stimulus exposure. A multi-epoch statistical analysis was performed to extract time-domain measures of HRV.

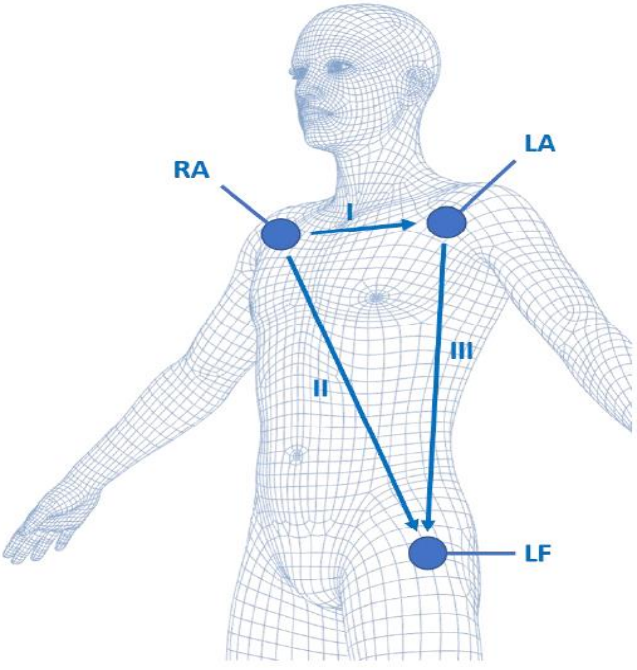

Figure 3.1: Electrode placements for ECG acquisitions in Einthoven configurations using the standard ECG sensor (Figure borrowed from Biosignalplux™, 2022)

ELECTROOCULOGRAPHY (EOG)

The Electrooculography (EOG) sensor by PLUX is bipolar with two measurement electrodes that can be used to detect electrical potentials in the chosen temporal or facial region relative to a reference electrode placed in an area of low bioelectrical activity (see Figure 3.2). As the difference between these two leads is amplified, the resulting signal eliminates any common unwanted signals. The electrodes of the EOG sensor were positioned, as illustrated in Figure 3.2, to measure horizontal eye movements. This positioning allows the measurement of conjugate eye movements (yoked movements of the left and right eyes), where horizontal eye movement to the left triggers a positive peak, and horizontal eye movement to the right triggers a negative peak. The electrode amplifier was AC coupled, and therefore constant signals during fixation drifted back to 0 V; as a result, the changes in potential at each fixation were used for calibration rather than steady-state levels. The electrodes were arranged to record horizontal eye movements, and calibration was based on the horizontally-spaced targets. The vertical calibration targets and fixations were used to ensure there was minimal cross-coupling of vertical eye movements.

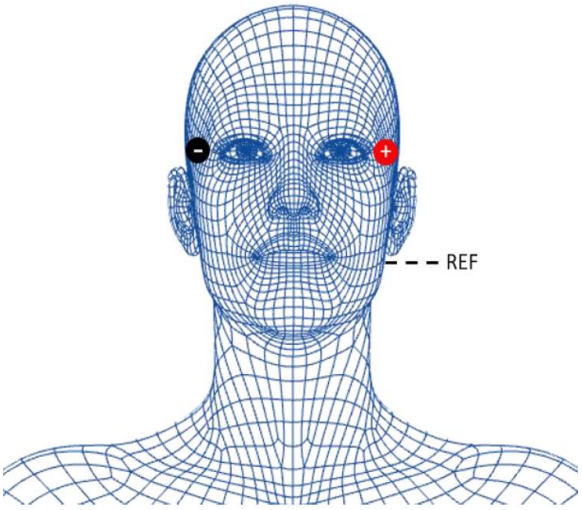

Figure 3.2. Placement of the EOG sensor electrodes to measure horizontal eye movements. (Figure borrowed from Biosignalplux™, 2022)

RESPIRATION

Respiration patterns were measured using an inductive respiration sensor from PLUX. The sensor is embedded in an adjustable nylon fabric belt, spanning the entire chest length. The belt was placed around 5 cm below the participant's underarm at the maximum respiratory expansion level. The RIP sensor measures the overall displacement of the thorax or abdomen, making it less susceptible to motion-induced artifacts. The elastic strap can be adjusted in length to accommodate different anatomies and body locations. According to Ambekar and Prabhu (2015), healthy adults typically have a resting respiration rate of between

12 and 18 breaths per minute. However, the respiratory rate has been found to increase during MS symptoms, such as nausea (Javaid et al., 2019).

ELECTRODERMAL ACTIVITY (EDA)

Two gelled self-adhesive Ag/AgCl surface electrodes (model EL507) were placed on the participant's non-dominant hand's middle finger (ground electrode) and index finger (active electrode) to measure the EDA. The emphasis is on observing changes in skin conductance level (SCL) to reflect stable modifications in skin conductance that can be noticed over time. Typically, SCL activity ranges from two micro siemens (2μS) to 20μS (Dawson et al., 2007).

ELECTROENCEPHALOGRAM (EEG)

The Muse™ Headband was employed to measure the electroencephalogram (EEG). The Muse™ Headband is a wearable wireless device with five dry electrodes located at AF7, AF8, TP9, TP10 and AUXR with a sampling frequency of 256 Hz. These electrodes are roughly equivalent to the analogous electrodes in the 10-20 International electrode system (Krigolson et al., 2017, Wilkinson et al., 2020, Chan et al., 2021) and correspond to placements behind the left ear, on the left and right forehead, behind the right ear and a right auxiliary, respectively. The Muse™ headband was chosen for measuring EEG because it is a commercially available EEG device with the fewest electrodes, as any real application will be limited in the number of placement electrodes incorporated into a wearable device.

The Muse headband was fully charged before its use for most recording sessions, and participants' skin was cleaned to remove dirt or the buildup of natural oils on the skin. A thin layer of water was applied to the dry electrodes of the Muse™ Headband using a cotton ball for both the frontal metallic sensors and the conductive silicone rubber mastoid sensors located behind the ears to improve signal quality and reduce impedance. Also, its fit was tightened or loosened as required based on the size of the participant's head while ensuring there was no hair between the sensors and the skin, especially behind the ears. In addition, participants were made to wear the headband about three minutes before starting the experiment to ensure the signals settled into a consistent state.

The Muse™ also has an onboard digital signal processing (DSP) module capable of noise filtering and integrates with the MindMonitor™ software installed on an iPhone 13 device with iOS (iPhone Operating System) version 16 for data recording. In addition to data recording, the Mindmonitor app allowed checking of electrode contact where a fully coloured circle on the horseshoe display denoted a good and acceptable

level of electrode connectivity with the skin. A visual inspection of the raw EEG waveforms was also performed, and the headset was re-adjusted if the signal was too noisy.

3.4 BEHAVIOURAL MEASURES

HEAD AND BODY MOVEMENT

In addition to using the Muse™ Headband to measure EEG, the head movement of the participant was recorded using the Muse™ inertial sensors consisting of the triaxial accelerometer and gyroscope sampled at 256 Hz. The measurement of head motion was motivated by the significant theoretical role of postural stability in the literature on airsickness and seasickness. Therefore evaluating this was a crucial subgoal of this project because it is unclear how well it applies to car sickness.

3.5 SUBJECTIVE MEASURES

Two questionnaire methods were used to measure motion sickness before, during, and after each condition. The first method involved participants rating their level of MS every two minutes using the Fast Motion Sickness Scale (FMS). The second method involved using the standardized Simulator Sickness Questionnaire (SSQ) before each of the conditions and after the last condition (see section 2.5.1).

3.6 DATA PREPROCESSING

All the physiological signals except the EEG were collected at a sampling rate of 300 Hz and preprocessed using Biosppy libraries in Python. In contrast, the EEG was collected at a sampling rate of 256 Hz and preprocessed using Matlab and EEGLAB. The raw digital sensor readings from the Biosignalsplux device corresponding to the EOG and EDA were converted to the appropriate units using relevant conversion factors. Specifically, the raw EDA signals were converted to microsiemens before further processing using the Biosspy libraries, while the EOG signals were converted to millivolts. Subsequently, large artifacts in the raw signal, such as noise spikes or equipment failures that deviated from the median by at least three times the interquartile range, were considered outliers and corrected by interpolating values to replace the artifacts in the respective channel(s).

A Butterworth low-pass digital filter with a cutoff of 5 Hz was applied to the EDA channel to remove high-frequency noise, while for the respiration signals, a Butterworth bandpass filter with a lower frequency of 0.1Hz and higher frequency of 0.35Hz was applied to filter the signal. For the ECG signals, a Finite Impulse Response (FIR) bandpass filter set at 45Hz with a lower cutoff limit of 3Hz was applied to correct for baseline drift and movement in the ECG signal. Analyses were conducted for each physiological measure

to extract relevant features such as the mean and standard deviation to observe changes over time within the sample. For the EOG data, a lowpass Butterworth filter was employed to remove noise, then artifacts such as blinks were removed using visual inspection techniques before applying each participant's calibration values to convert the signals from millivolts to angular degrees.

Perhaps, one of the greatest difficulties faced during this study was in setting up participants with the MUSE™ Headband for data collection. The EEG, including accelerometer and gyroscope data for head/body movement, was recorded using the Muse™. It was not easy obtaining adequate data quality from the MUSE™ headband, and this difficulty was largely due to insufficient connection between the participants' heads with the respective electrodes' scalp locations on the headband. Specifically, certain head shapes, head sizes and hairstyles made data collection quite difficult despite gaining adequate expertise with the MUSE headband during the pilot tests. Data was streamed from the Muse headband directly to the Mindmonitor application via Bluetooth connection and at a sampling frequency of 256 Hz. The EEGLAB was employed for the pre-processing of the EEG data. Firstly, excessively noisy or faulty electrodes were removed, then eye movement artifacts were removed using visual inspection techniques and corrected using independent component analysis before employing high-pass filtering. Subsequently, a second round of semi-automated and visual inspection-based rejection of bad data segments on the derived components was performed before a second ICA (Delorme and Makeig, 2004; Luck, 2014).

The accelerometer and gyroscope data were extracted from the original Muse CSV files containing the EEG data by selecting the relevant columns: Accelerometer_X, Accelerometer_Y, Accelerometer_Z, Gyro_X, Gyro_Y and Gyro_Z using Python libraries. Subsequently, relevant statistical features such as the standard deviation were extracted from the data.

CHAPTER FOUR – RESULTS

4.1 INTRODUCTION

This chapter is organized into six major sections, with section 4.2 describing the reading task performance and section 4.3 reviewing the driving simulator vehicle's dynamics data and conformance with the desired motion profiles. Subsequently, the experimental results and analysis for the physiological, behavioural and subjective measures, including the correlation between these measures, are provided in sections 4.3 to 4.6. Thereafter, the development and performance of machine learning models predicting car sickness are presented in section 4.7.

4.2 TASK PERFORMANCE AND RELATION TO CAR SICKNESS

The study recruited 40 participants (female=20 and male=20) with a mean age of 29.38 years (SD = 8.80). The experiment involved two different conditions: a Non-Driving Related Task (NDRT), which involved reading on a mobile device's screen, and a no-task condition. The reading task yielded a higher FMS rating (M = 4.34) in comparison with the no-task (M= 4.09, see Figure 4.1). However, this effect was not statistically significant ($F_{1,38}$ = 0.258, p = .615). Also, the effect of the group on the FMS ratings was not statistically significant ($F_{1,38}$ = 0.590, p = .447), which means that counterbalancing of the conditions worked and had the desired result of offsetting the task order effect. Finally, the task x group interaction effect was not statistically significant ($F_{1,38}$ = 2.581, p = .116).

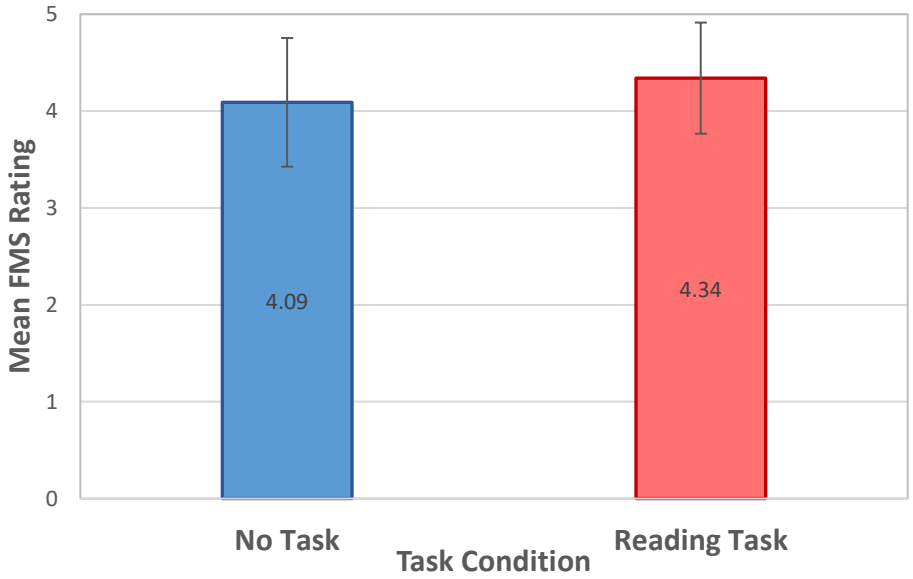

Figure 4.1. Results of Mean FMS Rating versus Task Condition. Error bars show ± 1 standard error of the mean (*SEM)*.

4.3 VEHICLE MOTION

The specified profile for the motion base simulator for this experiment was 0.2 Hz peak-to-peak sinusoidal motion in pitch. To confirm the motion profile moved at a frequency of 0.2 Hz in the pitch axis, the Muse™ Headset was strapped to the seat of the motion-base driving simulator during a sample drive with no participant to record the actual vehicular motion. In Figure 4.2, the raw and noisy Muse™ gyroscope data representing the movement of the motion-base platform in the pitch axis is presented alongside the heavily filtered version processed using a cut-off frequency of 0.5 Hz.

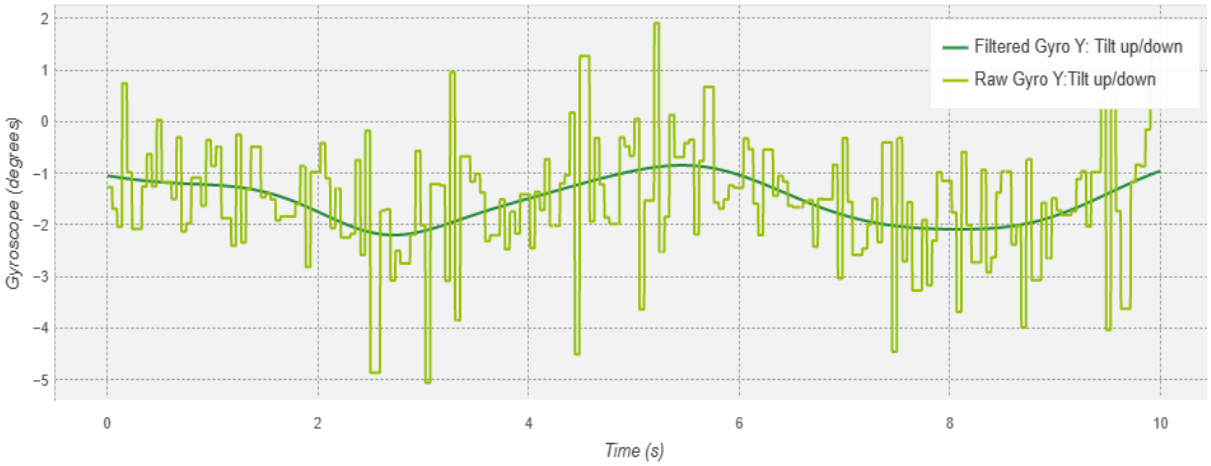

Figure 4.2. Motion simulator vehicle dynamics measured using an IMU.

4.4 SUBJECTIVE MEASURES

The stimulus was provocative in eliciting motion sickness symptoms: 31 participants reported FMS ratings of 4 and above (see Figures 4.3 a-c), while 29 participants had an SSQ nausea subscale score of 20 or higher across the second and third simulator sickness questionnaires (see Figures 4.4a and 4.4b). Five participants recorded a total score of 20 or higher for the first simulator sickness questionnaire. Using a combination of the peak FMS ratings and the SSQ nausea subscale score, participants who reported a peak FMS score of 4 or higher and an SSQ nausea score of 20 or higher across the second and third simulator sickness questionnaires were classified as motion sick. Consequently, of the 40 participants, 29 were classified as motion sick (72.5%), while 11 were classified as not motion sick (27.5%). The distribution of the peak FMS ratings over the course of the experiment is presented in Figure 4.3a. On average, the self-reported sickness levels increased with exposure time for both conditions. Additional charts showing the FMS ratings of the 40 participants as measured every two minutes using the FMS questionnaire for each task condition are available in the Appendix section and show this was generally true for individual participants as well, although there is considerable intersubject variation in reported sickness (See Appendices A, B and C).

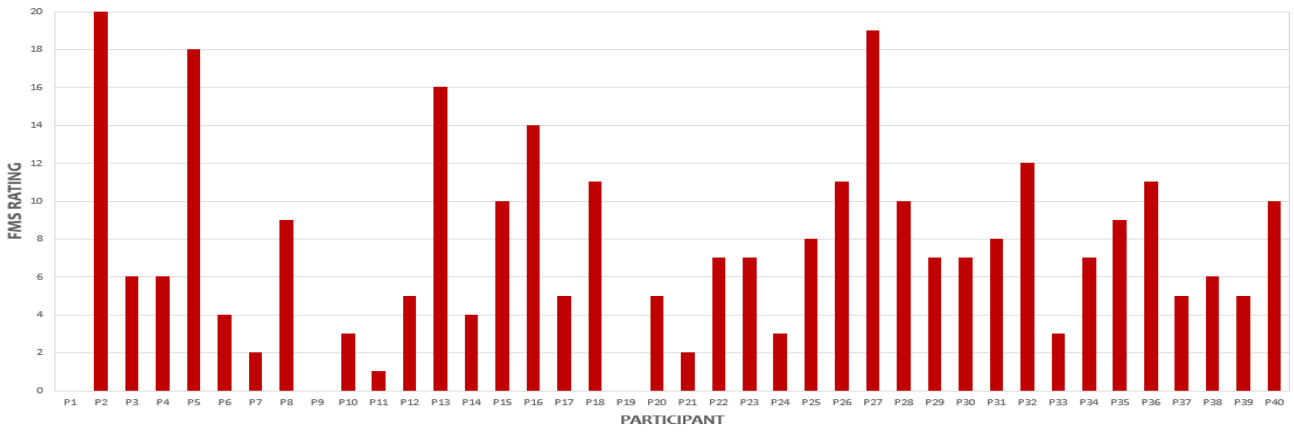

Figure 4.3 a. Highest FMS Rating per participant

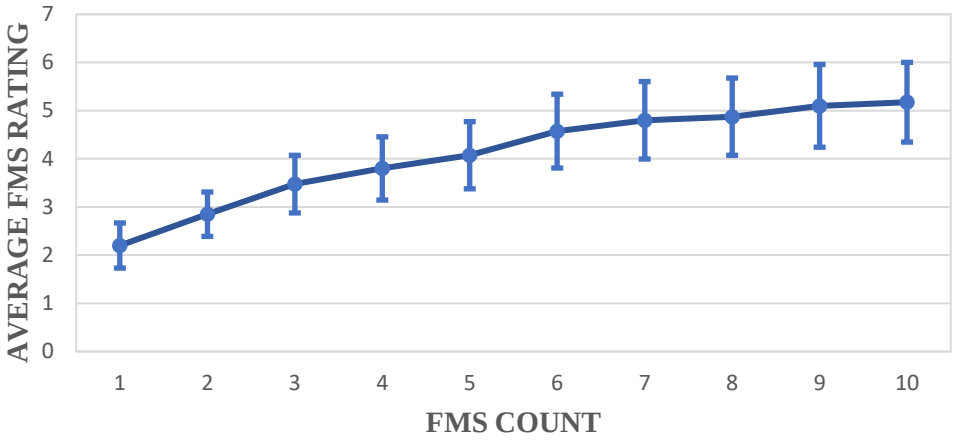

Figure 4.3 b. Average FMS Rating per FMS count for Condition 1. Error bars show ± 1 *SEM*

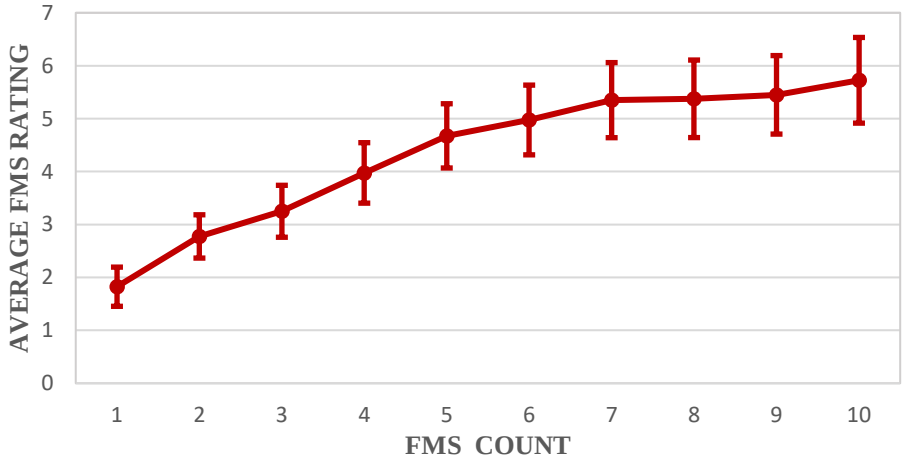

Figure 4.3 c. Average FMS Rating per FMS count for Condition 1. Error bars show ± 1 *SEM*

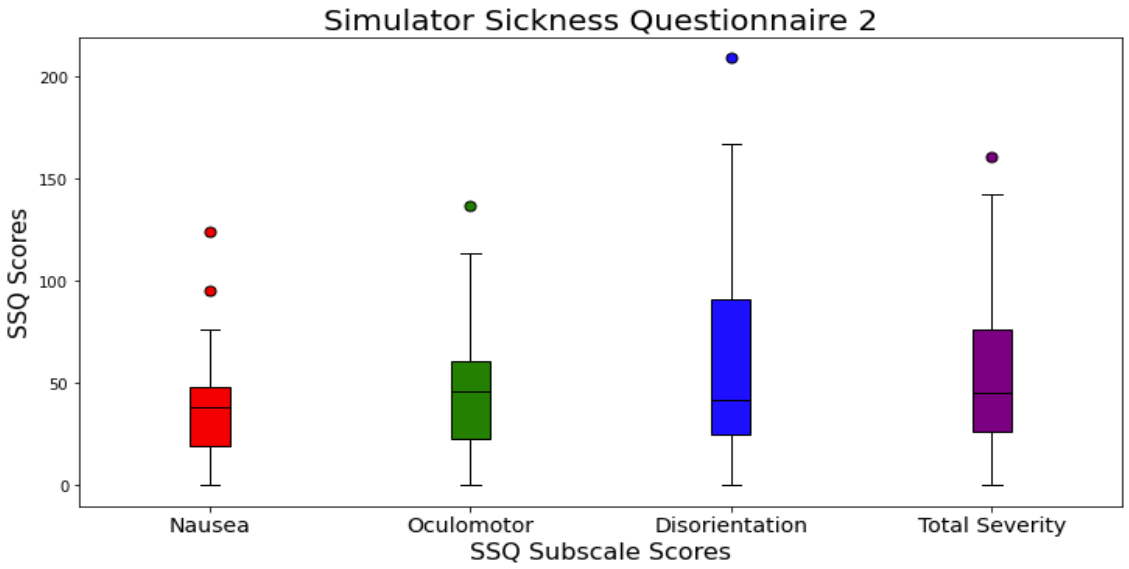

Figure 4.4 a. Simulator sickness questionnaire 2 (SSQ2) subscale scores for all participants. The Box-and-Whisker Plot includes these parts: the mean (denoted by a square), the median (denoted by a horizontal bar in the box), the 25th percentile (denoted by the bottom edge of the box), the 75th percentile (denoted by the top edge of the box), the 5th percentile (denoted by the bottom edge of the whisker), the 95th percentile (denoted by the top edge of the whisker), and the dots denote the data distribution.

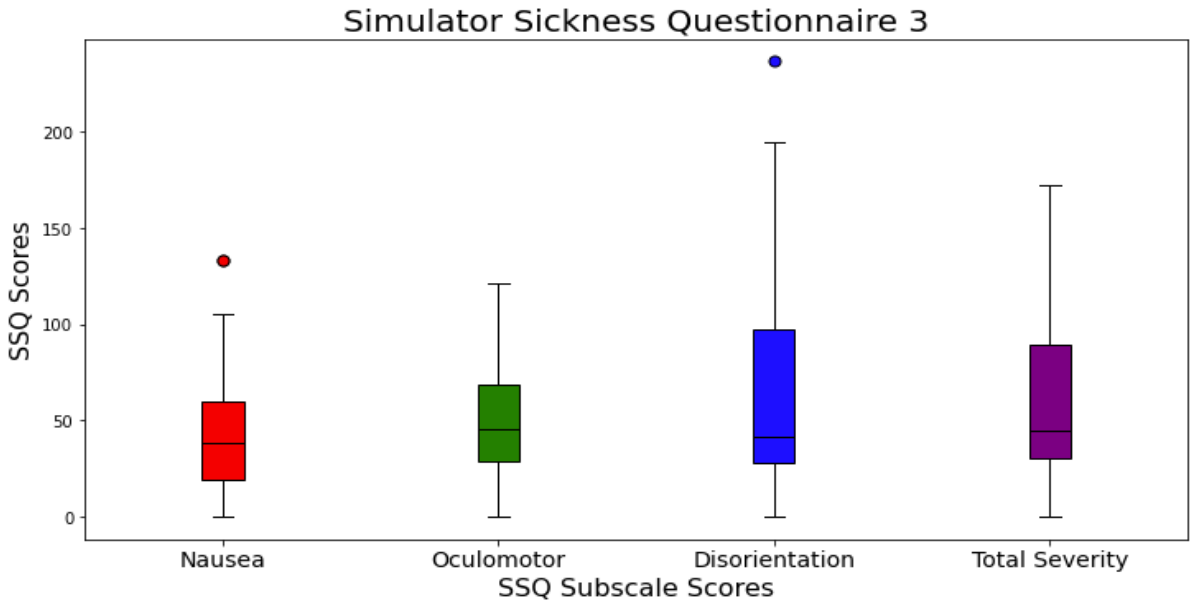

Figure 4.4 b. Simulator sickness questionnaire 3 (SSQ3) subscale scores for all participants.

4.4.1 CORRELATIONS FOR SUBJECTIVE MEASURES

Pearson's correlations were calculated to explore the relationship between the SSQ subscales, the SSQ total score, the FMS score and the MSSQ scores (see Figures 4.5a and b). The strongest correlations with the

FMS score were with the third SSQ nausea subscale score (r = 0.85) and the total score (r = 0.80), as shown in Figure 4.5b, while the MSSQ subscales for the child (r = 0.01) and adult (r = 0.29) showed weak correlations.

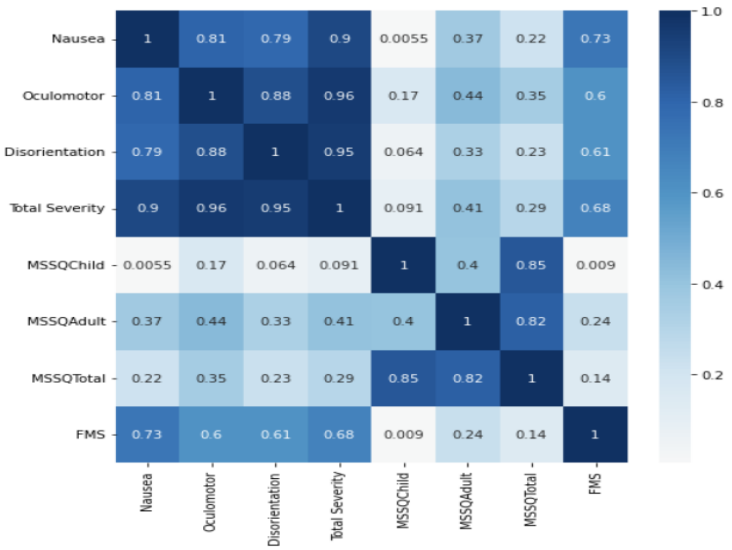

Figure 4.5 a. Pearson correlation matrix for the 10th FMS score, second SSQ subscales scores (nausea, disorientation, oculomotor and total scores), and the MSSQ subscales (child and adult) for all participants

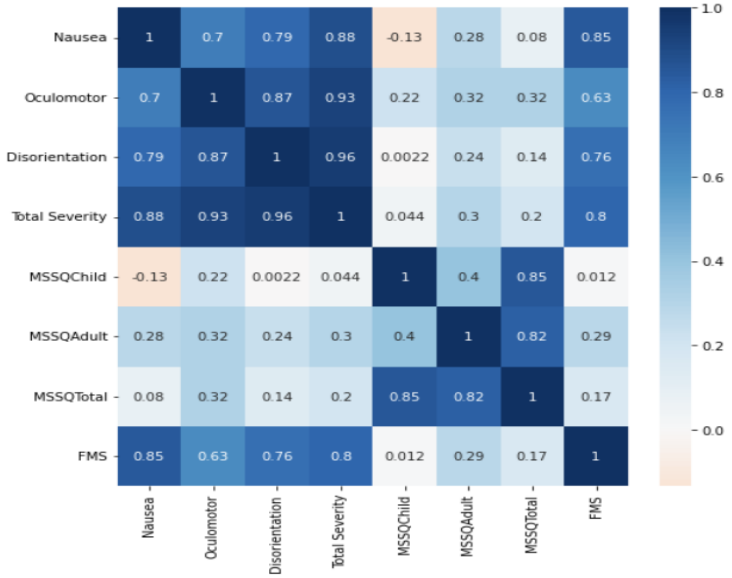

Figure 4.5 b. Pearson correlation matrix for the 20th FMS score, third SSQ subscales scores (nausea, disorientation, oculomotor and total scores), and the MSSQ subscales (child and adult) for all participants

4.5 PHYSIOLOGICAL MEASURES

The correlation between physiological measures and subjective motion sickness was analyzed in two ways. The first analysis associated the instantaneous physiological and behavioural measures (e.g. heart rate, respiration rate, skin conductance, accelerometer and gyroscope readings) with FMS ratings at the time

when the FMS was administered. Correlations between these instantaneous signals, the time elapsed since the start of the experiment, and the simultaneous FMS ratings were computed using the applicable Python programming libraries such as Biosppy, sci-kit, and numpy.

The second analysis involved computing the variability of the physiological and behavioural data over 60-second time segments centred on the times when the FMS rating was recorded. This analysis was necessary to extract time-series data congruent with the FMS ratings of motion sickness for subsequent analysis of the relationship between variability (e.g. mean and standard deviation) and FMS ratings. Nine participants were removed from the physiological measures analysis because eight reported zero FMS values throughout the experiment, and one participant had partially missing physiological data resulting in a final sample size of 31 participants and 620 data points corresponding to 20 FMS points per participant across the entire experiment.

ELECTROCARDIOGRAM (ECG)

The raw ECG signals measured in millivolts show the characteristic cardiac potential waveform as shown in Figure 4.6, with the key features for heart rate estimation being the R wave peak of the QRS component and the interval between subsequent R peaks (RR interval). As discussed in section 3.6, the Biosppy package was used to analyze the RR intervals to extract heart rate in beats per minute (bpm) and related measures of variability.

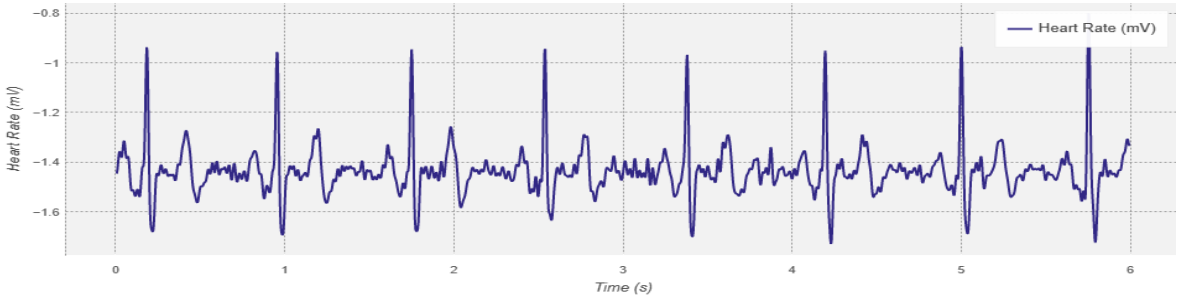

Figure 4.6 . Sample Heart Rate of a participant measured over 6 seconds

Pearson's correlations were computed between the FMS scores and the mean of the heart rate over 60 seconds time intervals surrounding the times when the FMS questionnaire was administered (see Figures 4.7a to c). Heart rate showed low correlations with FMS rating (r = 0.029) for condition 1. Similarly, for condition 2, heart rate showed little correlation with FMS ratings (r = 0.063). In addition, heart rate showed a moderate correlation with skin conductance at r = 0.37 across the first condition, and this relationship was found to be statistically significant (p = .04); however, the combined correlation (r = 0.32) across both

conditions was not statistically significant (p = .08) (see Figures 4.7 a to c). Interestingly, for the subset of participants who had the reading task as the second condition, there is a moderately strong correlation between heart rate and FMS rating (r = 0.43), as shown in Figure 4.8. Additionally, a subset of participants with FMS ratings of 8 and above (N = 13) showed a statistically significant high correlation between conductance and heart rate for the first condition (r (13) = 0.6, p = .030), moderate correlation for both the second condition (r(13) = 0.43, p = .143) and the combined conditions (r (13) = 0.52, p = .069) (see Figures 4.9a to c).

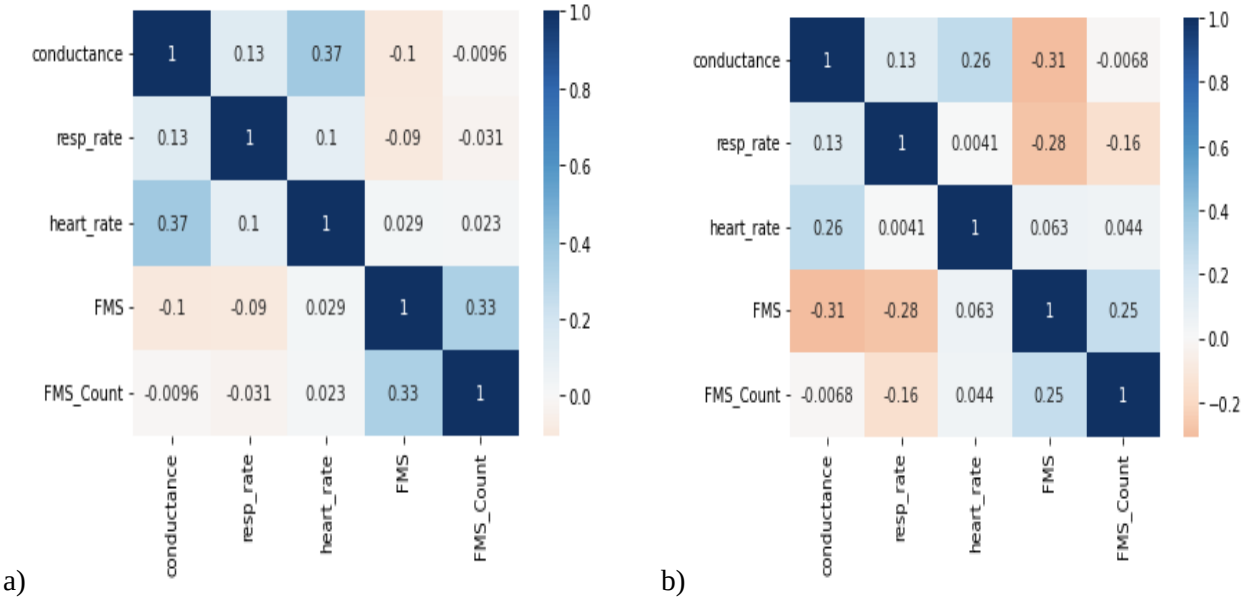

Figure 4.7 a - c. Pearson's correlation chart of the mean of physiological measures with each other, FMS and FMS Count across conditions 1, 2 and across both conditions pooled together.

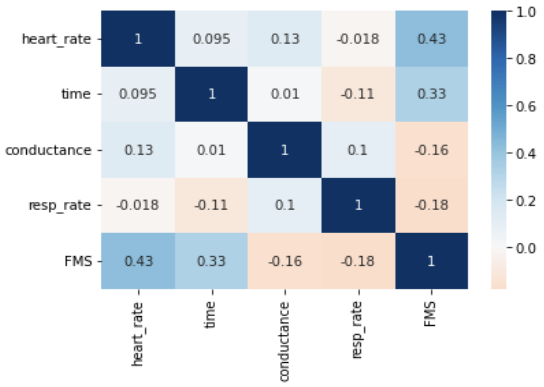

Figure 4.8 . Pearson's correlation charts of physiological measures with each other, time and FMS for participants that observed Reading Task as the second condition

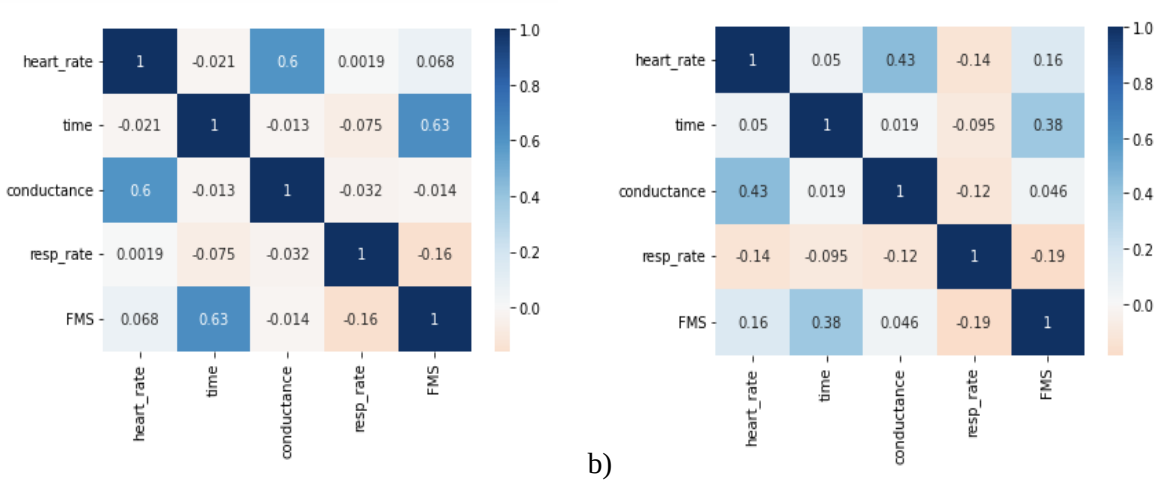

a) b)

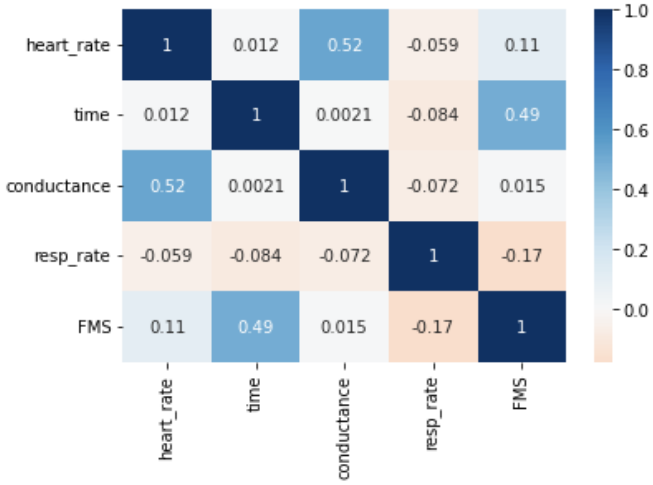

c)

Figure 4.9 a - c. Pearson's Correlation chart of physiological measures with time and FMS across conditions 1, 2 and the two conditions pooled together for a subset of participants with FMS ratings > 8

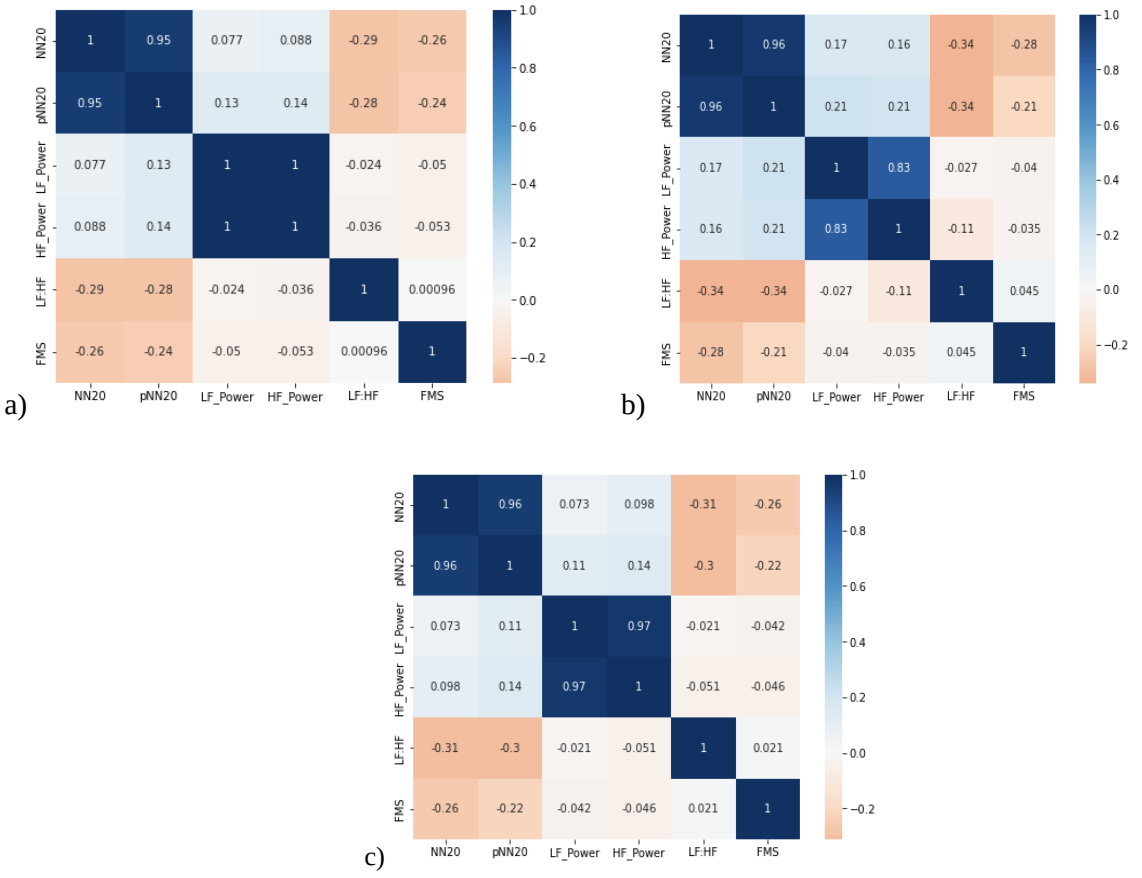

Figure 4.10 a-c. Pearson's correlation chart of heart rate variability parameters with each other, time and FMS across conditions 1 and 2 and the two conditions pooled together, respectively

RESPIRATION

Raw respiration signals were converted to chest displacement in percentage (see Figure 4.11) and then used to calculate respiration rate in Hz (see Figures 4.12 a and b). Respiration rate showed low negative correlations with FMS for condition 1 (r = -0.09) and similarly for condition 2 (r = -0.28) for the correlation relationships computed between the FMS scores and the mean of the respiration rate over 60 seconds time intervals surrounding the times when the FMS questionnaire was administered (see Figures 4.7 a to c),

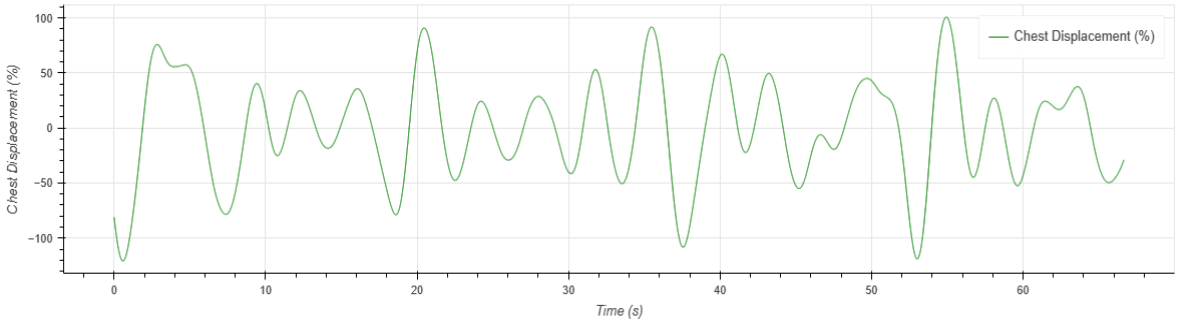

Figure 4.11. Chest displacement of a participant over 60 seconds during condition 1

SKIN CONDUCTANCE

Recorded electrodermal activity was directly converted to skin conductance in microSiemens. For the Pearson's correlations computed between the FMS scores and the mean of the skin conductance over 60 seconds time intervals surrounding the times when the FMS questionnaire was administered (see Figures 4.7 d to f), skin conductance showed moderately low negative correlations with FMS for condition 1 (r = -0.1) and similarly for condition 2 (r = -0.31).

ELECTROCULOGRAM (EOG)

After preprocessing the horizontal eye movements data from the ac-coupled EOG sensor, as discussed in section 3.6, eye blinks artifacts were removed via visual inspection techniques using the EEGLAB software. The calibration factor for each participant was also computed and used to convert the EOG data from millivolts to degrees. A custom algorithm was developed to compute the total number of saccades over a 60-second time interval when the FMS questionnaire was administered based on whenever the eye velocity exceeds a specified threshold of 30 degrees per second (Dai et al., 2021).

This velocity threshold was necessary to filter out noise or small eye movements and ensure only meaningful saccades are included in the analysis. Additionally, a minimum duration threshold of 20 milliseconds was also specified to filter out high-frequency movements that are unlikely to be saccades. Pearson correlations were calculated to explore the relationship between the number of saccades computed over 60 seconds time intervals centred on when the FMS questionnaire was administered with the FMS ratings (see Figures 4.12a to c). The number of saccades and the FMS rating had a moderately low negative correlation r = -0.12 (see Figure 4.12c).

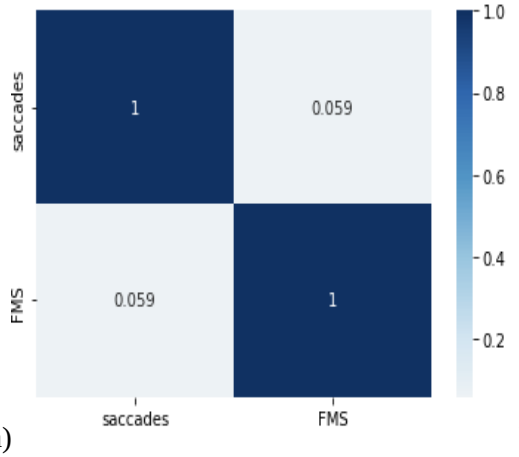

a)

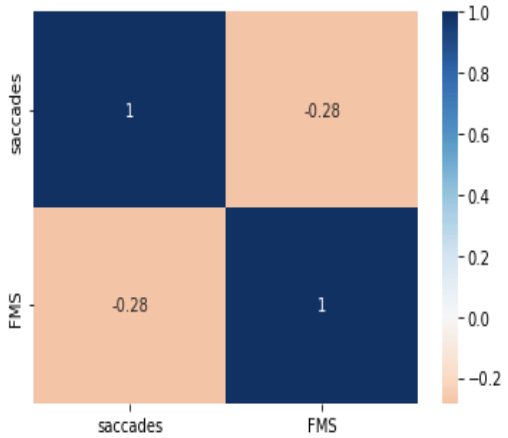

b)

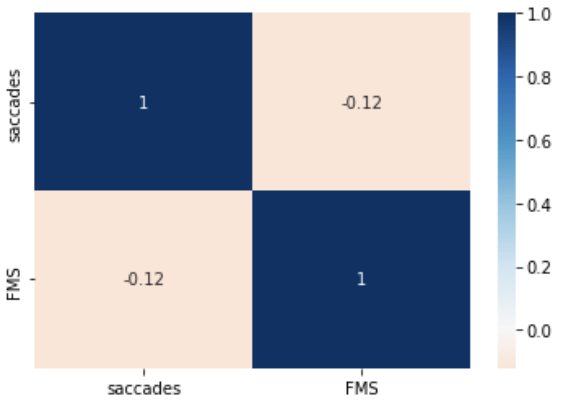

c)

Figure 4.12 a-c. Pearson's correlation chart of the number of saccades with FMS rating during the reading task for participants in group 1, group 2 and both groups pooled together, respectively.

ELECTROENCEPHALOGRAM (EEG)

The data processing stage for the EEG data collected using the Muse Headset is shown in Figure 4.13a

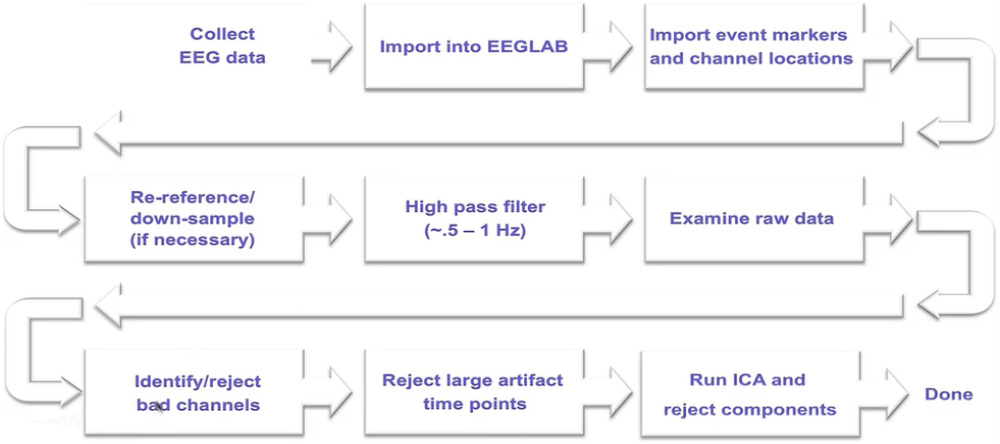

Figure 4.13 a. Processing steps for the Muse EEG data (figure borrowed from Delorme and Makeig, 2004)

The researcher performed the recommended steps by the original equipment manufacturer (OEM) to ensure good signal quality on the Muse Headset. However, a preliminary exploration of the recorded EEG data using the mind-monitor application revealed frequent bad-fit data markers in individual recordings across several participants. A bad fit data marker indicates possible bad recording caused by data quality dropping below the minimum requirements. This Area of bad quality data is typically displayed on the chart with the markers "BF" for "Bad Fit" or a "J" for "Jaw Clench", which produces a lot of Electromyography (EMG) interference that can override the EEG signal and invalidate the results (see Table 4.1 and Figure 4.13b). Ideally, for good data quality, the raw EEG data should have a 50uV difference between its minimum and maximum values, with large spikes only when blinking.

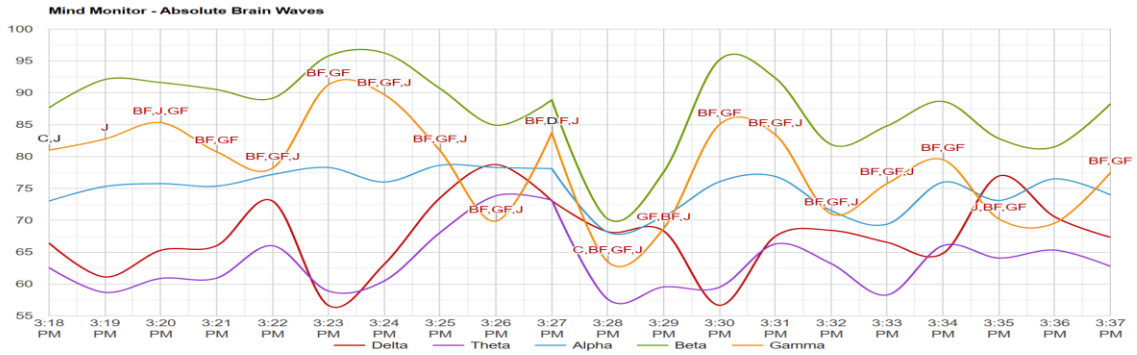

Figure 4.13 b. Sample visualization of the EEG data for a participant using the mind monitor application

Table 4.1: Error Messages from the Muse Headset EEG Data Recordings

Participant	Condition 1	Sample error message from mind-monitor.com	Condition 2	Sample error message from mind-monitor.com
P01	☑		☑	
P02	☑		☑	
P03	☒	Interference-NAN data	☒	Interference-NAN data
P04	☑		☒	9 BadFit Markers
P05	☑		☑	
P06	☑		☑	
P07	☑		☑	
P08	☒	4 BadFit Markers	☒	10 BadFit Markers
P09	☒	70 BadFit Markers	☒	7 BadFit Markers
P10	☒	26, 55 BadFit Markers	☒	26, 55 BadFit Markers
P11	☒		☑	3 BadFit Markers
P12	☑		☑	
P13	☑		☒	121 BadFit Markers
P14	☑		☑	
P15	☑		☑	
P16	☒	5 BadFit Markers	☒	15 BadFit Markers
P17	☑		☑	
P18	☒	8 BadFit Markers	☒	4 BadFit Markers
P19	☑		☑	
P20	☑		☑	
P21	☑		☑	
P22	☒	3 BadFit Markers	☑	
P23	☑		☑	
P24	☒	8 BadFit Markers	☑	
P25	☒	21 BadFit Markers	☑	
P26	☒	342 BadFit Markers	☒	36 BadFit Markers
P27	☒	17 BadFit Markers	☒	274 BadFit Markers
P28	☒	49 BadFit Markers	☒	16 BadFit Markers
P29	☒	13 BadFit Markers,	☑	
P30	☒	4 BadFit Markers	☒	21 BadFit Markers
P31	☒	13 BadFit Markers	☒	53 BadFit Markers
P32	☒	58 BadFit Markers	☒	42 BadFit Markers
P33	☒	87 BadFit Markers	☒	21 BadFit Markers
P34	☒	NAN+44 BadFitMarkers	☒	3 Bad Fit Marker
P35	☒	357 BadFitMarkers	☒	8 BadFitMarkers
P36	☑		☒	12 BadFitMarkers
P37	☑		☑	
P38	☒	5 BadFitMarkers	☑	
P39	☒	NAN Values	☑	
P40	☑		☑	

Although the EEG may be a potential biomarker in determining motion sickness, the use of the Muse Headset in measuring EEG is impractical for large-scale experiments. Specifically, data quality issues were found in more than half of the participants and data collection was challenging with certain head shapes, head sizes, and hairstyles; this is an important factor to consider when using portable EEG equipment like the Muse Headset (Krigolson et al., 2017). Consequently, the EEG data is removed from further analysis to avoid erroneous results.

4.6 BEHAVIOURAL MEASURES

Pearson correlations were computed between the FMS scores and the standard deviation of the accelerometer and gyroscope readings over 60 seconds time intervals surrounding the times when the FMS questionnaire was administered (see Figures 4.14a to c). Accelerometer_X, Accelerometer_Y and Accelerometer_Z refer to the standard deviation of acceleration along the head forward, lateral and vertical axes. Thus, they mainly respond to changes in the orientation of the head with respect to gravity; specifically, head tilt up and down (X), tilt left and right (Y) and both directions of tilt and vertical motion up and down (Z). Gyro_X, Gyro_Y and Gyro_Z provide angular rotation while tilting left and right (roll), tilting up and down (pitch) and rotating left and right (yaw), respectively. The strongest correlation with the FMS score was found for the Accelerometer_Y axis, and this relationship was statistically significant ($r = 0.43$, $p = .015$), suggesting that participants tended to vary the tilt of their heads more with increasing car sickness.

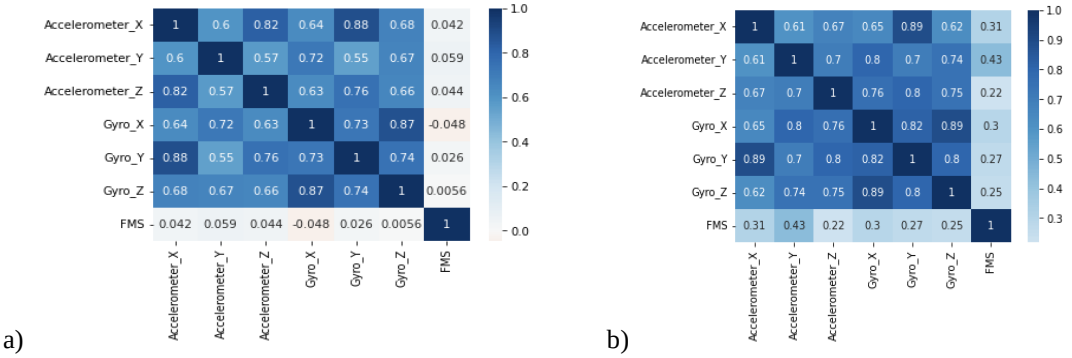

a) b)

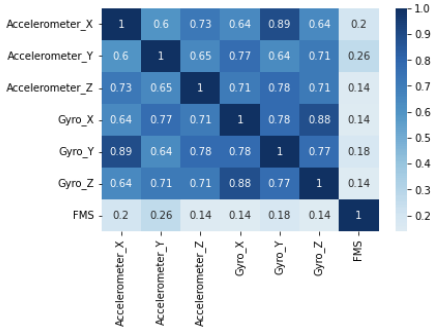

Figure 4.14 a – c. Pearson Correlation chart of the standard deviation of accelerometer and gyroscope measures with FMS scores for task order 1,2 and combined task, respectively

4.7 GENDER COMPARISON

As shown in Figure 4.15 and Appendices D and E, for the No Task condition, females had a higher mean FMS score of 4.74 while males had a lower mean FMS score of 3.47 for the No Task condition; however, this effect was not statistically significant ($F_{1,38} = .877$, $p = .355$). Similarly, for the Reading Task condition, females had a higher mean FMS score of 4.80 compared to males at 3.88; however, this effect was also not statistically significant ($F_{1,38} = .644$, $p = .427$). For the correlation of the physiological measures with FMS scores, the females had a higher positive correlation between heart rate and FMS scores with r = 0.24 for condition one, r = 0.39 for condition two and r = 0.29 across both conditions pooled together (see Figures 4.16a to c). While the males had a negative correlation between heart rate and FMS scores with r = -0.14 for condition one, r = -0.39 for condition two and r = -0.24 across both conditions pooled together (see Figures 4.17a to c).

The final FMS score in a condition should be most comparable with the SSQ scores taken immediately following the condition. The Pearson correlation matrix computed between the 10th FMS score, the second SSQ subscales score (nausea, disorientation, oculomotor and total scores), and the MSSQ subscales (child and adult) are shown in Figure 4.18 a and b grouped by female versus male participants. Similarly, Figure 4.19 a and b shows the Pearson correlation matrix for the 20th FMS score, the second SSQand the MSSQ. In general, all of the SSQ subscale scores correlated with FMS ratings; females had their highest correlation score as the nausea subscale score at r = 0.74 and 0.89, while males had the highest correlation score as the disorientation subscale score at r = 0.73 and 0.84 (see Figures 4.18 a-b and Figures 4.19 a-b).

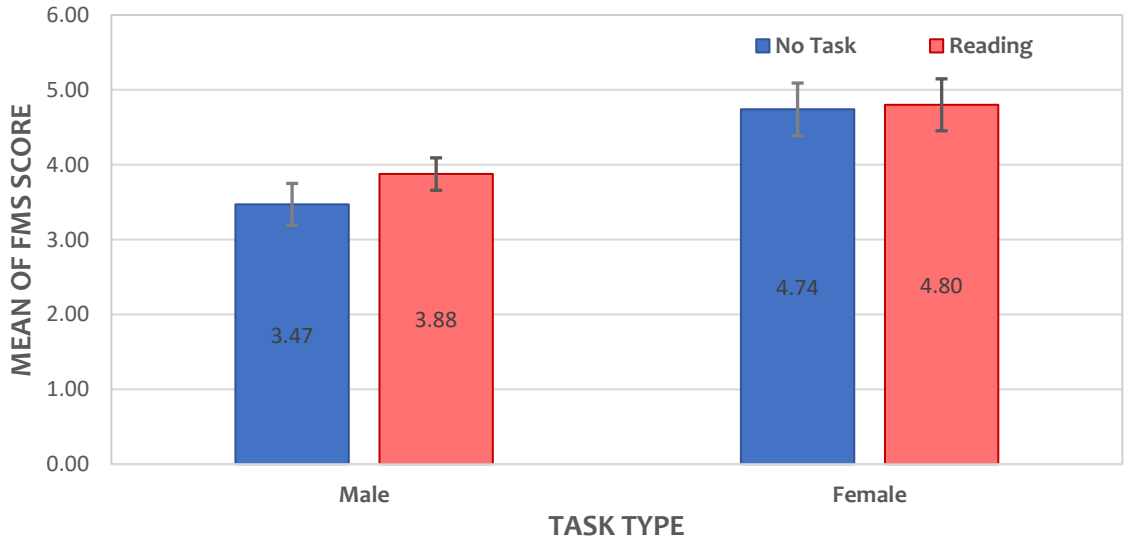

Figure 4.15 . Results of Mean FMS Rating versus Task Condition for Male and Female. Error bars show ± 1 *SEM*.

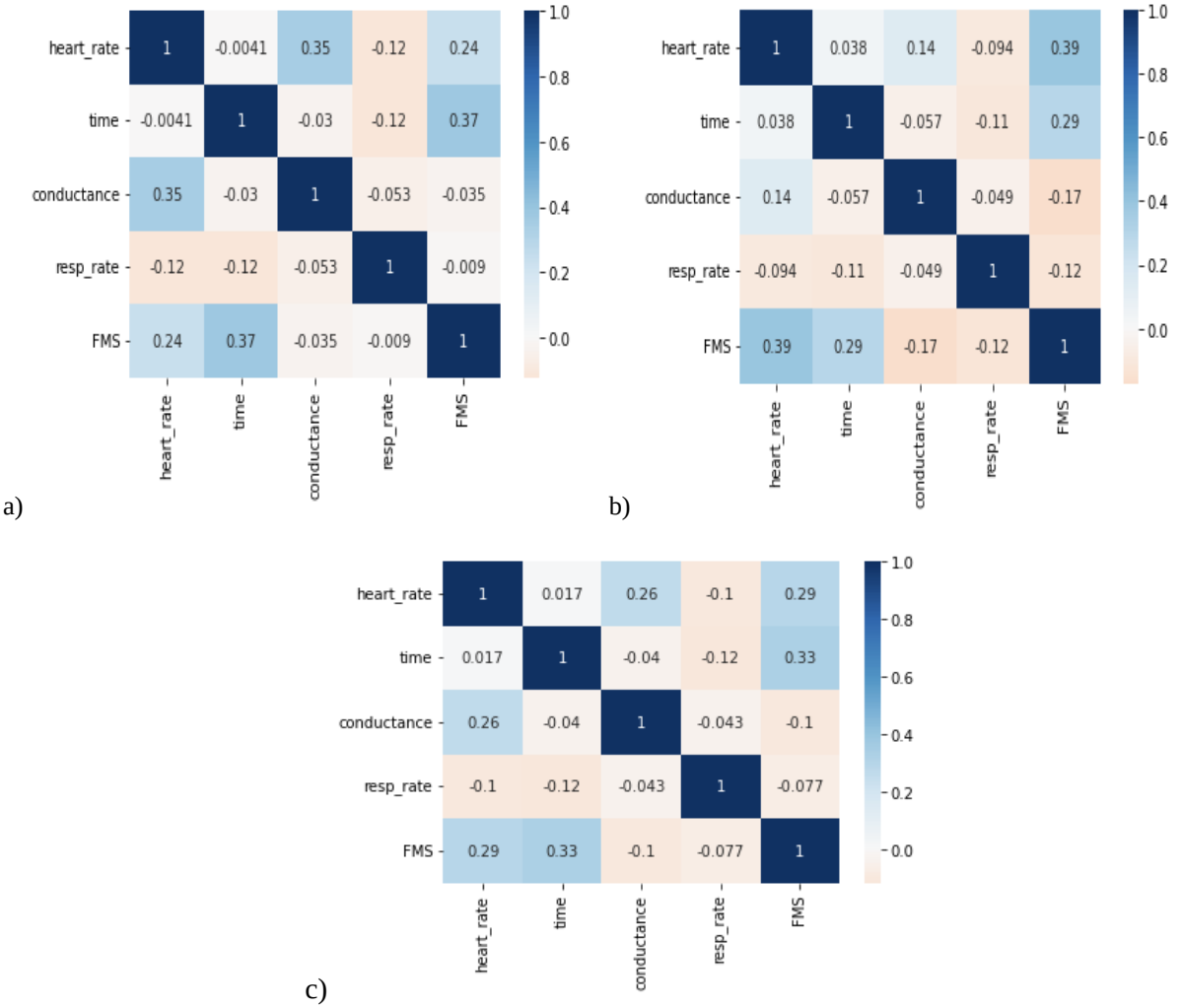

Figure 4.16 a-c. Correlation of physiological measures for female participants across conditions 1, 2 and both conditions pooled together

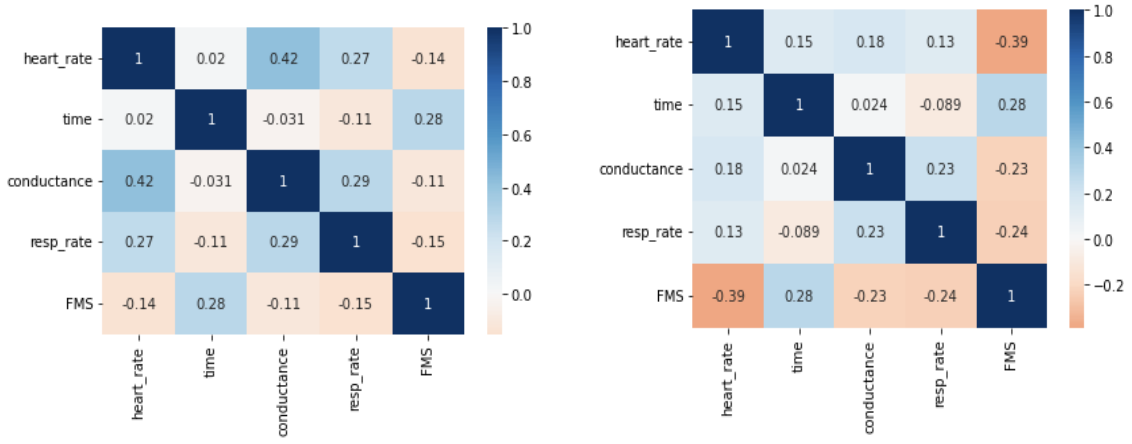

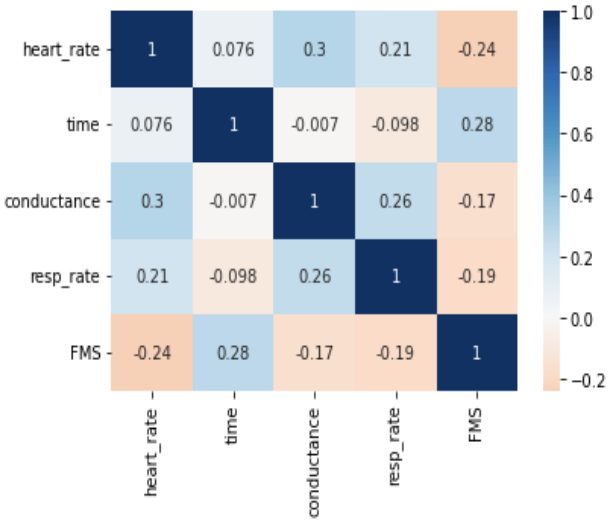

c)

Figure 4.17 a-c. Correlation of physiological measures for male participants across conditions 1, 2 and both conditions pooled together

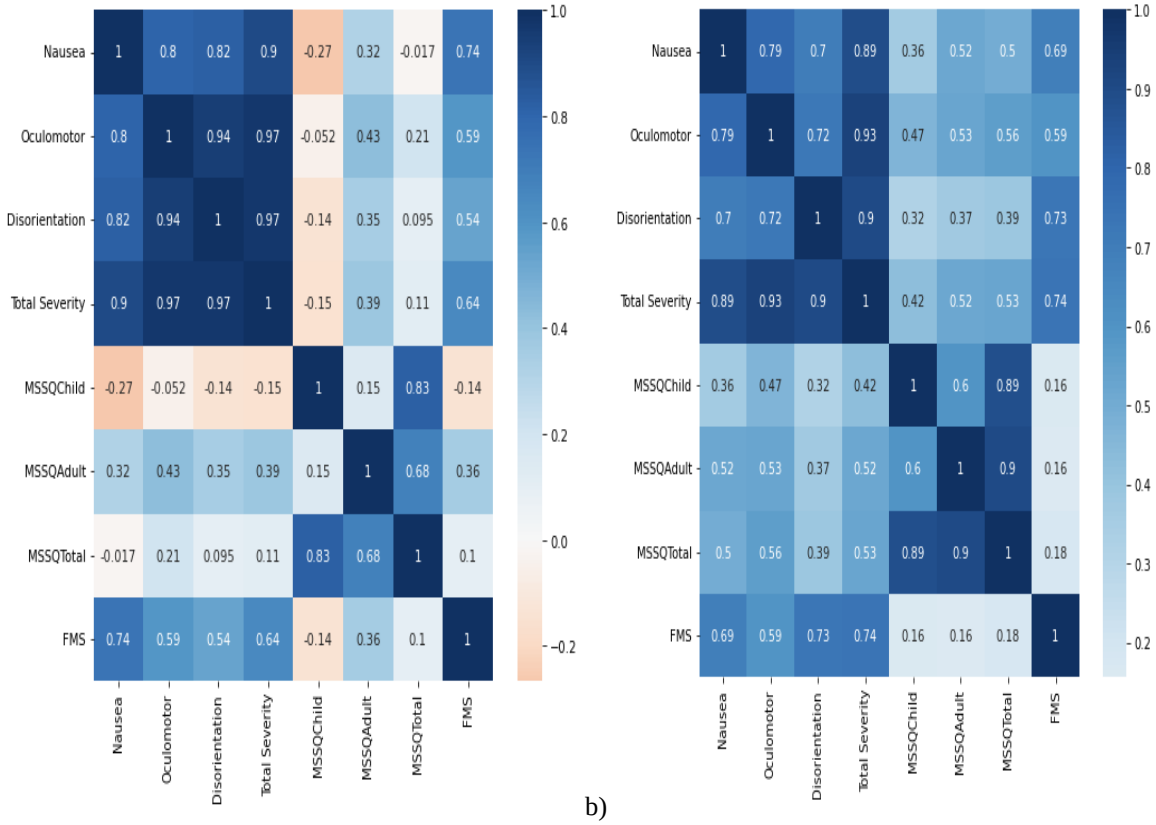

a) b)

Figure 4.18 a-b. Pearson correlation matrix for the 10th FMS score, second SSQ subscales scores (nausea, disorientation, oculomotor and total scores), and the MSSQ subscales (child and adult) for Female participants (left) versus Males (right) participants, respectively

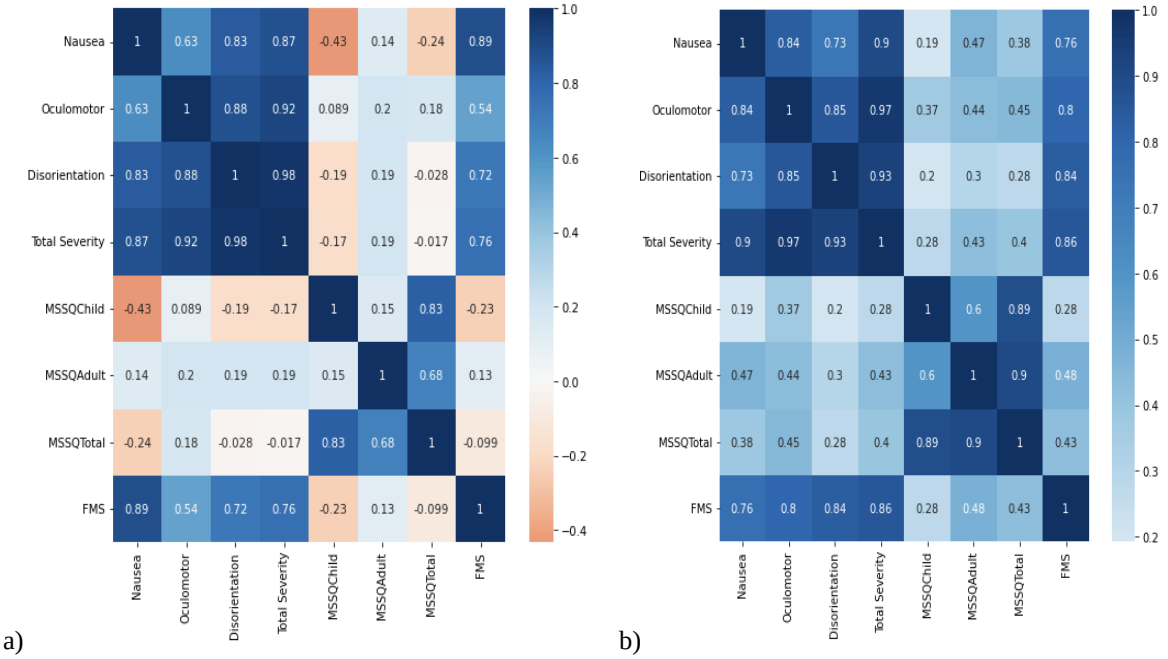

Figure 4.19 a-b. Pearson correlation matrix for the 20th FMS score, third SSQ subscales scores (nausea, disorientation, oculomotor and total scores), and the MSSQ subscales (child and adult) for Female participants versus Male participants, respectively

4.8 MODELLING

This section describes the two types of prediction tasks performed: regression and classification. For the regression analysis, a model was fitted to estimate the FMS score time series, while for the classification model, the goal was to distinguish between motion-sick and non-motion-sick participants based on an appropriate threshold selected from the FMS score where a score of four or higher indicated the presence of car sickness.

4.8.1 REGRESSION ANALYSIS

Multiple linear regressions using a stepwise iterative construction of a regression model with all physiological measures as predictors and the FMS score as a dependent variable were calculated to estimate the amount of variance explained by the physiological measures and examine each feature's statistical significance. The stepwise regression technique is helpful for selecting statistically significant predictors in a traditional regression model, removing insignificant variables and preventing multicollinearity. The detailed results of the stepwise regression analysis for the FMS score are presented in Figures 4.20 and 4.21. Based on the Ordinary Least Squares regression (OLS) results, the model consists of a constant and five backward-selected predictors: conductance, Accelerometer_X, Accelerometer_Y, Gyro_X and pNN20 as shown in Figure 4.20.

The other predictors of heart_rate, resp_rate, Accelerometer_X, Accelerometer_Z, Gyro_Y and Gyro_Z were not included based on $p > .05$. Therefore, a linear regression model was created using these five predictors, and it was confirmed that the selected predictors were still statistically significant at $p < .05$ (see Figure 4.21). The amount of variance explained was 15% ($R^2 = 0.149$, adjusted $R^2 = 0.142$ and $p < .001$) and similar for both the forward and backward stepwise regression techniques. In addition to the multiple linear regressions, a linear mixed-effects model was done to account for the repeated measures (see Figure 4.22).

Dep. Variable:	FMS	**R-squared:**	0.158
Model:	OLS	**Adj. R-squared:**	0.144
Method:	Least Squares	**F-statistic:**	11.39
Date:	Wed, 26 Apr 2023	**Prob (F-statistic):**	5.15e-18
Time:	11:50:22	**Log-Likelihood:**	-1730.4
No. Observations:	620	**AIC:**	3483.
Df Residuals:	609	**BIC:**	3532.
Df Model:	10		
Covariance Type:	nonrobust		

	coef	std err	t	P>|t|	[0.025	0.975]
const	11.6236	2.171	5.355	0.000	7.361	15.886
heart_rate	-0.0240	0.019	-1.264	0.207	-0.061	0.013
conductance	-0.2006	0.042	-4.729	0.000	-0.284	-0.117
resp_rate	-8.0090	4.487	-1.785	0.075	-16.821	0.803
Accelerometer_X	6.7761	5.464	1.240	0.215	-3.954	17.506
Accelerometer_Y	36.9604	6.356	5.815	0.000	24.479	49.442
Accelerometer_Z	-10.7142	9.179	-1.167	0.244	-28.740	7.312
Gyro_X	-0.6549	0.224	-2.922	0.004	-1.095	-0.215
Gyro_Y	0.0880	0.166	0.531	0.595	-0.237	0.413
Gyro_Z	0.0057	0.138	0.041	0.967	-0.265	0.277
pNN20	-0.0458	0.010	-4.526	0.000	-0.066	-0.026

Omnibus:	97.694	**Durbin-Watson:**	0.400
Prob(Omnibus):	0.000	**Jarque-Bera (JB):**	161.528
Skew:	0.983	**Prob(JB):**	8.41e-36
Kurtosis:	4.544	**Cond. No.**	5.58e+03

Figure 4.20. OLS result of the model with all predictors

Dep. Variable:	FMS	**R-squared:**	0.149
Model:	OLS	**Adj. R-squared:**	0.142
Method:	Least Squares	**F-statistic:**	21.45
Date:	Wed, 26 Apr 2023	**Prob (F-statistic):**	8.17e-20
Time:	12:23:11	**Log-Likelihood:**	-1733.7
No. Observations:	620	**AIC:**	3479.
Df Residuals:	614	**BIC:**	3506.
Df Model:	5		
Covariance Type:	nonrobust		

	coef	std err	t	P>|t|	[0.025	0.975]
const	7.3976	0.578	12.790	0.000	6.262	8.533
conductance	-0.2198	0.041	-5.373	0.000	-0.300	-0.139
Accelerometer_X	7.6804	3.142	2.445	0.015	1.511	13.850
Accelerometer_Y	36.0500	6.173	5.840	0.000	23.927	48.173
Gyro_X	-0.6351	0.152	-4.184	0.000	-0.933	-0.337
pNN20	-0.0374	0.008	-4.818	0.000	-0.053	-0.022

Omnibus:	99.634	**Durbin-Watson:**	0.397
Prob(Omnibus):	0.000	**Jarque-Bera (JB):**	165.782
Skew:	0.998	**Prob(JB):**	1.00e-36
Kurtosis:	4.561	**Cond. No.**	2.20e+03

Figure 4.21. OLS result of the model with selected predictors based on the backward regression technique

```
          Mixed Linear Model Regression Results
============================================================
Model:              MixedLM Dependent Variable: FMS
No. Observations:   620     Method:             REML
No. Groups:         31      Scale:              6.4282
Min. group size:    20      Log-Likelihood:     -1508.9159
Max. group size:    20      Converged:          Yes
Mean group size:    20.0
------------------------------------------------------------
                Coef.  Std.Err.   z    P>|z| [0.025 0.975]
------------------------------------------------------------
Intercept        4.171    2.518  1.656 0.098 -0.764  9.106
heart_rate       0.009    0.030  0.305 0.760 -0.049  0.067
Accelerometer_X  5.699    2.316  2.460 0.014  1.159 10.238
Accelerometer_Y 13.213    4.604  2.870 0.004  4.190 22.236
Gyro_X          -0.235    0.107 -2.196 0.028 -0.445 -0.025
pNN20           -0.014    0.011 -1.269 0.204 -0.035  0.008
PARTICIPANT Var  8.823    0.968
============================================================
```

Figure 4.22. Linear Mixed-Effect Model with selected predictors based on the backward regression technique

4.8.2 RANDOM FOREST MODEL

The Random Forest model is an ML technique that is frequently the classification algorithm of choice because it performs well with small data sets, is less prone to overfitting even when the number of features is very high, can handle unbalanced data, is resistant to outliers and does not require feature normalization. The Python scikit-learn module was used for all the ML analyses. A random forest model was trained to estimate the FMS score time series based on the physiological and behavioural measures at the instant the FMS was administered and in the preceding and subsequent 30 seconds.

Specifically, the physiological and behavioural measures were first processed to extract their instantaneous values at the specific times the FMS was administered and divided into one-minute segments to compute relevant statistical features such as mean and standard deviation. In total, 30 features were computed for the physiological and behavioural measurements. Nine participants were removed from the machine learning analysis because eight reported zero FMS values throughout the experiment, and one participant had partially missing physiological data resulting in a final sample size of 31 participants and 620 data points corresponding to 20 FMS points per participant across the entire experiment.

4.8.2.1 FEATURE SELECTION

Feature selection is important because it increases the prediction power of the model by selecting the most critical variables and eliminating the redundant and irrelevant ones to avoid overfitting. The available features were ranked according to their importance using a Random Forest classifier, and only top-ranking features were used for the random forest model's final training and evaluation. Figure 4.23 illustrates the result of the feature extraction process where a longer bar corresponds to higher importance.

4.8.2.2 CLASSIFICATION ANALYSIS

For the classification analysis, a cut-off score of 4 (representing the 50th percentile) was selected for the FMS scale to separate motion-sick participants with an FMS score of four or higher and non-motion-sick participants with an FMS score of three or lower. This cut-off score was chosen to ensure a near-balance distribution of the classes in the random forest model. Although having equal classes is not critical in a random forest model, it can affect the performance and interpretation of the model. Random forest models are generally robust to class imbalance and perform well even when unequal classes exist. However, when one class is much smaller than the other, the model may be biased towards the majority class by prioritizing features that are more predictive of this class while overlooking features that are important for the minority class leading to poor performance on the minority class. Consequently, it is useful to balance the classes to improve the model's interpretation and ensure it considers all features equally.

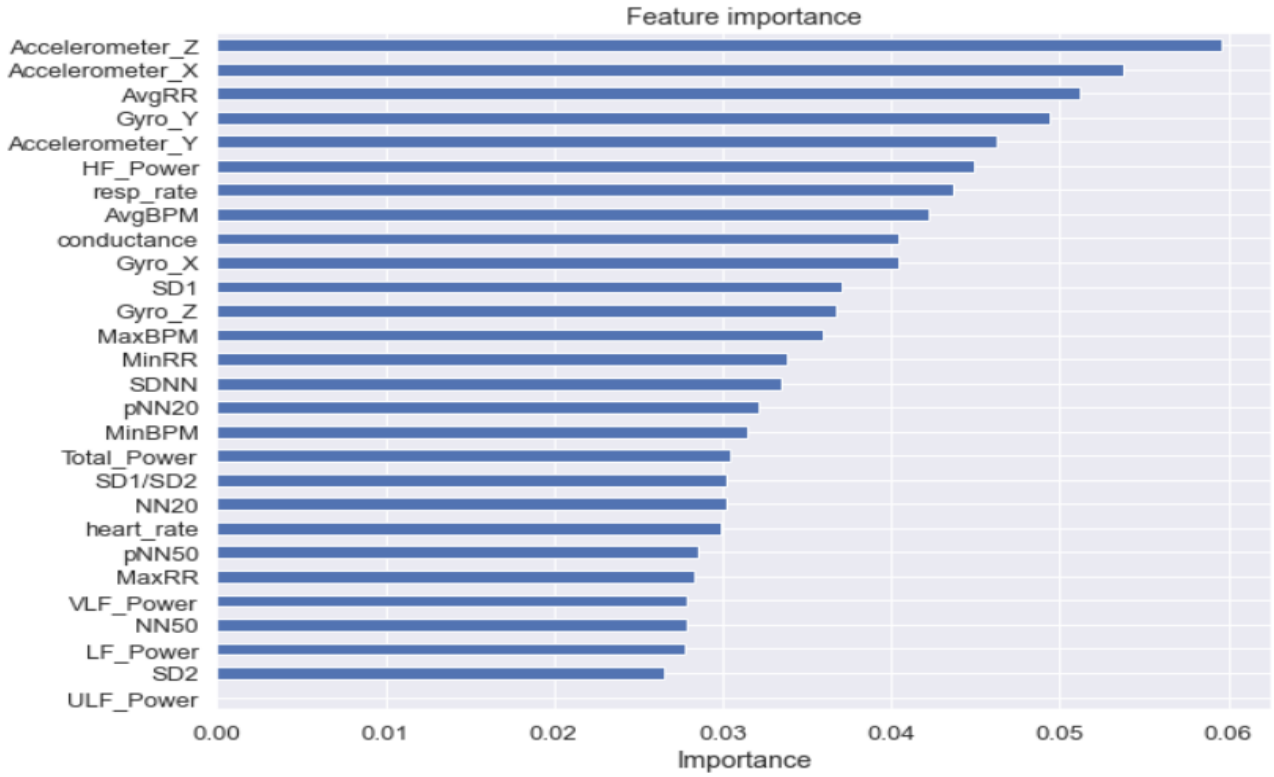

Figure 4.23. Average importance rank of features for Random Forest Model

The model's overall accuracy is 77% (see Figure 4.25). The confusion matrix is a performance measurement for machine learning classifications and is useful for measuring recall, precision, specificity and accuracy. The confusion matrix (see Figure 4.24) shows that the number of samples correctly predicted to belong to the "High Motion Sickness" class is 79%, while that of the "Low Motion Sickness class is 75%.

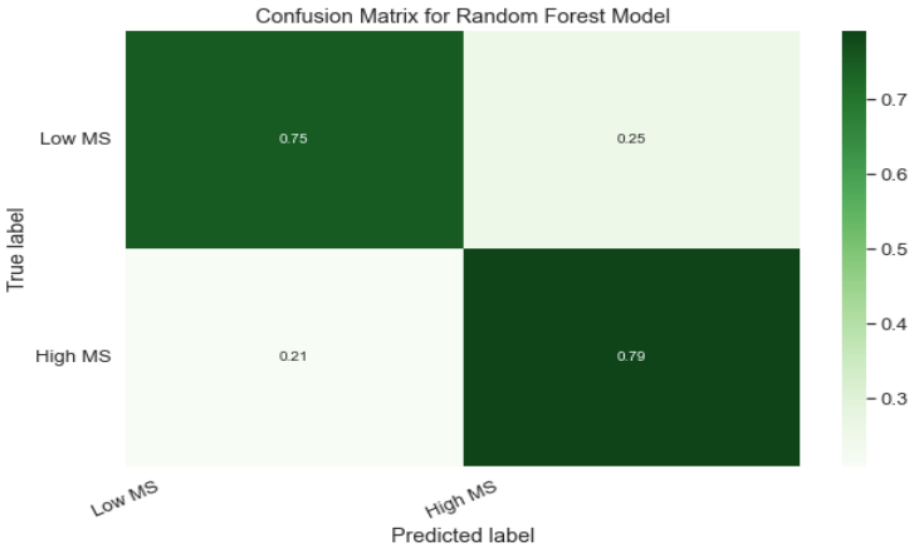

Figure 4.24: Confusion Matrix for Random Forest Model

	precision	recall	f1-score	support
1	0.72	0.75	0.74	52
2	0.81	0.79	0.80	72
accuracy			0.77	124
macro avg	0.77	0.77	0.77	124
weighted avg	0.78	0.77	0.77	124

Figure 4.25: Classification report for Random Forest Model

CHAPTER FIVE – DISCUSSION AND CONCLUSIONS

This thesis aimed to determine if physiological, behavioural and subjective measures can reliably detect and predict the presence of car sickness. The results of the quantitative analysis demonstrated the relationship between the psychological and physiological states of car sickness and its associated symptoms, with physiological measures accounting for 14.9 % of the variance in the reported FMS ratings. The machine learning analysis showed a moderate correlation between some physiological measures and the FMS rating.

The ability of the random forest model to classify participants as sick or not-sick can be considered acceptable, with an overall accuracy of 77%. Although these results are sufficient to be useful, they demonstrate that physiological measures alone cannot be relied upon to reliably detect or predict the onset or severity of car sickness. Therefore, these findings are consistent with similar research that reached comparable conclusions in other motion sickness contexts (Smyth et al., 2021; Kesharvarz et al., 2022).

Overall, as outlined in the research goals, the ML techniques adopted in this thesis were able to perform the following: (1) detect and identify changes in physiological and behavioural measures linked to the onset of car sickness and (2) categorize participants as sick or not sick based on physiological and behavioural measures. The next section presents the role of each physiological measure in relation to earlier findings and underlying theoretical assumptions.

5.1 SKIN CONDUCTANCE

One of the primary symptoms of motion sickness is cold sweating (Lackner, 2014). As a result, electrodermal activity has frequently been examined as a possible correlate of car motion sickness. While some investigations (Hu et al., 1991; Warwick-Evans et al., 1987) found an increase in skin conductance levels as motion sickness severity increased, other studies (Dahlman et al., 2009; Smyth et al., 2021) were unable to detect a difference in skin conductance levels between motion-sick and non-motion-sick participants. In this study, skin conductance level was one of the important measures of motion sickness and was among the features selected for the machine learning analysis. Skin conductance levels generally increased over the experiment for several participants; however, this alone was not a reliable predictor of how severe car sickness was, as a few participants who reported zero FMS ratings also had increasing skin conductance levels, possibly reflecting drifts in the electrode-skin interfaces. Skin conductance was measured by placing gelled electrodes on the participants' fingers, a popular site to identify sweat activity

linked to elevated sympathetic nervous system activity. However, some studies have suggested that the forehead appears to be more sensitive to changes in motion sickness (Golding, 1992; Wan et al., 2003).

5.2 ELECTROCARDIOGRAM

The relevance of cardiovascular measures such as heart rate and heart rate variability for detecting car sickness remains inconclusive. While heart rate showed a moderate correlation with skin conductance level, its correlation with motion sickness severity measured by the FMS ratings was small and not statistically significant. However, it is noteworthy to mention that a subset of participants who performed reading as the second condition showed a moderately strong correlation between heart rate and FMS rating. Similarly, Graybiel and Lackner (1980) and Mullen et al. (1998) found no relationship between heart rate and the level of MS, while some previous studies' results (Dahlman et al., 2009; Holmes et al., 2001; Hu et al., 1991; Ohyama et al., 2007) found a relationship. Despite the overall weak correlation, average heart rate and some heart rate variability parameters such as high-frequency power and average RR peaks (the time elapsed between two successive R-waves of the QRS signal on the electrocardiogram RR peaks, which is the inverse of instantaneous heart rate) were relevant parameters in the machine learning analyses. This suggests that these features carry diagnostically useful information but only in combination with other measures.

5.3 RESPIRATION

Given the strong relationship between respiration and cardiovascular functions (Grossman, 1983), it is plausible that car sickness may also impact respiration. However, in this thesis, respiration measures showed no strong correlations with car sickness ratings, although it was one of the influential measures in the machine learning analysis. This former finding is similar to some previous studies, such as Cowings et al. (1986) and Gianaros et al. (2003), that did not find a relationship between respiration rate and motion sickness severity. However, some other studies suggested a role for respiration. For instance, Himi et al. (2004), Javaid et al. (2019), and Kim et al. (2005) found that participants who reported motion sickness after being exposed to visual stimuli had higher respiration rates than those who did not. Some studies have also shown that controlled breathing can delay the onset of motion sickness (Denise et al., 2009; Yen Pik Sang et al., 2003). This biofeedback loop complicates the interpretation of respiration rate and may have contributed to the mixed findings here and in the literature.

5.4 ELECTROOCULOGRAM

According to Reason and Brand (1975), eye movements, such as those made while reading or looking at a screen, can increase the likelihood of experiencing motion sickness in a moving vehicle because the eyes

constantly shift focus and provide new visual information, which can cause a greater discrepancy between the visual and vestibular inputs to the brain. The negative correlation between the number of saccades and the FMS scores suggests that participants slowed down their reading pace as they experienced a higher severity of car sickness. This finding is similar to studies that suggest that reading increases the incidence and severity of motion sickness (e.g., Leung & Coenegrachts, 2011; Koch et al., 2018; Golding & Gresty, 2015; Krueger et al., 2017; Leung & Hon, 2019; Schmidt et al., 2020) especially because the frequency and intensity of eye movements can exacerbate the sensory conflict that leads to motion sickness.

5.5 BEHAVIOURAL MEASURE

Head movement had an explanatory role in this study, as shown by the moderately high correlations with the FMS ratings. It was also one of the significant measures in the random forest analysis. Previous studies have discussed measures of sway magnitude during quiet stances, such as differences in the velocity or positional variability of the head, torso, or centre of pressure, between individuals who are motion sick and those who are not (e.g., Bonnet et al., 2006, 2008; Stoffregen & Smart, 1998; Stoffregen et al., 2008; Villard et al., 2008). In this thesis, there is evidence that head movement does correlate with the intensity of car sickness, suggesting that it is a crucial aspect that should be considered when detecting and predicting car sickness.

5.6 SUBJECTIVE MEASURES

The SSQ nausea subscale score correlated highly with the FMS ratings. This result is similar to findings in previous studies where the FMS has been validated to correlate highly with SSQ subscale scores and the Total Scores (up to r = 0.80) (e.g., Keshavarz and Hecht, 2011; Keshavarz et al., 2014 and D'Armour et al., 2017).

5.7 GENDER COMPARISON

Although the FMS ratings were greater for females than males across the reading and no task conditions; however, this was not statistically significant. The FMS ratings for the females correlated more highly with SSQ nausea subscale scores (up to r = 0.89) in comparison with the male SSQ nausea subscale scores at 0.76 (e.g., Keshavarz and Hecht, 2011; Keshavarz et al., 2014 and D'Armour et al., 2017). Additionally, females had a higher and positive correlation between heart rate and FMS scores in comparison to the males, similar to the results in existing studies (e.g., Ryan et al., 1994, Holmes and Griffin, 2001)

5.8 LIMITATIONS OF THE RESEARCH

One limitation of the present study is the sample size. We had a significant sample of men and women and could compare these groups. However, before testing, we did not know how many participants would get

sick. Specifically, the motion-base driving simulator induced motion sickness in most participants, with only eight of the 40 reporting no motion sickness at all. Consequently, it was not possible to conduct insightful statistical comparisons between these groups and those experiencing some symptoms due to the imbalance in participant numbers. Some interesting indicators, such as skin conductance and heart rate, might have been able to distinguish between the sick and non-motion-sick participants if a stricter criterion for 'not sick' had been used. However, more data is required to corroborate this.

Another limitation of this study is that car sickness was induced in seated participants with limited movement under controlled laboratory conditions. This setting was necessary to increase the likelihood of detecting physiological changes related to car sickness, given that some physiological measures are known to be susceptible to motion artifacts. For instance, the ECG signal is highly prone to motion artifacts caused by changes in body position and would be less reliable under real-world conditions. Therefore, the findings do not offer conclusive evidence on whether or not physiological changes linked to car sickness are robust in situations where participants are actively moving.

Additionally, the use of driving simulators in investigating car sickness because of the limited motion envelope or limitations on position, velocity, and acceleration poses a constraint. For example, xy-platforms provide a much wider range of motion, while Stewart platforms are constrained in their displacements when used in moving base simulators. Motion in the frequency range of 0.2 Hz has repeatedly been shown to be most provocative for vertical (O'Hanlon and McCauley, 1972; ISO 2631-1, 1997) and similarly for horizontal motion (Golding et al., 2001); therefore, the frequency capabilities of the motion platform are of particular interest in terms of motion sickness. Therefore, careful consideration should be given to a motion base simulator's frequency and acceleration capabilities to maximize provocativeness, as restricted motion might not elicit sufficient levels of motion sickness ratings for investigation (Golding, 2006b). Another constraint is the generalization issues with results obtained from driving simulators to real-life scenarios and other tasks (Stocco et al., 2022).

5.9 RECOMMENDATION AND FUTURE WORK

Although the findings of this study are promising, they suggest that physiological measures alone are not an accurate method to detect or predict car sickness in real-time reliably. Heart rate, skin conductance and head tilt showed the most promising results of the applied physiological measures. Additionally, the number of saccades computed from the EOG data to detect changes in participants' reading rates using custom-developed algorithms is a promising method for further investigation in the future. Specifically, detailed saccade analysis, in combination with measures of heart rate, skin conductance and head tilt, could be

particularly interesting and may advise on potential solutions to reduce or prevent the onset of car sickness, especially while engaged in tasks such as reading or texting. This is because of their notable effects in the current study, their non-invasive nature, and the ease of measurement; a further investigation of these measures as potential indicators of car sickness is recommended.

In car sickness studies, eye movement analysis is crucial in understanding the underlying mechanisms and psychological impacts of car sickness on individuals. EOG sensors have historically been used to measure horizontal eye movements. In this thesis, the EOG sensors used could measure only horizontal eye movements. However, adopting EOG electrode configurations that can track both horizontal and vertical eye movements can offer additional information and help with a more thorough analysis of car sickness. Vertical eye movements, such as upward and downward gaze shifts, can reveal how people visually engage with their surroundings while driving by indicating the monitoring of traffic conditions, scanning of the environment, or the awareness of visual cues.

Furthermore, integrating vertical eye movement data can improve the precision of detecting oculomotor patterns linked to motion sickness. Certain eye movements, such as nystagmus or saccades, in horizontal and vertical directions may help to determine the intensity or susceptibility of motion sickness (Golding, 2003). By examining these multidimensional eye movement patterns, it may be possible to establish more precise relationships between ocular responses and subjective symptoms of motion sickness. Additionally, integrating vertical eye movement data can facilitate the design of tailored interventions that target particular visual processing difficulties based on understanding the interactions between horizontal and vertical eye movements during motion sickness. Interventions can optimize visual cues, modify visual displays, or give adaptive visual feedback to reduce sensory conflicts.

This study recruited a significant number of men and women for comparison; however, further studies could increase the number of recruited subjects, as having more data would allow improvements in the performance of the ML model and facilitate conducting insightful statistical comparisons between the groups of participants experiencing no motion-sickness symptoms and those experiencing some symptoms. Future research may also involve conducting longitudinal validation studies to evaluate the effectiveness and reliability of the real-time predictive model and any proposed mitigation solutions, collecting data from diverse driving scenarios and various environmental conditions to assess the model's generalizability. Such longitudinal studies can provide insights into the long-term efficacy of the designed intervention measures and reveal potential issues such as habituation or sensitization.

In addition, future studies could combine the predictive capability of the ML model with real-time data obtained from smart sensors and Application Programming Interfaces (APIs). The real-time integration of physiological signals such as heart rate, skin conductance, and breathing rate, in addition to eye and head movement, could improve an understanding of the physiological underpinnings of motion sickness. Additionally, combining data on external elements that may affect a person's susceptibility to motion sickness through access to real-time environmental data such as traffic updates, weather forecasts, or road conditions through APIs could also help to produce more accurate predictions.

Integrating real-time data streaming could also assist with continuous retraining of the model to improve its accuracy, responsiveness and adaptive capabilities. Thus ensuring that the model stays up to date and can account for individual variations, changes in driving circumstances, and other important elements that enhance the model's capacity to forecast the onset of motion sickness in real-time. Further improvements can include creating a user-friendly interface that displays real-time predictions and mitigation options. A simple, intuitive and friendly user interface providing detailed directions for carrying out suggested interventions to lessen motion sickness symptoms can improve passenger safety and comfort during car rides. These advancements will bring us closer to developing practical applications for mitigating motion sickness during car travel.

Other improvements that could significantly enhance future studies include adopting personalization techniques that integrate participants' general well-being and level of discomfort through a routine collection of their subjective feedback. Such personalization techniques would enable a more thorough study of individual responses to motion stimuli to assist in customizing interventions. Also, establishing baseline physiological measurements is crucial for serving as reference points for comparison against subsequent data, enabling the identification of patterns and trends related to participants' susceptibility to motion sickness and detecting the onset of motion sickness. Thus, researchers could observe how these metrics change over time by monitoring physiological indicators before, during, and after exposure to motion stimuli.

This information is valuable for understanding an individual's unique physiological response to motion sickness and could aid in predicting susceptibility or detecting the early signs of motion sickness. By monitoring physiological indicators like heart rate, skin conductance, and pupil dilation, researchers could observe how these metrics fluctuate in response to motion stimuli as people develop motion sicknesses, thus enhancing evaluation significantly. Implementing improved susceptibility measures may also create a better and more dependable way to predict a person's likelihood of experiencing motion sickness using

criteria such as genetic markers, vestibular function, or other important factors. By incorporating these improvements, researchers could optimize motion sickness measurement and ultimately contribute to designing targeted interventions for improved mitigation of this discomforting condition.

Although motion-base simulators provide controlled and reproducible environments for studying car sickness, conducting motion sickness experiments on a real road can offer unique insights and bridge the gap between simulated and real-world experiences. Compared to research conducted in simulated environments, real-road experiments are more ecologically valid and provide opportunities to capture real-world driving conditions' complexities and dynamic nature. Therefore, adopting a real road for future car sickness research efforts offers several advantages and opportunities for understanding the phenomenon as participants will have a more realistic driving experience due to road imperfections, traffic patterns, and environmental signals (such as visual scenery and sounds) that are present in their natural context. This increased ecological validity improves the generalizability of the findings to real-life scenarios.

Additionally, conducting motion sickness experiments in a real car and on a real road enables the integration of a wider variety of sensory inputs. Participants may feel fluctuations in road vibrations, sounds, and airflow in addition to visual and motion cues, which can add to the overall sensory experience of driving. Investigating motion sickness in various naturalistic driving situations can reveal important details about how varied driving conditions affect motion sickness susceptibility and severity. Different road types (e.g., highways, urban roads, and winding roads), driving manoeuvres (e.g., acceleration, braking, and turning), and traffic conditions (e.g., congested traffic and varying speeds) may also impact how a vehicle behaves and ultimately assist in curating targeted interventions for specific driving conditions.

In conclusion, adopting real-road experiments for motion sickness studies could foster collaboration between researchers and the automotive industry, thus facilitating access to cutting-edge sensing technologies, vehicle instrumentation, and telematics data. This partnership may offer insightful information about how car sickness is affected by vehicle design, technologies such as autonomous driving, and in-vehicle interventions aimed at improving passenger comfort and reducing motion sickness in future vehicle designs and technology.

5.10 CONCLUSION

Car sickness is a serious concern for modern technologies, such as self-driving vehicles, as autonomous driving can potentially increase its incidence greatly. Thus, detecting and predicting the early onset of car sickness is important to prevent users' severe side effects and increase adoption. This thesis involved an

investigation into whether or not the objectives measures can assist in the detection of car sickness. Car sickness symptom was successfully elicited in participants using a motion-base driving simulator while avoiding simulator sickness. Head movement showed the strongest correlation with car sickness, and there was a moderate correlation between heart rate and skin conductance. Also, with a subset of participants, heart rate had a moderate correlation with car sickness. Interestingly, the number of saccades for participants reduced as car sickness increased, suggesting a reduction in the reading rate. Combined with other measures, a low variance for the overall severity of car sickness (up to 15%) was explained. Also, the Random Forest model had an acceptable accuracy score of 77%, distinguishing between sick and non-sick participants.

REFERENCES

[1] Akiduki, H., Nishiike, S., Watanabe, H., Matsuoka, K., Kubo, T., & Takeda, N. (2003). Visual-vestibular conflict induced by virtual reality in humans. *Neuroscience Letters*, *340*(3), 197–200.

[2] Andersen, G. J., & Braunstein, M. L. (1985). Induced self-motion in central vision. *Journal of Experimental Psychology: Human Perception and Performance*, *11*(2), 122.

[3] Annett, J. (2002). Subjective rating scales: Science or art? *Ergonomics*, *45*(14), 966–987.

[4] Arcioni, B., Palmisano, S., Apthorp, D., & Kim, J. (2019). Postural stability predicts the likelihood of cybersickness in active HMD-based virtual reality. *Displays*, *58*, 3–11.

[5] Ash, A., & Palmisano, S. (2012). Vection during conflicting multisensory information about the axis, magnitude, and direction of self-motion. *Perception*, *41*(3), 253–267.

[6] Ash, A., Palmisano, S., & Kim, J. (2011). Vection in depth during consistent and inconsistent multisensory stimulation. *Perception*, *40*(2), 155–174.

[7] Banerjee, A., Pal, M., Datta, S., Tibarewala, D. N., & Konar, A. (2014). Eye movement sequence analysis using electrooculogram to assist autistic children. *Biomedical Signal Processing and Control*, *14*, 134–140.

[8] Banerjee, A., Pal, M., Tibarewala, D. N., & Konar, A. (2015). Electrooculogram based blink detection to limit the risk of eye dystonia. *2015 Eighth International Conference on Advances in Pattern Recognition (ICAPR)*, 1–6.

[9] Barra, J., Marquer, A., Joassin, R., Reymond, C., Metge, L., Chauvineau, V., & Pérennou, D. (2010). Humans use internal models to construct and update a sense of verticality. *Brain*, *133*(12), 3552–3563.

[10] Bertin, R. J. V., Collet, C., Espié, S., & Graf, W. (2005). Objective measurement of simulator sickness and the role of visual-vestibular conflict situations. *Driving Simulation Conference North America*, 280–293.

[11] Bles, W., Bos, J. E., De Graaf, B., Groen, E., & Wertheim, A. H. (1998). Motion sickness: Only one provocative conflict? *Brain Research Bulletin*, *47*(5), 481–487.

[12] Bonnet, C. T., Faugloire, E., Riley, M. A., Bardy, B. G., & Stoffregen, T. A. (2006). Motion sickness preceded by unstable displacements of the center of pressure. *Human Movement Science*, *25*(6), 800–820.

[13] Bonnet, C. T., Faugloire, E., Riley, M. A., Bardy, B. G., & Stoffregen, T. A. (2008). Self-induced motion sickness and body movement during passive restraint. *Ecological Psychology*, *20*(2), 121–145.

[14] Borojeni, S. S., Weber, L., Heuten, W., & Boll, S. (2018). From reading to driving: Priming mobile users for take-over situations in highly automated driving. *Proceedings of the 20th International Conference on Human-Computer Interaction with Mobile Devices and Services*, 1–12.

[15] Bos, J. E. (2011). Nuancing the relationship between motion sickness and postural stability. *Displays*, *32*(4), 189–193.

[16] Bos, J. E., Bles, W., & Groen, E. L. (2008). A theory on visually induced motion sickness. *Displays*, *29*(2), 47–57.

[17] Bos, J. E., MacKinnon, S. N., & Patterson, A. (2005). Motion sickness symptoms in a ship motion simulator: Effects of inside, outside, and no view. *Aviation, Space, and Environmental Medicine*, *76*(12), 1111–1118.

[18] Bronstein, A. M., Golding, J. F., & Gresty, M. A. (2020). Visual vertigo, motion sickness, and disorientation in vehicles. *Seminars in Neurology*, *40*(01), 116–129.

[19] Cain, B. (2007). *A review of the mental workload literature*.

[20] Cha, Y.-H. (2009). Mal de debarquement. *Seminars in Neurology*, *29*(05), 520–527.

[21] Chakraborty, S., Dasgupta, A., & Routray, A. (2020). Localization of eye Saccadic signatures in Electrooculograms using sparse representations with data driven dictionaries. *Pattern Recognition Letters*, *139*, 104–111.

[22] Chan, K. S. N., Srisurangkul, C., Depaiwa, N., & Pangkreung, S. (2021). Detection of driver drowsiness from EEG signals using wearable brain sensing headband. *Journal of Research and Applications in Mechanical Engineering*, *9*(2).

[23] Chen, D. J., Bao, B., Zhao, Y., & So, R. H. (2016). Visually induced motion sickness when viewing visual oscillations of different frequencies along the fore-and-aft axis: Keeping velocity versus amplitude constant. *Ergonomics*, *59*(4), 582–590.

[24] Chen, Y.-C., Duann, J.-R., Chuang, S.-W., Lin, C.-L., Ko, L.-W., Jung, T.-P., & Lin, C.-T. (2010). Spatial and temporal EEG dynamics of motion sickness. *NeuroImage*, *49*(3), 2862–2870.

[25] Cheung, B. S., Howard, I. P., & Money, K. E. (1991). Visually-induced sickness in normal and bilaterally labyrinthine-defective subjects. *Aviation, Space, and Environmental Medicine*.

[26] Cheung, B., & Vaitkus, P. (1998). Perspectives of electrogastrography and motion sickness. *Brain Research Bulletin*, *47*(5), 421–431.

[27] Cho, H.-J., & Kim, G. J. (2022). RideVR: Reducing Sickness for In-Car Virtual Reality by Mixed-in Presentation of Motion Flow Information. *IEEE Access*, *10*, 34003–34011.

[28] Choukèr, A., Kaufmann, I., Kreth, S., Hauer, D., Feuerecker, M., Thieme, D., Vogeser, M., Thiel, M., & Schelling, G. (2010). Motion sickness, stress and the endocannabinoid system. *PloS One*, *5*(5), e10752.

[29] Chuang, S.-W., Chuang, C.-H., Yu, Y.-H., King, J.-T., & Lin, C.-T. (2016). EEG alpha and gamma modulators mediate motion sickness-related spectral responses. *International Journal of Neural Systems*, *26*(02), 1650007.

[30] Claremont, C. A. (1931). The psychology of seasickness. *Psyche*, *11*, 86–90.

[31] Cloutier, A., & Watt, D. G. (2006). Motion sickness provoked by torso rotation predicts that caused by head nodding. *Aviation, Space, and Environmental Medicine*, *77*(9), 909–914.

[32] Cobb, S. V. G. (1999). Measurement of postural stability before and after immersion in a virtual environment. *Applied Ergonomics*, *30*(1), 47–57.

[33] Cohen, B., Yakushin, S. B., Holstein, G. R., Dai, M., Tomko, D. L., Badakva, A. M., & Kozlovskaya, I. B. (2005). Vestibular experiments in space. *Advances in Space Biology and Medicine*, *10*, 105–164.

[34] Cowings, P. S., Suter, S., Toscano, W. B., Kamiya, J., & Naifeh, K. (1986). General autonomic components of motion sickness. *Psychophysiology*, *23*(5), 542–551.

[35] Cowings, P. S., & Toscano, W. B. (1993). *Autogenic-feedback training (AFT) as a preventive method for space motion sickness: Background and experimental design*.

[36] Crampton, G. H. (1990). *Motion and space sickness*. CRC Press.

[37] Dahlman, J., Sjörs, A., Lindström, J., Ledin, T., & Falkmer, T. (2009). Performance and autonomic responses during motion sickness. *Human Factors*, *51*(1), 56–66.

[38] Dai, W., Selesnick, I., Rizzo, J.-R., Rucker, J., & Hudson, T. (2021). Detection of normal and slow saccades using implicit piecewise polynomial approximation. *Journal of Vision*, *21*(6), 8–8.

[39] D'Amour, S., Bos, J. E., & Keshavarz, B. (2017). The efficacy of airflow and seat vibration on reducing visually induced motion sickness. *Experimental Brain Research*, *235*, 2811–2820.

[40] Davis, S., Nesbitt, K., & Nalivaiko, E. (2014). A systematic review of cybersickness. *Proceedings of the 2014 Conference on Interactive Entertainment*, 1–9.

[41] de Winkel, K. N., Pretto, P., Nooij, S. A., Cohen, I., & Bülthoff, H. H. (2021). Efficacy of augmented visual environments for reducing sickness in autonomous vehicles. *Applied Ergonomics*, *90*, 103282.

[42] Delorme, A., & Makeig, S. (2004). EEGLAB: an open-source toolbox for analysis of single-trial EEG dynamics, including independent component analysis. *Journal of Neuroscience Methods*, *134*(1), 9–21.

[43] Denise, P., Vouriot, A., Normand, H., Golding, J. F., & Gresty, M. A. (2009). Effect of temporal relationship between respiration and body motion on motion sickness. *Autonomic Neuroscience*, *151*(2), 142–146.

[44] Dennison, M. S., & D'Zmura, M. (2017). Cybersickness without the wobble: Experimental results speak against postural instability theory. *Applied Ergonomics*, *58*, 215–223.

[45] Dennison, M. S., Wisti, A. Z., & D'Zmura, M. (2016). Use of physiological signals to predict cybersickness. *Displays*, *44*, 42–52.

[46] Diels, C., & Bos, J. E. (2015). User interface considerations to prevent self-driving carsickness. *Adjunct Proceedings of the 7th International Conference on Automotive User Interfaces and Interactive Vehicular Applications*, 14–19.

[47] Diels, C., & Bos, J. E. (2016). Self-driving carsickness. *Applied Ergonomics*, *53*, 374–382.

[48] Diels, C., Bos, J. E., Hottelart, K., & Reilhac, P. (2016). Motion sickness in automated vehicles: The elephant in the room. *Road Vehicle Automation 3*, 121–129.

[49] Dobie, T. G. (2019). *Motion sickness: A motion adaptation syndrome* (Vol. 6). Springer.

[50] Dong, X., Yoshida, K., & Stoffregen, T. A. (2011). Control of a virtual vehicle influences postural activity and motion sickness. *Journal of Experimental Psychology: Applied*, *17*(2), 128.

[51] Ebenholtz, S. M., Cohen, M. M., & Linder, B. J. (1994). The possible role of nystagmus in motion sickness: A hypothesis. *Aviation, Space, and Environmental Medicine*, *65*(11), 1032–1035.

[52] Erkaymaz, H., Ozer, M., & Orak, İ. M. (2015). Detection of directional eye movements based on the electrooculogram signals through an artificial neural network. *Chaos, Solitons & Fractals*, *77*, 225–229.

[53] Estrada, A., LeDuc, P. A., Curry, I. P., Phelps, S. E., & Fuller, D. R. (2007). Airsickness prevention in helicopter passengers. *Aviation, Space, and Environmental Medicine*, *78*(4), 408–413.

[54] Feenstra, P. J., Bos, J. E., & van Gent, R. N. (2011). A visual display enhancing comfort by counteracting airsickness. *Displays*, *32*(4), 194–200.

[55] Flanagan, M. B., May, J. G., & Dobie, T. G. (2004). The role of vection, eye movements and postural instability in the etiology of motion sickness. *Journal of Vestibular Research*, *14*(4), 335–346.

[56] Foulkes, A. J., Rushton, S. K., & Warren, P. A. (2013). Flow parsing and heading perception show similar dependence on quality and quantity of optic flow. *Frontiers in Behavioral Neuroscience*, *7*, 49.

[57] Gahlinger, P. M. (1999). Motion sickness: How to help your patients avoid travel travail. *Postgraduate Medicine*, *106*(4), 177–184.

[58] Gallagher, M. (2020). *Cybersickness: A Visuo-Vestibular Multisensory Integration Approach*. Royal Holloway, University of London.

[59] Gianaros, P. J., Muth, E. R., Mordkoff, J. T., Levine, M. E., & Stern, R. M. (2001). A questionnaire for the assessment of the multiple dimensions of motion sickness. *Aviation, Space, and Environmental Medicine*, *72*(2), 115.

[60] Gianaros, P. J., Quigley, K. S., Muth, E. R., Levine, M. E., Vasko, J., & Stern, R. M. (2003). Relationship between temporal changes in cardiac parasympathetic activity and motion sickness severity. *Psychophysiology*, *40*(1), 39–44.

[61] GJ, K. (1954). Passenger comfort in commercial air travel with reference to motion sickness. *International Record of Medicine and General Practice Clinics*, *167*(12), 661–668.

[62] Golding, J. F. (1992). Phasic skin conductance activity and motion sickness. *Aviation, Space, and Environmental Medicine*.

[63] Golding, J. F. (1998). Motion sickness susceptibility questionnaire revised and its relationship to other forms of sickness. *Brain Research Bulletin*, *47*(5), 507–516.

[64] Golding, J. F. (2006). Motion sickness susceptibility. *Autonomic Neuroscience*, *129*(1–2), 67–76.

[65] Golding, J. F. (2016). Motion sickness. *Handbook of Clinical Neurology*, *137*, 371–390.

[66] Golding, J. F., Bles, W., Bos, J. E., Haynes, T., & Gresty, M. A. (2003). Motion sickness and tilts of the inertial force environment: Active suspension systems vs. Active passengers. *Aviation, Space, and Environmental Medicine*, *74*(3), 220–227.

[67] Golding, J. F., & Gresty, M. A. (2015). Pathophysiology and treatment of motion sickness. *Current Opinion in Neurology*, *28*(1), 83–88.

[68] Golding, J. F., Mueller, A. G., & Gresty, M. A. (2001). A motion sickness maximum around the 0.2 Hz frequency range of horizontal translational oscillation. *Aviation, Space, and Environmental Medicine*, *72*(3), 188–192.

[69] Graybiel, A., & Lackner, J. R. (1980). Evaluation of the relationship between motion sickness symptomatology and blood pressure, heart rate, and body temperature. *Aviation, Space, and Environmental Medicine*.

[70] Griffin, M. J., & Newman, M. M. (2004). Visual field effects on motion sickness in cars. *Aviation, Space, and Environmental Medicine*, *75*(9), 739–748.

[71] Groen, E. L., & Bos, J. E. (2008). Simulator sickness depends on the frequency of the simulator motion mismatch: An observation. *Presence*, *17*(6), 584–593.

[72] Grossman, P. (1983). Respiration, stress, and cardiovascular function. *Psychophysiology*, *20*(3), 284–300.

[73] Guedry Jr, F. E. (1965). Psychophysiological studies of vestibular function. *Contributions to Sensory Physiology*, *1*, 63–135.

[74] Guna, J., Geršak, G., Humar, I., Song, J., Drnovšek, J., & Pogačnik, M. (2019). Influence of video content type on users' virtual reality sickness perception and physiological response. *Future Generation Computer Systems*, *91*, 263–276.

[75] Harris, L. R., Herpers, R., Jenkin, M., Allison, R. S., Jenkin, H., Kapralos, B., Scherfgen, D., & Felsner, S. (2012). The relative contributions of radial and laminar optic flow to the perception of linear self-motion. *Journal of Vision*, *12*(10), 7–7.

[76] Heer, M., & Paloski, W. H. (2006). Space motion sickness: Incidence, etiology, and countermeasures. *Autonomic Neuroscience*, *129*(1–2), 77–79.

[77] Henry, E. H., Bougard, C., Bourdin, C., & Bringoux, L. (2022). Changes in Electroencephalography Activity of Sensory Areas Linked to Car Sickness in Real Driving Conditions. *Frontiers in Human Neuroscience*, *15*, 809714.

[78] Herron, D. G. (2010). The ups and downs of motion sickness. *AJN The American Journal of Nursing*, *110*(12), 49–51.

[79] Hettinger, L. J., & Haas, M. W. (2003). *Virtual and adaptive environments: Applications, implications, and human performance issues*. CRC Press.

[80] Hill, K. J., & Howarth, P. A. (2000). Habituation to the side effects of immersion in a virtual environment. *Displays*, *21*(1), 25–30.

[81] Himi, N., Koga, T., Nakamura, E., Kobashi, M., Yamane, M., & Tsujioka, K. (2004). Differences in autonomic responses between subjects with and without nausea while watching an irregularly oscillating video. *Autonomic Neuroscience*, *116*(1–2), 46–53.

[82] Holmes, S. R., & Griffin, M. J. (2001). Correlation between heart rate and the severity of motion sickness caused by optokinetic stimulation. *Journal of Psychophysiology*, *15*(1), 35.

[83] Hromatka, B. S., Tung, J. Y., Kiefer, A. K., Do, C. B., Hinds, D. A., & Eriksson, N. (2015). Genetic variants associated with motion sickness point to roles for inner ear development, neurological processes and glucose homeostasis. *Human Molecular Genetics*, *24*(9), 2700–2708.

[84] Hu, S., Grant, W. F., Stern, R. M., & Koch, K. L. (1991). Motion sickness severity and physiological correlates during repeated exposures to a rotating optokinetic drum. *Aviation, Space, and Environmental Medicine*.

[85] Irmak, T., Pool, D. M., & Happee, R. (2021). Objective and subjective responses to motion sickness: The group and the individual. *Experimental Brain Research*, *239*, 515–531.

[86] Iskander, J., Attia, M., Saleh, K., Nahavandi, D., Abobakr, A., Mohamed, S., Asadi, H., Khosravi, A., Lim, C. P., & Hossny, M. (2019). From car sickness to autonomous car sickness: A review. *Transportation Research Part F: Traffic Psychology and Behaviour*, *62*, 716–726.

[87] ISO, I. (1997). Mechanical Vibration and Shock—Evaluation of human exposure to whole body vibrations (2631-1). *International Standards Organization*.

[88] Javaid, A., Chouhna, H., Varghese, B., Hammam, E., & Macefield, V. G. (2019). Changes in skin blood flow, respiration and blood pressure in participants reporting motion sickness during sinusoidal galvanic vestibular stimulation. *Experimental Physiology*, *104*(11), 1622–1629.

[89] Karjanto, J., Yusof, N. M., Wang, C., Terken, J., Delbressine, F., & Rauterberg, M. (2018). The effect of peripheral visual feedforward system in enhancing situation awareness and mitigating motion sickness in fully automated driving. *Transportation Research Part F: Traffic Psychology and Behaviour*, *58*, 678–692.

[90] Kennedy, R. S., Lane, N. E., Berbaum, K. S., & Lilienthal, M. G. (1993). Simulator sickness questionnaire: An enhanced method for quantifying simulator sickness. *The International Journal of Aviation Psychology*, *3*(3), 203–220.

[91] Kennedy, R. S., Lane, N. E., Lilienthal, M. G., Berbaum, K. S., & Hettinger, L. J. (1992). Profile analysis of simulator sickness symptoms: Application to virtual environment systems. *Presence: Teleoperators & Virtual Environments*, *1*(3), 295–301.

[92] Kennedy, R. S., & Stanney, K. M. (1996). Postural instability induced by virtual reality exposure: Development of a certification protocol. *International Journal of Human-Computer Interaction*, *8*(1), 25–47.

[93] Keshavarz, B., & Hecht, H. (2011). Validating an efficient method to quantify motion sickness. *Human Factors*, *53*(4), 415–426.

[94] Keshavarz, B., Hecht, H., & Lawson, B. D. (2014). Visually induced motion sickness: Characteristics, causes, and countermeasures. *Handbook of Virtual Environments: Design, Implementation, and Applications*, 648–697.

[95] Keshavarz, B., Hettinger, L. J., Kennedy, R. S., & Campos, J. L. (2014). Demonstrating the potential for dynamic auditory stimulation to contribute to motion sickness. *PloS One*, *9*(7), e101016.

[96] Keshavarz, B., Peck, K., Rezaei, S., & Taati, B. (2022). Detecting and predicting visually induced motion sickness with physiological measures in combination with machine learning techniques. *International Journal of Psychophysiology*, *176*, 14–26.

[97] Keshavarz, B., Riecke, B. E., Hettinger, L. J., & Campos, J. L. (2015). Vection and visually induced motion sickness: How are they related? *Frontiers in Psychology*, *6*, 472.

[98] Kim, Y. Y., Kim, H. J., Kim, E. N., Ko, H. D., & Kim, H. T. (2005). Characteristic changes in the physiological components of cybersickness. *Psychophysiology*, *42*(5), 616–625.

[99] Kiryu, T., Tada, G., Toyama, H., & Iijima, A. (2008). Integrated evaluation of visually induced motion sickness in terms of autonomic nervous regulation. *2008 30th Annual International Conference of the Ieee Engineering in Medicine and Biology Society*, 4597–4600.

[100] Klosterhalfen, S., Kellermann, S., Pan, F., STOcKHORST, Urs., Hall, G., & ENcK, Pa. (2005). Effects of ethnicity and gender on motion sickness susceptibility. *Aviation, Space, and Environmental Medicine*, *76*(11), 1051–1057.

[101] Koch, A., Cascorbi, I., Westhofen, M., Dafotakis, M., Klapa, S., & Kuhtz-Buschbeck, J. P. (2018). The neurophysiology and treatment of motion sickness. *Deutsches Ärzteblatt International*, *115*(41), 687.

[102] Koenderink, J. J. (1986). Optic flow. *Vision Research*, *26*(1), 161–179.

[103] Krigolson, O. E., Williams, C. C., Norton, A., Hassall, C. D., & Colino, F. L. (2017). Choosing MUSE: Validation of a low-cost, portable EEG system for ERP research. *Frontiers in Neuroscience*, *11*, 109.

[104] Krueger, W. W., Bonato, F., & Bubka, A. (2017). Method to mitigate nystagmus and motion sickness with head-worn visual display during vestibular stimulation. *J Otolaryngol ENT Res*, *7*(5), 00216.

[105] Kuiper, O. X., Bos, J. E., Diels, C., & Cammaerts, K. (2019). Moving base driving simulators' potential for carsickness research. *Applied Ergonomics*, *81*, 102889.

[106] Kuiper, O. X., Bos, J. E., Schmidt, E. A., Diels, C., & Wolter, S. (2020). knowing what's coming: Unpredictable motion causes more motion sickness. *Human Factors*, *62*(8), 1339–1348.

[107] Lackner, J. R. (2014). Motion sickness: More than nausea and vomiting. *Experimental Brain Research*, *232*, 2493–2510.

[108] Lackner, J. R., & DiZio, P. (1991). Decreased susceptibility to motion sickness during exposure to visual inversion in microgravity. *Aviation, Space, and Environmental Medicine*.

[109] LaViola Jr, J. J. (2000). A discussion of cybersickness in virtual environments. *ACM Sigchi Bulletin*, *32*(1), 47–56.

[110] Lawther, A., & Griffin, M. J. (1986). The motion of a ship at sea and the consequent motion sickness amongst passengers. *Ergonomics*, *29*(4), 535–552.

[111] Lawther, A., & Griffin, M. J. (1988). A survey of the occurrence of motion sickness amongst passengers at sea. *Aviation, Space, and Environmental Medicine*, *59*(5), 399–406.

[112] Leung, A. K., & Coenegrachts, K. (2011). *Common Problems in Ambulatory Pediatrics: Anticipatory Guidance and Behavioral Pediatrics*. Nova Science.

[113] Leung, A. K., & Hon, K. L. (2019). Motion sickness: An overview. *Drugs in Context*, *8*.

[114] Li, C., Zhang, Z., Liu, Y., Zhang, T., Zhang, X., Wang, H., & Wang, X. (2022). Multi-dimensional and objective assessment of motion sickness susceptibility based on machine learning. *Frontiers in Neurology*, *13*.

[115] Li, Y., Liu, A., & Ding, L. (2019). Machine learning assessment of visually induced motion sickness levels based on multiple biosignals. *Biomedical Signal Processing and Control*, *49*, 202–211.

[116] Lin, C.-T., Chuang, S.-W., Chen, Y.-C., Ko, L.-W., Liang, S.-F., & Jung, T.-P. (2007). EEG effects of motion sickness induced in a dynamic virtual reality environment. *2007 29th Annual International Conference of the IEEE Engineering in Medicine and Biology Society*, 3872–3875.

[117] Lin, C.-T., Tsai, S.-F., & Ko, L.-W. (2013). EEG-based learning system for online motion sickness level estimation in a dynamic vehicle environment. *IEEE Transactions on Neural Networks and Learning Systems*, *24*(10), 1689–1700.

[118] Lo, W. T., & So, R. H. (2001). Cybersickness in the presence of scene rotational movements along different axes. *Applied Ergonomics*, *32*(1), 1–14.

[119] Löcken, A., Sadeghian Borojeni, S., Müller, H., Gable, T. M., Triberti, S., Diels, C., Glatz, C., Alvarez, I., Chuang, L., & Boll, S. (2017). Towards adaptive ambient in-vehicle displays and interactions: Insights and design guidelines from the 2015 AutomotiveUI dedicated workshop. *Automotive User Interfaces: Creating Interactive Experiences in the Car*, 325–348.

[120] Luck, S. J. (2014). *An introduction to the event-related potential technique*. MIT press.

[121] Malińska, M., Zużewicz, K., Bugajska, J., & Grabowski, A. (2015). Heart rate variability (HRV) during virtual reality immersion. *International Journal of Occupational Safety and Ergonomics, 21*(1), 47–54.

[122] Mayo, A. M., Wade, M. G., & Stoffregen, T. A. (2011). Postural effects of the horizon on land and at sea. *Psychological Science, 22*(1), 118–124.

[123] McCauley, M. E., Royal, J. W., Wylie, C. D., O'Hanlon, J. F., & Mackie, R. R. (1976). Motion sickness incidence: Exploratory studies of habituation, pitch and roll, and the refinement of a mathematical model. Goleta CA: Human Factors Research Division, Canyon Research. *Group Inc. Technical Report*, 1733–2.

[124] McCauley, M. E., & Sharkey, T. J. (1992). Cybersickness: Perception of self-motion in virtual environments. *Presence: Teleoperators & Virtual Environments*, *1*(3), 311–318.

[125] McGill, M., Ng, A., & Brewster, S. (2017). I am the passenger: How visual motion cues can influence sickness for in-car VR. *Proceedings of the 2017 Chi Conference on Human Factors in Computing Systems*, 5655–5668.

[126] Money, K. E. (1970). Motion sickness. *Physiological Reviews*, *50*(1), 1–39.

[127] Money, K. E. (1972). Measurement of susceptibility to motion sickness. *AGARD Conference Proceedings*, *109*, B2-1.

[128] Mullen, T. J., Berger, R. D., Oman, C. M., & Cohen, R. J. (1998). Human heart rate variability relation is unchanged during motion sickness. *Journal of Vestibular Research*, *8*(1), 95–105.

[129] Murdin, L., Golding, J., & Bronstein, A. (2011). Managing motion sickness. *Bmj*, *343*.

[130] Muth, E. R., Stern, R. M., & Koch, K. L. (1996). Effects of vection-induced motion sickness on gastric myoelectric activity and oral-cecal transit time. *Digestive Diseases and Sciences*, *41*, 330–334.

[131] Nalivaiko, E., Davis, S. L., Blackmore, K. L., Vakulin, A., & Nesbitt, K. V. (2015). Cybersickness provoked by head-mounted display affects cutaneous vascular tone, heart rate and reaction time. *Physiology & Behavior*, *151*, 583–590.

[132] Naqvi, S. A. A., Badruddin, N., Jatoi, M. A., Malik, A. S., Hazabbah, W., & Abdullah, B. (2015). EEG-based time and frequency dynamics analysis of visually induced motion sickness (VIMS). *Australasian Physical & Engineering Sciences in Medicine*, *38*, 721–729.

[133] Nichols, S., & Patel, H. (2002). Health and safety implications of virtual reality: A review of empirical evidence. *Applied Ergonomics*, *33*(3), 251–271.

[134] O'Hanlon, J. F., & McCauley, M. E. (1973). *Motion sickness incidence as a function of the frequency and acceleration of vertical sinusoidal motion*. CANYON RESEARCH GROUP INC GOLETA CA HUMAN FACTORS RESEARCH DIV.

[135] Ohyama, S., Nishiike, S., Watanabe, H., Matsuoka, K., Akizuki, H., Takeda, N., & Harada, T. (2007). Autonomic responses during motion sickness induced by virtual reality. *Auris Nasus Larynx*, *34*(3), 303–306.

[136] Oldenburg, M. (2018). 3.7 Kinetose und Reisediarrhoe. *Reisemedizin Und Impfen*, 96.

[137] Oman, C. M. (1990). Motion sickness: A synthesis and evaluation of the sensory conflict theory. *Canadian Journal of Physiology and Pharmacology*, *68*(2), 294–303.

[138] Otto, B., Riepl, R. L., Klosterhalfen, S., & Enck, P. (2006). Endocrine correlates of acute nausea and vomiting. *Autonomic Neuroscience*, *129*(1–2), 17–21.

[139] Paillard, A. C., Quarck, G., Paolino, F., Denise, P., Paolino, M., Golding, J. F., & Ghulyan-Bedikian, V. (2013). Motion sickness susceptibility in healthy subjects and vestibular patients: Effects of gender, age and trait-anxiety. *Journal of Vestibular Research*, *23*(4–5), 203–209.

[140] Palmisano, S., Allison, R. S., & Kim, J. (2020). Cybersickness in head-mounted displays is caused by differences in the user's virtual and physical head pose. *Frontiers in Virtual Reality*, *1*, 587698.

[141] Palmisano, S., Allison, R. S., Teixeira, J., & Kim, J. (2022). Differences in virtual and physical head orientation predict sickness during active head-mounted display-based virtual reality. *Virtual Reality*, 1–21.

[142] Pavard, B., Berthoz, A., & Lestienne, F. (1976). Role of peripheral vision in linear motion detection (linear vection). *Le Travail Humain: A Bilingual and Multi-Disciplinary Journal in Human Factors*.

[143] Peck, K., Russo, F., Campos, J. L., & Keshavarz, B. (2020). Examining potential effects of arousal, valence, and likability of music on visually induced motion sickness. *Experimental Brain Research*, *238*, 2347–2358.

[144] Peddareddygari, L. R., Kramer, P. D., Hanna, P. A., Levenstien, M. A., & Grewal, R. P. (2019). Genetic analysis of a large family with migraine, vertigo, and motion sickness. *Canadian Journal of Neurological Sciences*, *46*(5), 512–517.

[145] *PLUX Biosignals*. (n.d.). Retrieved March 21, 2023, from https://www.pluxbiosignals.com/

[146] Priesol, A. J. (2017). Motion sickness. *UpToDate, Waltham, MA*, 1–34.

[147] Ragan, E. D., Bowman, D. A., Kopper, R., Stinson, C., Scerbo, S., & McMahan, R. P. (2015). Effects of field of view and visual complexity on virtual reality training effectiveness for a visual scanning task. *IEEE Transactions on Visualization and Computer Graphics*, *21*(7), 794–807.

[148] Rahimzadeh, G., Tay, A., Travica, N., Lacy, K., Mohamed, S., Nahavandi, D., Pławiak, P., Qazani, M. C., & Asadi, H. (2023). Nutritional and Behavioral Countermeasures as Medication Approaches to Relieve Motion Sickness: A Comprehensive Review. *Nutrients*, *15*(6), 1320.

[149] Reason, J. T. (1969). Motion sickness—Some theoretical considerations. *International Journal of Man-Machine Studies*, *1*(1), 21–38.

[150] Reason, J. T. (1978). Motion sickness adaptation: A neural mismatch model. *Journal of the Royal Society of Medicine*, *71*(11), 819–829.

[151] Reason, J. T., & Brand, J. J. (1975). *Motion sickness.* Academic Press.

[152] Reavley, C. M., Golding, J. F., Cherkas, L. F., Spector, T. D., & MacGregor, A. J. (2006). Genetic influences on motion sickness susceptibility in adult women: A classical twin study. *Aviation, Space, and Environmental Medicine*, *77*(11), 1148–1152.

[153] Rebenitsch, L., & Owen, C. (2016). Review on cybersickness in applications and visual displays. *Virtual Reality*, *20*, 101–125.

[154] Recenti, M., Ricciardi, C., Aubonnet, R., Picone, I., Jacob, D., Svansson, H. Á., Agnarsdóttir, S., Karlsson, G. H., Baeringsdóttir, V., & Petersen, H. (2021). Toward predicting motion sickness using virtual reality and a moving platform assessing brain, muscles, and heart signals. *Frontiers in Bioengineering and Biotechnology*, *9*, 635661.

[155] Riccio, G. E., & Stoffregen, T. A. (1991). An ecological theory of motion sickness and postural instability. *Ecological Psychology*, *3*(3), 195–240.

[156] Rolnick, A., & Bles, W. (1989). Performance and well-being under tilting conditions: The effects of visual reference and artificial horizon. *Aviation, Space, and Environmental Medicine*.

[157] Rolnick, A., & Lubow, R. E. (1991). Why is the driver rarely motion sick? The role of controllability in motion sickness. *Ergonomics*, *34*(7), 867–879.

[158] Ryan, S. M., Goldberger, A. L., Pincus, S. M., Mietus, J., & Lipsitz, L. A. (1994). Gender and age-related differences in heart rate dynamics: Are women more complex than men? *Journal of the American College of Cardiology*, *24*(7), 1700–1707.

[159] Salter, S., Diels, C., Herriotts, P., Kanarachos, S., & Thake, D. (2019). Motion sickness in automated vehicles with forward and rearward facing seating orientations. *Applied Ergonomics*, *78*, 54–61.

[160] Samuel, O., & Tal, D. (2015). Airsickness: Etiology, Treatment, and Clinical Importance—A Review. *Military Medicine*, *180*(11), 1135–1139.

[161] Sang, Y. P. (n.d.). F., Billar, J., Gresty, MA, Golding, JF, 2005. Effect of a novel motion desensitization training regime and controlled breathing on habituation to motion sickness. *Percept. Mot. Skills*, *101*, 244–256.

[162] Saredakis, D., Szpak, A., Birckhead, B., Keage, H. A., Rizzo, A., & Loetscher, T. (2020). Factors associated with virtual reality sickness in head-mounted displays: A systematic review and meta-analysis. *Frontiers in Human Neuroscience*, *14*, 96.

[163] *SCANeR*. (2022). AVSimulation. https://www.avsimulation.com/scaner/

[164] Schmäl, F. (2013). Neuronal mechanisms and the treatment of motion sickness. *Pharmacology*, *91*(3–4), 229–241.

[165] Schmidt, E. A., Kuiper, O. X., Wolter, S., Diels, C., & Bos, J. E. (2020). An international survey on the incidence and modulating factors of carsickness. *Transportation Research Part F: Traffic Psychology and Behaviour*, *71*, 76–87.

[166] Schutz, L., Zak, D., & Holmes, J. F. (2014). Pattern of passenger injury and illness on expedition cruise ships to Antarctica. *Journal of Travel Medicine*, *21*(4), 228–234.

[167] Sclocco, R., Garcia, R. G., Kettner, N. W., Isenburg, K., Fisher, H. P., Hubbard, C. S., Ay, I., Polimeni, J. R., Goldstein, J., & Makris, N. (2019). The influence of respiration on the brainstem and cardiovagal response to auricular vagus nerve stimulation: A multimodal ultrahigh-field (7T) fMRI study. *Brain Stimulation*, *12*(4), 911–921.

[168] Sherwood, L. (2006). *Fundamentals of Physiology: A Human Perspective.‖ Thomson Brooks*. Cole.

[169] Smart Jr, L. J., Stoffregen, T. A., & Bardy, B. G. (2002). Visually induced motion sickness predicted by postural instability. *Human Factors*, *44*(3), 451–465.

[170] Smyth, J., Birrell, S., Woodman, R., & Jennings, P. (2021). Exploring the utility of EDA and skin temperature as individual physiological correlates of motion sickness. *Applied Ergonomics*, *92*, 103315.

[171] So, R. H., & Lo, W. T. (1999). Cybersickness: An experimental study to isolate the effects of rotational scene oscillations. *Proceedings IEEE Virtual Reality (Cat. No. 99CB36316)*, 237–241.

[172] Stanney, K. M., Hale, K. S., Nahmens, I., & Kennedy, R. S. (2003). What to expect from immersive virtual environment exposure: Influences of gender, body mass index, and past experience. *Human Factors*, *45*(3), 504–520.

[173] Stanney, K. M., Kennedy, R. S., & Drexler, J. M. (1997). Cybersickness is not simulator sickness. *Proceedings of the Human Factors and Ergonomics Society Annual Meeting*, *41*(2), 1138–1142.

[174] Stanney, K. M., Kennedy, R. S., Drexler, J. M., & Harm, D. L. (1999). Motion sickness and proprioceptive aftereffects following virtual environment exposure. *Applied Ergonomics*, *30*(1), 27–38.

[175] Steele, J. E. (1961). *Motion sickness and spatial perception. A theoretical study*. AERONAUTICAL SYSTEMS DIV WRIGHT-PATTERSON AFB OH.

[176] Stern, R. M., Hu, S., Anderson, R. B., Leibowitz, H. W., & Koch, K. L. (1990). The effects of fixation and restricted visual field on vection-induced motion sickness. *Aviation, Space, and Environmental Medicine*.

[177] Stern, R. M., Hu, S., Uijtdehaage, S. H., Muth, E. R., Xu, L. H., & Koch, K. L. (1996). Asian hypersusceptibility to motion sickness. *Human Heredity*, *46*(1), 7–14.

[178] Stocco, A., Pulfer, B., & Tonella, P. (2022). Mind the gap! A study on the transferability of virtual vs physical-world testing of autonomous driving systems. *IEEE Transactions on Software Engineering*.

[179] Stoffregen, T. A., Chang, C.-H., Chen, F.-C., & Zeng, W.-J. (2017). Effects of decades of physical driving on body movement and motion sickness during virtual driving. *PLoS One*, *12*(11), e0187120.

[180] Stoffregen, T. A., Chen, Y.-C., & Koslucher, F. C. (2014). Motion control, motion sickness, and the postural dynamics of mobile devices. *Experimental Brain Research*, *232*, 1389–1397.

[181] Stoffregen, T. A., Faugloire, E., Yoshida, K., Flanagan, M. B., & Merhi, O. (2008). Motion sickness and postural sway in console video games. *Human Factors*, *50*(2), 322–331.

[182] Stoffregen, T. A., & Smart Jr, L. J. (1998). Postural instability precedes motion sickness. *Brain Research Bulletin*, *47*(5), 437–448.

[183] Stoffregen, T. A., Villard, S., Chen, F. C., & Yu, Y. (2011). Standing body sway on land and at sea. *Ecological Psychology*, *23*, 19–36.

[184] Stoffregen, T. A., Yoshida, K., Villard, S., Scibora, L., & Bardy, B. G. (2010). Stance width influences postural stability and motion sickness. *Ecological Psychology*, *22*(3), 169–191.

[185] Takov, V., & Tadi, P. (2019). *Motion sickness*.

[186] Tal, D., Wiener, G., & Shupak, A. (2014). Mal de debarquement, motion sickness and the effect of an artificial horizon. *Journal of Vestibular Research*, *24*(1), 17–23.

[187] Treisman, M. (1977). Motion sickness: An evolutionary hypothesis. *Science*, *197*(4302), 493–495.

[188] Turner, M. (1999). Motion sickness in public road transport: Passenger behaviour and susceptibility. *Ergonomics*, *42*(3), 444–461.

[189] Turner, M., Griffin, M. J., & Holland, I. (2000). Airsickness and aircraft motion during short-haul flights. *Aviation, Space, and Environmental Medicine*, *71*(12), 1181–1189.

[190] Vickers, N. J. (2017). Animal communication: When I'm calling you, will you answer too? *Current Biology*, *27*(14), R713–R715.

[191] Villard, S. J., Flanagan, M. B., Albanese, G. M., & Stoffregen, T. A. (2008). Postural instability and motion sickness in a virtual moving room. *Human Factors*, *50*(2), 332–345.

[192] Vogel, H., Kohlhaas, R., & Von Baumgarten, R. J. (1982). Dependence of motion sickness in automobiles on the direction of linear acceleration. *European Journal of Applied Physiology and Occupational Physiology*, *48*, 399–405.

[193] Wan, H., Hu, S., & Wang, J. (2003). Correlation of phasic and tonic skin-conductance responses with severity of motion sickness induced by viewing an optokinetic rotating drum. *Perceptual and Motor Skills*, *97*(3_suppl), 1051–1057.

[194] Warren, P. A., & Rushton, S. K. (2008). Evidence for flow-parsing in radial flow displays. *Vision Research*, *48*(5), 655–663.

[195] Warwick-Evans, L. A., Church, R. E., Hancock, C., Jochim, D., Morris, P. H., & Ward, F. (1987). Electrodermal activity as an index of motion sickness. *Aviation, Space, and Environmental Medicine*.

[196] Warwick-Evans, L., & Beaumont, S. (1995). An experimental evaluation of sensory conflict versus postural control theories of motion sickness. *Ecological Psychology*, *7*(3), 163–179.

[197] Webb, N. A., & Griffin, M. J. (2002). Optokinetic stimuli: Motion sickness, visual acuity and eye movements. *Aviation, Space and Environmental Medicine*, *73*(4), 351–358.

[198] Webb, N. A., & Griffin, M. J. (2003). Eye movement, vection, and motion sickness with foveal and peripheral vision. *Aviation, Space, and Environmental Medicine*, *74*(6), 622–625.

[199] Wilkinson, C. M., Burrell, J. I., Kuziek, J. W., Thirunavukkarasu, S., Buck, B. H., & Mathewson, K. E. (2020). Predicting stroke severity with a 3-min recording from the Muse portable EEG system for rapid diagnosis of stroke. *Scientific Reports*, *10*(1), 18465.

[200] Xuan, R. P., Xiong, Y., Brietzke, A., & Marker, S. (2021). Thermal infrared imaging based facial temperature in comparison to ear temperature during a real-driving scenario. *Journal of Thermal Biology*, *96*, 102806.

[201] Yen Pik Sang, F. D., Golding, J. F., & Gresty, M. A. (2003). Suppression of sickness by controlled breathing during mildly nauseogenic motion. *Aviation, Space, and Environmental Medicine*, *74*(9), 998–1002.

[202] Zhang, H., Yang, T., Zhang, B., Liu, Z., Zhang, F., & Liu, G. (1998). Effect of hypoxia on motion sickness induced by optokinetic stimulation. *Hang Tian Yi Xue Yu Yi Xue Gong Cheng= Space Medicine & Medical Engineering*, *11*(1), 1–4.

[203] Zhang, L.-L., Wang, J.-Q., Qi, R.-R., Pan, L.-L., Li, M., & Cai, Y.-L. (2016). Motion sickness: Current knowledge and recent advance. *CNS Neuroscience & Therapeutics*, *22*(1), 15–24.

[204] Zużewicz, K., Saulewicz, A., Konarska, M., & Kaczorowski, Z. (2011). Heart rate variability and motion sickness during forklift simulator driving. *International Journal of Occupational Safety and Ergonomics*, *17*(4), 403–410. (N.d.).

APPENDICES

Appendix A: FMS Rating versus FMS Count for the 'No Task Condition'

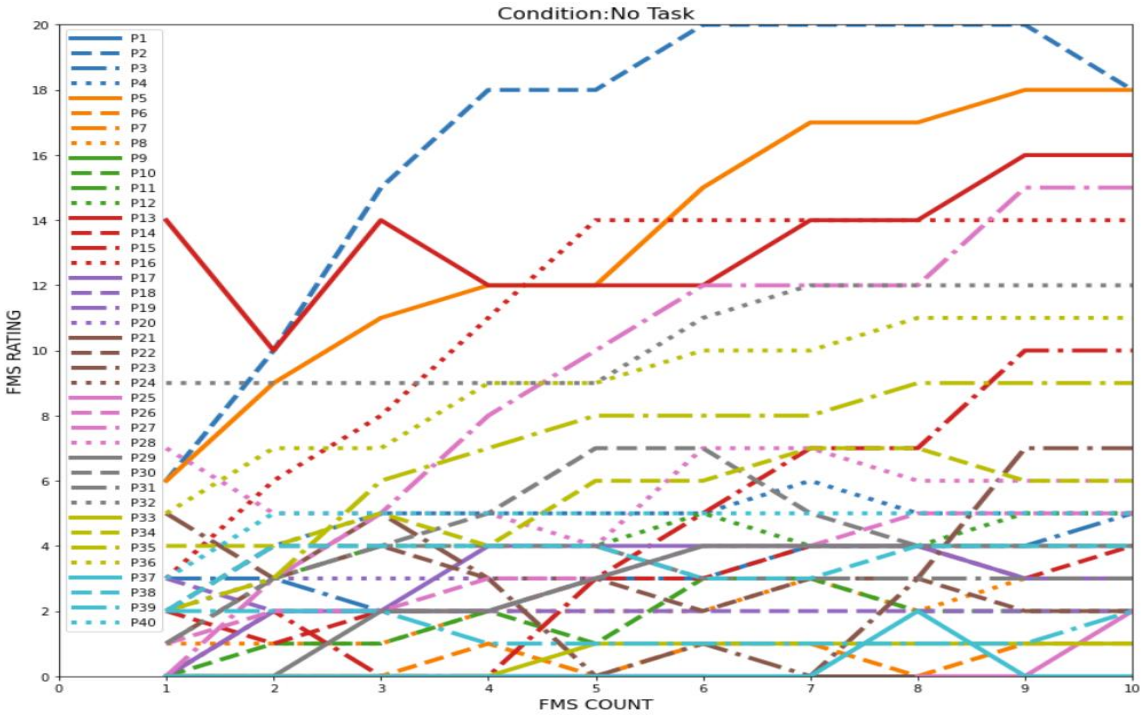

Appendix B: FMS Rating versus FMS Count for the 'Reading Task Condition'

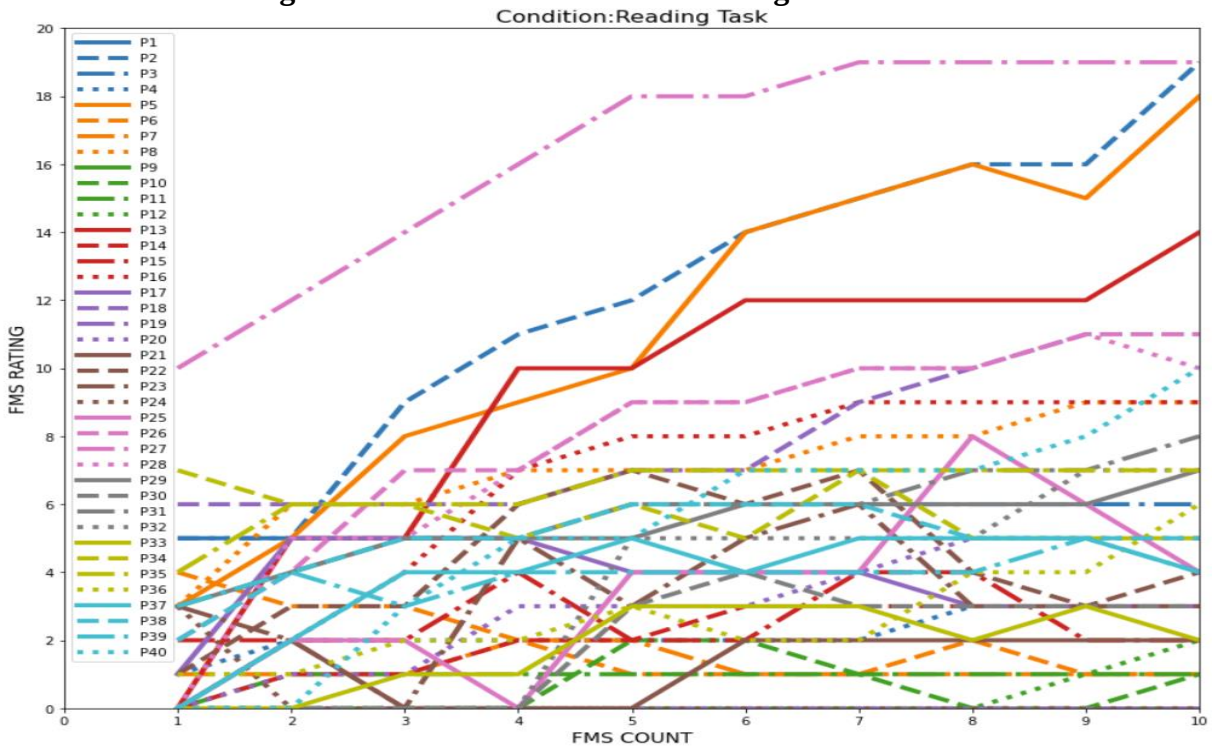

Appendix C: FMS Rating versus FMS Count for the entire experiment period

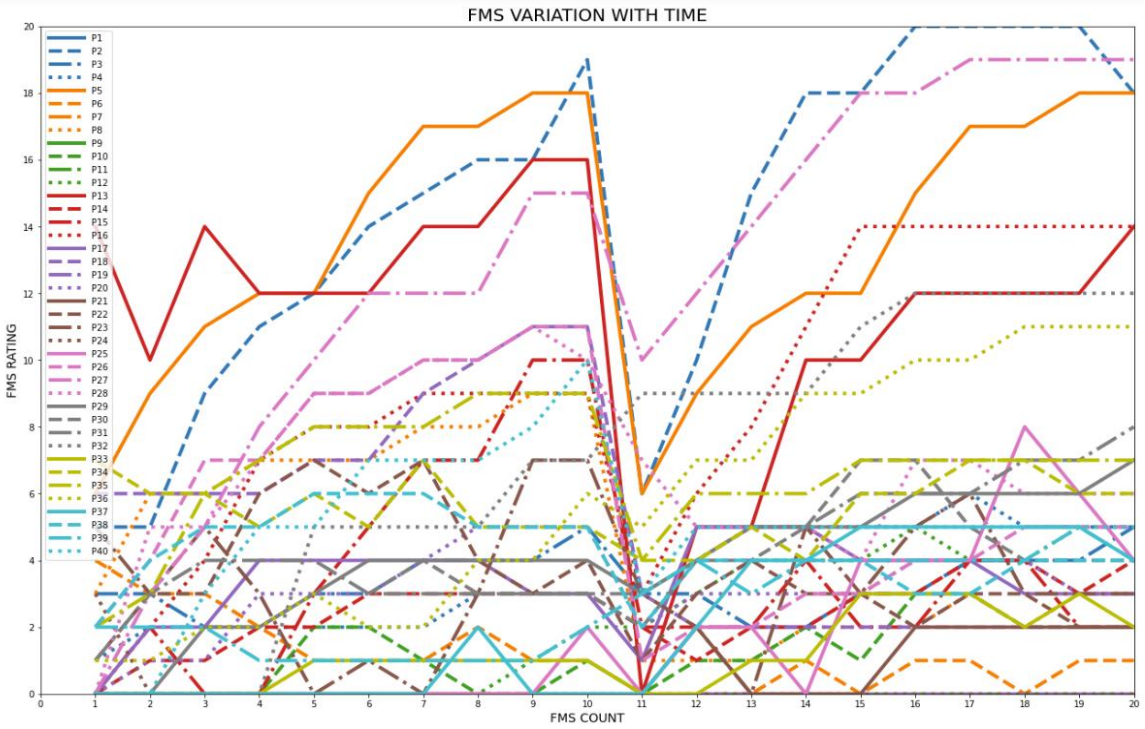

Appendix D: Comparison of Female versus Male over the No Task Condition

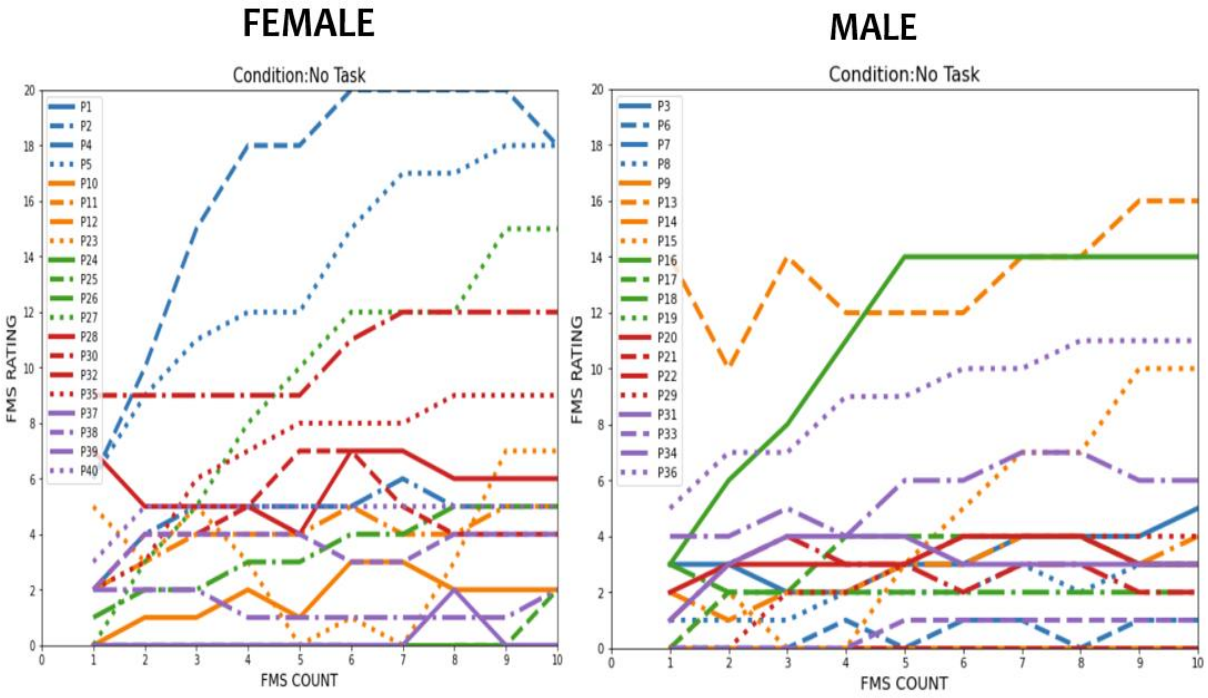

Appendix E: Comparison of Female versus Male over the Reading task condition

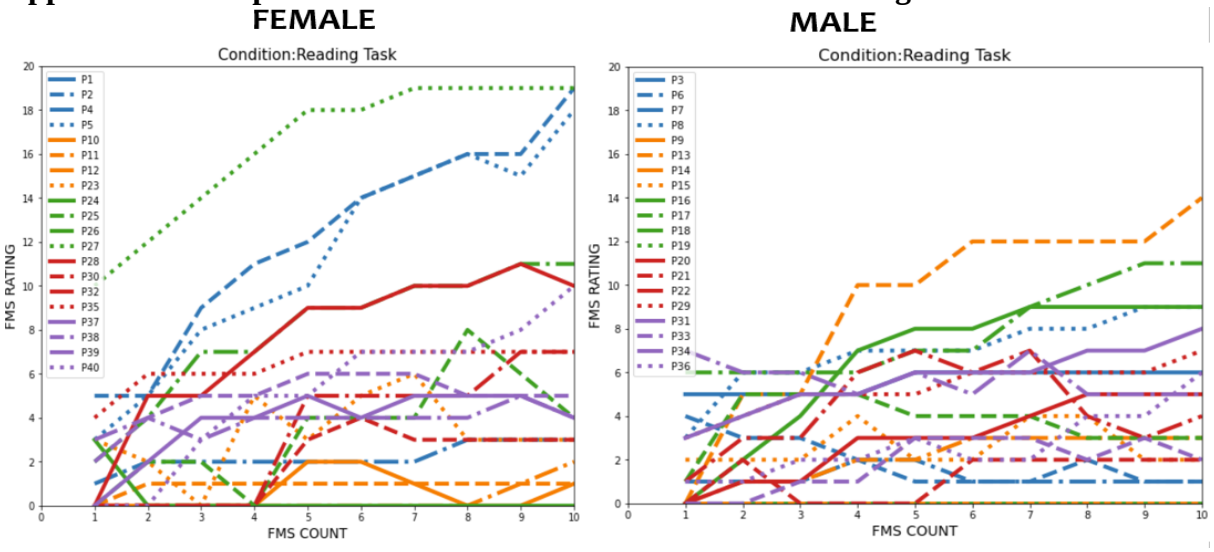

Appendix F: Correlation chart of heart rate variability parameters with FMS across the two conditions combined.